UNIVERSITY OF SOUTHERN QUEENSLAND

TWO-STAGE METHOD LINKING SPATIAL POINT PROCESSES AND LINEAR MIXED MODELS FOR PLANT ROOT TIP DATA

A THESIS SUBMITTED FOR THE AWARD OF

HONOURS THESIS

By Luke Neale

B.Sc.

Faculty of Health, Engineering and Sciences,

The University of Southern Queensland

December 2021

CERTIFICATION OF DISSERTATION

I certify that the ideas, experimental work, results, analyses, software and conclusions reported in this dissertation are entirely my own effort, except where otherwise acknowledged. I also certify that the work is original and has not been previously submitted for any other award, except where otherwise acknowledged.

Luke Neale   Date: 10/12/2021

Endorsement
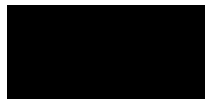
Signature of Supervisors   Date: 10/12/2021

Abstract

Spatial point processes allow for model fitting to spatial point pattern data. These spatial models estimate parameters, including covariates, based on the spatial location of points of interest. Despite the effectiveness of this methodology in analysing point pattern data, the software has difficulty in terms of computation for large, replicated experiments. In these circumstances, the inferences that can be made from spatial point processes are quite limiting and this promotes the use of a two-stage method. The presence of design parameters from a replicated experiment and research interest in relationships between genotypes advocates the implementation of the linear mixed model framework in the second stage of the analysis. The viability of such a two-stage method is investigated in this study with a weighted and unweighted use of the linear mixed model compared. The linking of spatial point processes and linear mixed models has not been investigated before, and the findings will therefore shape similar analyses in the future.

The development of spatial point pattern data can occur through the use of aeroponic platforms. In this study, the spatial point pattern data represents the position of plant root tips. This data was collected from a designed experiment on wheat plants grown in aeroponic platforms conducted at the Catholic University of Louvain in Belgium. The hidden nature of plant root traits make their measurement difficult and various methods have been implemented in an attempt to increase the accuracy in measuring below ground traits. Aeroponic platforms allow accessibility to plant root systems in a non-destructive manner, aiding the measurement of below ground traits. Often, the primary research aim in these trials is to determine variation between genotypes. A range of below ground traits can be investigated when attempting to determine genotypic variation in the root architecture of plants. Such traits can be measured and investigated using the spatial locations of plant root tips.

This study showed that linking spatial point processes and linear mixed models through the use of a two-stage method is viable. The estimated parameters from the spatial point processes were used as the response variable in the linear mixed models, where differences in the results were evident. The unweighted linear mixed models showed difficulty in estimating genetic variance across the width of the plant

root systems. This was not the case for the weighted linear mixed models, which accounted for the uncertainty in the parameter estimates to allow genetic variance to be estimated. This study also highlighted key components of this two-stage method which could be improved in the future.

Acknowledgements

I would like to sincerely thank the following people for their various contributions towards my honours project:

Contents

List of Tables

List of Figures

CHAPTER 1

Introduction

The architecture of a plant consists of both above ground and below ground compo-
nents. The measurement of above ground plant traits is generally easier than below
ground traits, due to easier access and visibility. Several methods have been attempted
to efficiently measure below ground traits, with the implementation of aeroponic plat-
forms one available option. An aeroponic platform suspends the plants in mid-air such
that plant root systems, which are usually below ground, are easily accessible (Draye
et al., 2018). In such plant trials, often a large number of genotypes are tested and
the purpose is to determine variation between them for a given set of traits. In recent
years, as aeroponic platforms have become increasingly viable for use in plant trials,
the spatial locations of plant root tips has become a focus of interest. The analysis of
these spatial locations can be conducted using spatial point processes.

For spatial data, each spatial location represents one occurrence of the object of
study (Baddeley et al., 2007). In this context, the object of study is a single plant root
tip at one point in time. The collection of spatial locations within a given spatial win-
dow create a spatial point pattern. Spatial point patterns are evident in many contexts
including those where points may represent the locations of cities, galaxies, crimes,
infectious disease cases or earthquake epicentres (Isham, 1981). Figure 1.1 displays a
spatial point pattern of the crime scene locations in Chicago. Spatial point processes
are used for the analysis of such patterns and often the objective is to predict future
locations of the object of study. Spatial point processes can also be used in an experi-
mental setting where multiple spatial point patterns are present in the data. Varying
spatial point processes can be fit to data based on the distribution of the spatial point
pattern, with each type of spatial point process requiring different assumptions to be
met. Often, computational issues impose a restricted implementation of spatial point
process analysis. For this reason, the use of linear mixed models in combination with
spatial point processes in the form of a two-stage analysis will be investigated to de-
termine its viability.

Figure 1.1: A spatial point pattern where each point represents a crime scene location in the city of Chicago (Baddeley et al., 2015).

A two-stage analysis method will be applied to the motivating dataset for this project which comes from an experiment conducted by the Catholic University of Louvain in Belgium. The experiment is partially replicated with 520 unique wheat genotypes included. In this case, partial replication refers to the unequal replication of these genotypes across the experiment. In this experiment, each plant root system had multiple images taken over an 18 day period to provide an overall spatial point pattern for the root tips within each root system. As such, there is an analysable spatial point pattern for each plant root system in the experiment. Through these spatial point patterns, the root tip data is intended to help understand the genotypic variation in plant root architecture. Further details regarding the motivating dataset and method

behind the development of the spatial point patterns are presented in Section 2.2.

The development of spatial point pattern analysis allows for the fitting of models by parameterising the explanatory variables of the experiment. That is, these statistical models can incorporate simple design terms of the experiment as well as any covariates which are present. A number of seismological applications as described by Ogata and Akaike (1982), Ogata (1983), Ogata and Katsura (1986) and Vere-Jones and Ozaki (1982) examine the relationship between point processes and their covariates. Berman and Turner (1992) raised the issue of many models resulting in negative estimated parameter values due to the statistical properties of the estimators lacking clarity. The major development to address this issue was the use of generalized linear models (GLMs). The GLM formulation resulted in reliable estimators and as such, progressed the accuracy and reliability of spatial point process models. This implementation of spatial point process models is central to the analysis of spatial point patterns, and this is the case for all types of patterns. The plant root tip data in use for this project will be modelled according to this formulation, although the specific form the model takes is dependent on the nature of the point pattern. There are several factors involved in selecting an appropriate spatial point process to fit to the data, and these will be discussed. Ultimately, spatial point processes will allow the key parameters of the plant root tip data to be captured with the implementation of an appropriate model.

The linear mixed model is an extension of a linear model in that it allows for the modelling of fixed, random and residual effects. Further to this, the implementation of different variance structures at the random and residual levels are possible. This enables extensions to point process models, such as capturing correlation between traits at both the genetic and residual levels. The ability to attribute variation to genotype and other design terms relating to the experiment is informative in drawing conclusions from the analysis. The need for the linear mixed model arises from the issues spatial point process modelling has in terms of computation. This is particularly the case with large datasets for replicated experiments (Baddeley and Turner, 2004). Given that this describes the motivating dataset for this project, a two-stage analysis combining spatial point processes and linear mixed models is necessary. Spatial point processes remain an important part of the analysis given the original data is a point pattern. The root tip study is attempting to determine genotypic variation in the architecture of the plant roots and as such, the ability of the linear mixed model to capture genetic correlations is useful. The challenge, then, is to efficiently use both spatial point patterns and linear mixed models sequentially, in a manner which produces meaningful results. Firstly, the theoretical context in which this project sits will be established before the implementation of these models in the R (R Core Team, 2019) program is explored. This will

be achieved through the use of the R packages **spatstat** (Baddeley and Turner, 2004) and **ASReml-R** (Butler et al., 2018).

1.1   The measurement of plant root traits

The identification and measurement of plant root traits has evolved considerably over recent years. The key evolution in this area has been the development of methods which allow root traits to be accurately measured during the growth of the plant without causing destruction to the root system. Root-related characteristics have been neglected in the past due to limited knowledge of root system growth and functions, as well as difficulty in measuring the traits themselves (Manschadi et al., 2006). The measurement of such traits was extremely difficult given the below ground nature of the plant roots in most trials. Due to the inherent variation in plant root traits, a lack of accuracy in measurement can significantly influence the final interpretation. As a result of this, the study of root traits via experiments was only deemed to be necessary when the root information could not be accurately generated from a model (Atkinson, 2000). As further research into plant root traits was conducted, the root data coming from such experiments was found to be useful. Subsequently, focus was quickly turned to alternate methods of conducting experiments where root traits were of interest. Developments were key in the areas of enhancing both accuracy and ease of measurement for plant root traits.

Automated high-throughput phenotyping is image-based technology which can produce multiple images for each plant in an experiment each day. The benefits of high-throughput phenotyping to agriculture include accelerated in-field measurements of biologically relevant phenotypes. These are required by plant breeders to determine which genomic characteristics and plant features are most critical to new plant development. Furthermore, the technology is rapid and non-destructive, allowing further measurements to be taken on the same plant over time where necessary (Sideli et al., 2020). Given this, the implementation of automated high-throughput phenotyping is ideal for the measurement of plant root traits. This specific technology has been implemented to create the root tip data for this analysis, which also makes use of aeroponic platforms to allow for ease of photography and access to the plant root systems.The automated high-throughput phenotyping platform used in this experiment that produced the motivating data for this research is shown in Figure 1.2.

Richard et al. (2015) and Das et al. (2015) both implement digital imaging in a high-throughput phenotyping setting. Richard et al. (2015) tested two methods, clear pots and growth pouches, to assess the angle and the number of seminal roots in wheat

Figure 1.2: The aeroponic high-throughput phenotyping platform which was used in the collection of the plant root tip data. Roots dangle freely and can easily be misted with water/nutrients. The camera can run underneath the platform to take many high quality images of the plant root systems in a non-destructive manner.

seedlings. The goal was to identify the best method for development of a low-cost high-throughput phenotyping method to facilitate the selection of desirable root architectural traits. It was found that the clear pot method had significant advantages over all other previous methods for measuring plant root traits (Richard et al., 2015). Das et al. (2015) also focus on improving methods for characterising crop root system architecture. However, the primary objective of the paper is the development of an open-source phenomics platform (DIRT). DIRT provides a storage solution for the metadata linked to such experiments, and allows intuitive access to the analysis methods and traits extracted from the images (Das et al., 2015). This was a critical step forward in the history of data collection of plant root traits and forms the basis of how such experiments are conducted today. The DIRT software may be altered for each experiment, but the underlying functionality remains consistent. In the case of Das et al. (2015), access to the data set and the accuracy of the data itself, would have been compromised without the use of this software.

The variation and flexibility of root architecture is largely influenced by physiological and genetic determinants (Hodge et al., 2009). Essentially, the growth of a root

system over space and time is genetically driven, but modified in accordance to its environmental conditions (Harper et al., 1991). There are two key concepts to address regarding root architecture; the shape and structure of the system. The shape of the plant root system refers to the manner in which the plant occupies the soil, or more specifically, the location of the roots in space. To capture this, the key traits to measure are lateral root expansion, root length density and root depth (Hodge et al., 2009). Together, these traits can be used to gain a fundamental understanding of the shape of a plant root system. The plant root structure relates to the internal makeup of the plant root system. That is, it describes the relationship between the number of components which are part of the root system. The key traits to describe plant root structure are topology (branch structure), connection between roots, and root gradients (Hodge et al., 2009). The variation in plant root architecture is significant, even within a species (Cannon, 1949; Kutschera, 1960; Weaver and Bruner, 1926). This represents the interest in conducting a trial with a large number of genotypes as is the case with the root tip dataset.

Root function is key in understanding the operation of the plant root system as a whole. The primary function of a root system in small plants is the uptake of water and nutrients. Anchorage is a secondary function, which is more vital in trees and similar species with extensive below ground structures (Hodge et al., 2009). It has been discovered that plant roots display both physiological and morphological plasticity, meaning that they can manipulate themselves to capture nutrients from transient patches in the soil (Hodge, 2004, 2006). A strong link has been found between root length and nutrient capture, where root length can be used as a predictor for nutrient capture (Hodge et al., 1999, 2000; Robinson et al., 1999). Relationships such as this are vital in understanding root function, and furthermore, the variability in efficiency of root function between genotypes. Intricate differences in plant root systems have been shown to correlate with significant differences in crop outputs (e.g. Yield). The details of these differences in the context of barley breeding trials are explored in Robinson et al. (2018). The development of designed experiments to measure plant root traits are critical to developing knowledge surrounding plant root function further. Automated high-throughput phenotyping methods as used to collect the plant root tip data, are central to this continued development and research.

1.2 Spatial point processes

1.2.1 Poisson processes

Poisson processes are central to analyses of spatial point patterns and have a large bearing on the way in which analyses are conducted. A Poisson process exhibits "no

interaction" and "complete spatial randomness" (Moller and Waagepetersen, 2003). That is to say, a spatial point pattern is Poisson if there is no detectable trend or dependence between the points. If a point pattern is Poisson, it may be either homogeneous or inhomogeneous. Homogeneous spatial point patterns exhibit constant intensity throughout the entire spatial window. Intensity in this context refers specifically to the number of points per unit area in the spatial window of interest. A homogeneous spatial point process is therefore one which displays constant intensity. If the intensity is not constant and varies throughout the spatial window, the pattern is an inhomogeneous spatial point process. Examples of these varying processes are evident through simulations shown in Figure 1.3. The concept of 'intensity' encompasses a large part of any analysis where deviation from the Poisson process is investigated. A number of functions and summary statistics have been developed to describe and parameterise spatial point patterns. These vary depending on whether the pattern is homogeneous or inhomogeneous.
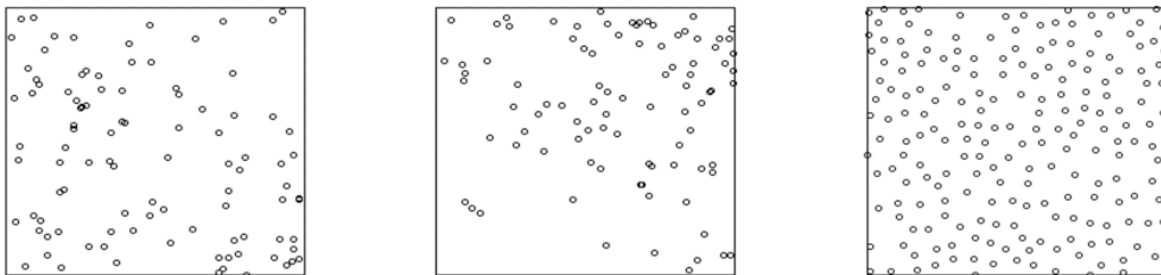
Figure 1.3: Spatial point patterns which have been simulated in R using the **spatstat** package (Baddeley and Turner, 2000). From left to right there is a homogeneous Poisson pattern, an inhomogeneous Poisson pattern and a non-Poisson pattern.

Determining whether a point pattern is Poisson is a key determinant for how a spatial point pattern analysis progresses. According to Ripley (1977), the methods used to identify whether spatial point processes are Poisson can be divided into four classes:

- Quadrat counts
- Distance or nearest-neighbour methods
- Second-order methods
- The "test-set" approach

Quadrat counts and nearest-neighbour methods tend to be appropriate in preliminary fieldwork while second-order methods and the "test-set" approach employ useful non-Poisson models to test against the fit of a proposed model (Ripley, 1977). The basis model of a point process is the uniform Poisson point process in the spatial window

with intensity defined by lambda (λ). According to Baddeley and Turner (2004), the properties of the basis model are:

- the number of points in a given region (A) has a Poisson distribution with mean (λ) x area (A)
- the locations of these points inside region A are independently and identically distributed and uniformly distributed
- the contents of two separate regions A and B are independent

The uniform Poisson process is usually employed as the 'null model' in point pattern analyses. Many analyses begin by establishing that the data does not conform to a uniform Poisson process, which proves to be the case in many point patterns. After confirming that the spatial point pattern is not uniform and Poisson, further investigations can be carried out to determine the specific nature of the point pattern. Methods for fitting point process models have been available since the 1970's, however most of these produced models that were specific to the chosen context and lacked generality (Baddeley and Turner, 2004). The R package **spatstat** has provided an improved method for model fitting and is now commonly used.

1.2.2 Spatstat

Baddeley and Turner (2000) describe an algorithm for fitting point process models of a very general form and developed this into the R package **spatstat**. This method uses approximate maximum pseudolikelihood to estimate the parameters of a spatial point process. The maximum pseudolikelihood estimator is a practical alternative to the maximum likelihood estimator (MLE). In cases where the variance-covariance matrix is complex, the approximate maximum pseudolikelihood estimator has been shown to be ideal (Baddeley and Turner, 2000). It is consistent and asymptotically normal under suitable conditions as well as satisfying unbiased estimating equations. That is, the estimated parameters are free from bias. This methodology opened up a wide variety of spatial point process models known as Gibbs models. These models were found to incorporate spatial trends, mark information, dependence on spatial covariates and interaction between points (Baddeley and Turner, 2000). The range of models which **spatstat** can fit is broad and as such, it is vital to implement appropriate modelling from the options available for a given spatial point pattern.

1.2.3 Cluster processes

Cluster processes were one of the earliest and most prominent class of models studied for the analysis of spatial point patterns (Neyman and Scott, 1972). In general, cluster

processes consist of a parent process which is usually Poisson, and a corresponding daughter process (Ripley, 1977). The cluster process is then a superposition of the daughter process. Nearest neighbour distances and the Clark-Evans' test are often used to determine the difference between a cluster process and a Poisson process. Nearest neighbour distances are used to compare what is believed to be a cluster process to a Poisson process. The distribution of the nearest neighbour distances give a clear indication of the nature of the process. That is to say, is the distribution of nearest neighbour distances Poisson, or are a number of these distances very close together indicating a cluster process? The Clark-Evans' test is commonly used to see if the data conform to a Poisson process and Figure 1.3 show simulations of various point patterns. This test accounts for edge corrections which is important in achieving an accurate result (Ripley, 1979). Edge corrections work on the principle that the spatial window is a sample from a greater population rather than being abruptly cut off at the windows peripheries. This ensures the spatial point pattern is represented as accurately as possible in the model being fitted. In turn, this allows summary statistics to be interpreted with confidence.

1.2.4 Marks and Covariates

Marked spatial point patterns and covariates add another element to analysis. Marks and covariates are commonly confused; however, the difference is that marks are linked to the point pattern response variable while covariates potentially explain the observed variation in the response variable. In environmental and agricultural data, marks and covariates are both often present and must be accounted for accordingly. The most common example of marks is when time is involved. That is, the spatial location is the response variable and the time of its occurrence is the mark. Covariates may be spatial or geostatistical such as elevation above sea level. Baddeley and Turner (2004) explain how covariates are included in the fitting of a point process model in terms of the **spatstat** package. Ultimately, the goal of estimating the parameters remains the same, and the covariates are estimated just as any other parameters in the analysis are when fitting a model. The maximum pseudolikelihood approach used for estimation is explained in section 1.2.2. Each explanatory variable in the model, including any covariates, are fit through this parameterisation process. This methodology can be appropriately applied to the analysis of plant root architecture and growth patterns.

Analysis surrounding plants has tended to be predominantly outcome based throughout history. That is, understanding response variables such as yield, dry weight and soil moisture content have been at the forefront of research. The architectural makeup of plants and how this architecture develops over time is a much less known field,

and one which spatial point processes can help to address. Plant root architecture varies depending on several covariates. Environmental factors may play a key role in both architecture and growth; however, it is likely that the genetics of the plant is the dominant reason for variation. The application of spatial point processes to a designed experiment of plants allows for a meticulous analysis of plant root architecture. Furthermore, if points are taken over time, growth patterns can also be analysed. Forming spatial point processes of the plants allows for a model to be fitted as a space-time process, as described by Chang and Schoenberg (2011). By parameterising the genotypic variation an elaborate understanding of how intensity varies among genotypes, and the rate of this variation over time can be established. The use of inhomogeneous point process methods are appropriate in this case given the variable intensity which is evident across the spatial window. This is due to the greater intensity of plant root tips created around the base of the seminal roots in contrast to the far less intense peripheries of the plant (lateral roots). The use of linear mixed models can enhance this analysis and provide more comprehensive results.

1.3 Linear Mixed Models

1.3.1 Background/Methodology

Linear mixed models are being increasingly used in applied statistics, and have wide applications in an agricultural context. They have the ability to handle large datasets for replicated experiments and can do so in a highly flexible manner. The flexibility comes from the linear mixed model's ability to partition effects into fixed, random and residual components. Linear mixed models are an extension to linear models, with some important differences. Perhaps the most important of these is that linear mixed models have both regression (fixed) and variance (random) parameters (Muller et al., 2013). The random effects are assumed to follow a Gaussian distribution which exhibits a mean of zero and homogeneity of variance. The other key strength of the linear mixed model is its ability to fit correlations between terms at both the random and residual levels. In many agricultural experiments, this provides advantages for researchers who are often interested in correlations modelled between genotypes. This is not limited to a single experiment or genetic correlations. Correlations may be fit between different traits or environments which are both useful in certain circumstances. The different variance structures which can be fit at the random and residual levels of the linear mixed model are discussed in section 1.3.2.

There are several approaches to choosing a model, with the goal generally being to select the most parsimonious. The Akaike information criterion, AIC (Akaike, 1973), and Bayesian information criterion, BIC (Schwarz, 1978), are two key tools used in this

process, where minimisation of these two values is sought after. Whilst these tools are useful in model selection, they should not strictly decide which model is implemented. The REML process of Patterson and Thompson (1971), as described in section 1.3.2, seeks to maximise the log-likelihood in the model fitting process. Models can then be compared using the log-likelihood ratio test (LRT) which determines whether the difference in log-likelihood is significant enough to justify the extra parameters. The degrees of freedom for this test are calculated by the difference in the number of parameters between the two models. The LRT, along with the AIC and BIC are key in determining the parsimony of models and therefore aid in the model selection process.

Estimation of effects in linear mixed models are done in two ways. The fixed effects are estimated using Best Linear Unbiased Estimation (BLUE) while the random effects are estimated using Best Linear Unbiased Prediction (BLUP). Both estimation procedures rely on the estimated variance parameters from the REML model fitting process when they are unknown prior to model fitting. In reality, this is usually the case. In this analysis, a two-stage approach is implemented, meaning that a set of parameters from the spatial point processes are estimated first, before moving to the linear mixed model. The spatial point process estimates will provide the response variable(s) in the linear mixed model which then allow the estimation of variance components. Subsequently, these variance components are used in the estimation of the BLUEs and BLUPs.

1.3.2 ASReml-R software

ASReml-R implements the method of residual maximum likelihood (REML) to estimate the parameters of the linear mixed model. Linear mixed models are an extensive and flexible tool among many statistical applications which the implementation of **ASReml-R** adequately supports. The analysis of balanced and unbalanced designed experiments, multi-environment trials (METs), repeated measures, longitudinal and multivariate data as well as regular or irregular spatial data are common use of the linear mixed model. **ASReml-R** seeks to provide flexibility in the syntax for specifying variance models for the random effects (Butler et al., 2018). This expands the approaches which can be taken to any given analysis. **ASReml-R** warns users of the dangers of overfitting or trying to fit inappropriate variance structures to small or highly unbalanced datasets. The REML process itself uses the average information (AI) algorithm in combination with sparse matrix methods to allow the efficient modelling of large and complex datasets. The algorithm behind the computational engine used by REML is that of Gilmour et al. (1995). The linear mixed model consists of fixed effects, random effects and an error term. **ASReml-R** separates the model into these three sets of effects, where both the random effects and residual errors have an

underlying variance structure. The variance of the random effects is known as the G structure and the variance of the residual errors is known as the R structure.

In **ASReml-R** (Butler et al., 2018), there are several variance structures which can be fit at both the random and residual levels of the model. These structures may be fit to terms such as genotype, environment and/or trait. Ideally, an unstructured variance model is fitted as this does not restrict any estimation of the variance parameters. This ensures that the model is capturing as much of the variation in the data as possible. The opposite end of the scale is the independent, or 'diag' model, which only estimates heterogeneous variances and no covariances. This is very restrictive and, as such, does not provide a comprehensive model. Despite this, the independent model is commonly used as a starting point to ensure that the model is behaving as expected. Often the unstructured model can be too difficult to estimate; this is particularly the case when there are a large number of parameters. Ultimately, this depends on what **ASReml-R** can handle computationally, and as such, there are other variance structures which can be fit. Perhaps the most common of these is the factor analytic (FA) structure. The statistical intricacies of the FA structure will not be discussed in this section, however the variance matrix is modelled as a combination of the factor loadings, subject scores and the specific variances (Butler et al., 2018). Generally, lower order FA models (fewer parameters estimated) are somewhat restrictive, however, the higher the order of FA model, the closer it gets to the unstructured estimate (Smith et al., 2015). Often, models which implement different variance structures are compared by way of a log-likelihood ratio test (LRT). The purpose of a log-likelihood ratio test is to investigate whether a statistically significant difference is evident between the log-likelihoods of the two models. Ultimately, model selection is a case by case basis and there are no concrete rules specifying which model to select. The options discussed are the frequently used tools in model selection and give a strong indication of which model is the most parsimonious.

The *asreml*() function itself gives an object of class asreml which has many accompanying functions. These include *fitted*(), *resid*(), *summary*(), *plot*(), *coef*(), *anova*(), *predict*(), *variogram*() and *wald*() which are key in both model selection and the production of meaningful results. The Wald test (Searle, 1971) is the standard test used to determine the significance of fixed effects, whether this be main or interaction effects. The *predict*() function (Welham et al., 2004) is used to provide estimates of certain factors within the model and does so based on the *asreml*() model fit. The output of using the *predict*() function will be either a set of BLUPs or BLUEs depending on the effects being estimated. Functions such as *resid*(), *plot*() and *variogram*() are useful visual tools in the sense that they indicate whether a transformation of the response variable is

required to adhere to the assumption of homogeneity of variance. They are also key in determining if spatial terms should be included in the model. Perhaps the most useful function is *summary*() which provides key information regarding the fitted model. This ranges from AIC and BIC values to the variance components of the fitted model. Thus, it is ideal for ensuring the model is doing what you expect while providing some key summary statistics as well.

1.4   Two stage methods

1.4.1   Background/Methodology

As the name suggests, two-stage methods have two parts. Depending on the context in which a two-stage method is applied, the process may vary. In general, the first stage involves determining some response or estimation to use in the second stage. In most circumstances, the need for a two-stage method is required for two reasons. The first of these is the inability of a given methodology to complete the analysis in one stage through lack of computational ability (Gogel et al., 2018). In such cases, an estimate of some form is predicted during stage one of the analysis which requires less computational power, and is then carried forward to stage two of the analysis. Another reason for the implementation of a two-stage method, perhaps less common, is the linkage of two separate methodologies. In these cases, an initial estimation is determined from the first methodology in stage one, and this is taken to complete stage two using the second methodology. This process is usually completed to take advantage of certain aspects of both methodologies, which can benefit in answering key research questions. Ultimately, the goal of a two-stage analysis is to achieve a result as close as possible to what the one-stage analysis would have (Kackar and Harville, 1981).

In terms of the plant root tip analysis, the first stage is the fitting of spatial point process models. The estimated parameters of the spatial covariates from the spatial point process models provide the response variables for the second stage of analysis in the linear mixed model. In any two-stage analysis, the second stage is to proceed as if the estimated values from stage one are the true values (Kackar and Harville, 1981). When dealing with large datasets for replicated experiments, one-stage analyses require significant computing resources and computational times are lengthy. In some cases, the one-stage approach may not be feasible at all. This issue is exacerbated further in **spatstat** which requires significant computational time and power to fit spatial point processes to large datasets for replicated experiments (Baddeley and Turner, 2004). This problem surrounding one-stage analyses encompasses the need for two-stage methods and infers the effectiveness of their use in these circumstances. This is particularly the case for the plant root tip data, which in a one-stage analysis

in **spatstat** would attempt to fit one spatial point process model which accounts for all covariates in the experiment. This is computationally intense, and coupled with the effectiveness of the linear mixed model at handling large datasets for replicated experiments, indicates the necessity of a two-stage method.

One of the common applications of a two-stage approach is for multi-environment trial (MET) analysis. Such trials include data from multiple experiments with the aim of combining all of this data across experiments into a single statistical model. When this is not computationally feasible, a two-stage analysis is implemented. Initially, each environment within the MET is analysed as an individual trial. This constitutes stage one of the analysis, with the genotype means from each trial taken with their variances as weights to stage two of the analysis (Gogel et al., 2018). Weighting methods will be discussed in detail in Section 1.4.2, but ultimately, they allow the differences in uncertainty surrounding the response from stage one to be incorporated into stage two of the analysis. In stage two, a more complex model is fit using all of the genotype means from stage one. Gogel et al. (2018) describe a two-stage approach of this specific nature.

In the MET context, the two-stage approach allows the full set of genotype by environment effects to be included, and their associated variance structure to be estimated when the one-stage analysis is not feasible (Gogel et al., 2018). In the case of Gogel et al. (2018), the linear mixed model framework is used in both stages of the analysis. There are several aspects of a two-stage analysis which impact the effectiveness and efficiency of the analysis. The biggest compromise moving from a one-stage to a two-stage analysis is in the fullness of the variance-covariance matrix which is taken from stage one to stage two (Gogel et al., 2018). If in a two-stage analysis the full variance-covariance matrix is utilised in stage two, the result of the two-stage analysis will mirror that of a one-stage analysis (Gogel et al., 2018). In many cases this is not achievable and as such a diagonal approximation is used, introducing a compromise to the full analysis. The more sophisticated the model is in terms of genetic effects, the greater the impact of a diagonal approximation is. The effectiveness of a two-stage analysis is also hindered by the less accurate estimation of the non-genetic variance parameters. Depending on the circumstance, significant information can be lost at this point. Finally, it is vital that genotype lines are replicated as best as possible. Partial replications, particularly with a low proportion replicated, prevent a two-stage analysis' ability to provide reasonable estimates (Gogel et al., 2018).

In recent years computing power has grown significantly, improving **ASReml-R**'s ability to analyse large and complex multi-environment genotype trial data sets using the one-stage approach. While the need for two-stage approximation is now needed to

a lesser extent, there are still situations which require their use. The plant root tip data in use for this analysis is one of these situations and requires the use of a two-stage method.

1.4.2 Weighted and unweighted methods

When using two-stage methods with a linear mixed model in stage two, a weighted or unweighted approach can be taken. A key benefit of two-stage methods is the reduction in computing power required. Estimates are taken in the first stage to be used in the second stage and a challenge in two-stage methods is how these estimates should be weighted for the second stage. Möhring and Piepho (2009) propose four published and three unpublished methods of weighting in a two-stage analysis of plant breeding trials. Generally speaking, the use of a weighted diagonal matrix is attractive given the speed the REML analysis runs with when it is used. The weighting methods discussed in Möhring and Piepho (2009) are various combinations of the following:

- standard error of differences
- variance of differences
- standard error of the mean
- least squares estimate

For the methods involving least squares, the goal of the method generally involves minimising the sum of the least squares. Various weighting methods are more appropriate than others depending on the circumstance. These circumstances include the experimental design; this may be a completely randomised block design, incomplete block design, partially replicated design, etc. The results of the analyses conducted by Möhring and Piepho (2009) revealed that most of the weighting methods provided acceptable estimates. For the unweighted method, the variance-covariance matrix from stage one is not used to create the diagonal matrix. The ignoring of this information equates to the unweighted two-stage method which does not allow the separation of the genotype by environment interaction and the residual variance (Möhring and Piepho, 2009). As such, the estimated residual variance absorbs both the genotype by environment interaction and the residual error. Many authors including Damesa et al. (2017), Welham et al. (2010), Gogel et al. (2018) and Möhring and Piepho (2009) used a weighting approach where two-stage methods were used. This is to account for the heterogeneity present and thus, ensure the estimators are as reliable as possible. As mentioned, the weighting method chosen is important and there is no straightforward answer to which method is the best. The goal is to minimise the loss of information and get as close to the estimate which a one-stage method would achieve.

Damesa et al. (2019) compared weighted and unweighted stage wise analysis for genome-wide association studies and genomic selection. For the dataset used by Damesa et al. (2019), considerable heterogeneity was evident and this is where weightings can be particularly valuable in a two-stage analysis. Spatial modelling techniques help to account for the existing spatial variability and increase the efficiency of analysis. Weighted methods tend to perform better than unweighted methods, however the degree of difference between the two varies. In Damesa et al. (2019), the study concluded that the weighted method was more highly correlated with the one-stage analysis and therefore better than the unweighted method. Although this was the case, the difference between the two was quite small and showed that the unweighted method is by no means inaccurate. As expected, the full variance-covariance matrix provides the best result when using two-stage methods and as such this should be used where it is feasible. Ultimately, the selection of a weighted or unweighted method, and if weighted which method to use, is a circumstantial decision but should be treated with great importance given the impact it can have on the analysis (Möhring and Piepho, 2009). The ability to account for heterogeneity is key to any linear mixed model analysis and allows for conclusions to be drawn with confidence in the knowledge that the analysis has been completed in an accurate manner. The importance of two-stage methods is clear given that one-stage methods are not always feasible. Therefore, it is important to know that there is a reliable method to employ in this event and this is why two-stage methods are critical to many analyses.

Two stage methods are frequently used for multi-environment trial (MET) analyses but are not strictly limited to these. In MET analyses linear mixed models contain residual variation which consists of the genotype by environment interaction and any within trial error variation (Frensham et al., 1997). Heterogeneity of variance may be present within each of these components and as mentioned, weights can play a key role in accounting for this. Estimates of a variable are often what is taken from the first stage to the second stage and as such it is the task of the weights to account for the varying levels of uncertainty surrounding these estimates. In terms of the plant root tip analysis, the estimated parameters from the spatial point process models will have varying levels of error surrounding them. As such, a weighting method which effectively accounts for the uncertainty in these estimates must be employed in the second stage of analysis (the linear mixed model). The analysis would lose vital amounts of information if the uncertainty present is not dealt with appropriately. It is clear that this is a case by case situation and the impact of the factors discussed varies. It will therefore be important to determine the effect of conducting a two-stage analysis on the plant root tip data, as well as the difference in results depending on whether a

weighted or unweighted method is utilised.

1.5 Research Questions

The analysis of the plant root tip data will merge the two methodologies of spatial point processes and linear mixed models through the utilisation of a two-stage approach. Firstly, spatial point processes will be fit to the root tip data for each plant root system separately and explored using estimated model parameters. This will allow the determination of an appropriate response variable(s) to then take into the linear mixed model framework. The linear mixed model framework will allow for all estimates from the spatial point process models to be fit in one model. This is necessary due to the lack of computational power of **spatstat**, which cannot fit one spatial point process model inclusive of all plant root systems in the experiment. For this reason, the use of a two-stage approach provides a more comprehensive analysis of the plant root tip data through it's ability to include all experimental information in one model. The implementation of the linear mixed model will allow the examination of relationships between estimated parameters through the modelling of covariance, and therefore, the analysis may provide new knowledge relating to the root architecture of particular wheat genotypes. This encompasses the need for a two-stage analysis of the plant root tip data, but it is important to implement this in an appropriate manner. Depending on the circumstance, there are a selection of different weighting methods which can be used in a two-stage approach. The difference in estimation through the use of a two-stage approach will be investigated and compared for a weighted and unweighted method. This will aid in the determination of whether a weighted or unweighted method results in meaningful differences, or whether the use of either is arbitrary. Furthermore, this will indicate the confidence with which conclusions can be made from this analysis. Ultimately, analysing the outcome of the two-stage method will show the worth of such an analysis and indicate the depth of interpretation the linear mixed model can provide after being translated from the spatial point process methodology. As such, the research questions to be answered in this analysis are:

1. What is an appropriate spatial point process model to fit to the root tip data?
2. Can a linear mixed model be used in a two-stage approach for analysis of spatial point patterns from replicated experiments?
3. Is there a difference in accuracy when a weighted or unweighted two-stage method is used?

1.6 Importance of Research

The overarching importance of this research lies in the application of a two-stage approach for analysing data from large, replicated experiments where the response

variable is a spatial point pattern. While analysis techniques used for spatial point processes provide a useful introduction to what might be occurring at the plant level in this experiment, the ability of linear mixed models to provide more comprehensive model formulation and variance modelling is crucial to the research question. Computational power is a legitimate concern for spatial point process modelling when the dataset is large and arises from a replicated experiment. The ability of linear mixed models to handle large datasets from replicated experiments and as such, include all information from an experiment in one model, is vital to the production of quality results. Another advantage lies within linear mixed models' ability to model correlations, thus providing further insight into the relationships between estimated parameters within the experiment. For these reasons, it is critical to determine an efficient two-stage method for analyses such as this which link spatial point processes and linear mixed models.

The difference in results from the two-stage method will be explored through the comparison of weighted and unweighted two-stage models. The use of a two-stage method allows the spatial point processes to capture the key spatial characteristics of each plant root system. As such, carrying the estimated parameters from the initial spatial point processes into the linear mixed model analysis brings key information into the second stage. The importance of respecting the uncertainty in the parameter estimates from stage one of a two-stage analysis varies depending on the experiment. Due to the ability of weighting methods to account for uncertainty, determining the difference in results between the weighted and unweighted methods will be vital in concluding how similar analyses should be conducted in the future. Ultimately, the determination of an appropriate two-stage method linking spatial point processes and linear mixed models is central to this analysis and encompasses the importance of this research. A flow chart describing the different components of this project is shown in Figure 1.4.

From a practical perspective, the method developed through this research will demonstrate the accuracy of measurement of root traits using an aeroponic high-throughput phenotyping platform. It will lead to critical knowledge regarding the root architecture of different wheat genotypes as well as the relationship between estimated parameters from the spatial point processes. Subsequently, future analyses may show links between plant architecture and critical traits to plant performance such as yield. This research is not limiting and could include links to root function or even response to varying pathogens. Such analyses may only be possible through the implementation of a similar method to that developed here. Therefore, the research

conducted throughout this analysis is critical to future research into root architecture and the effect it has on other plant traits.
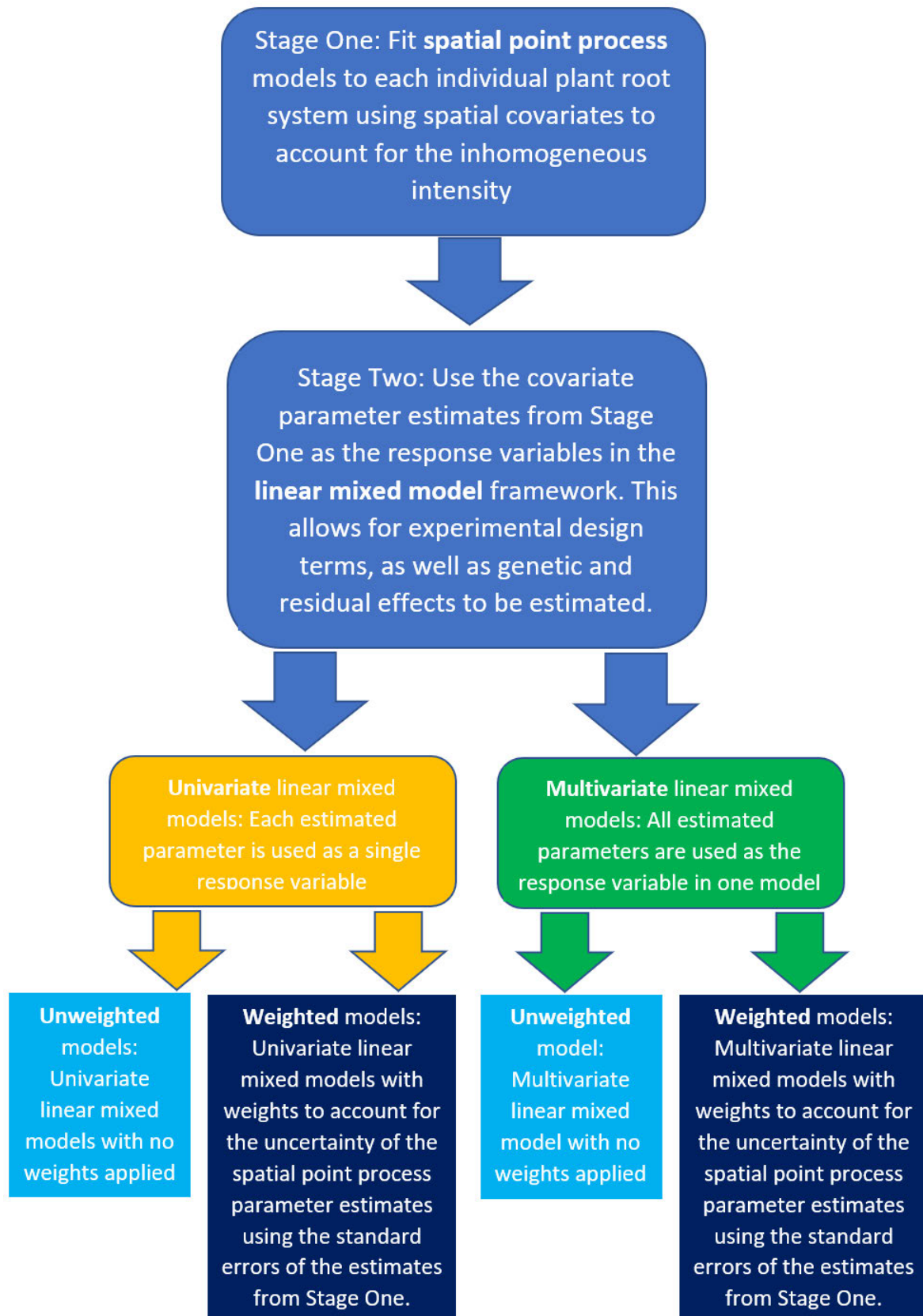
Figure 1.4: Flow chart of the analysis process carried out during the completion of this project. It summarises how spatial point process models were used in stage one of the analysis before linear mixed models were implemented in stage two. The different forms of analysis using the linear mixed model framework are described.

CHAPTER 2

Methods

2.1 Statistical methods

In this chapter, the statistical methods employed throughout this project will be detailed. Section 2.1.1 discusses the statistical theory behind spatial point process models. This includes the theory behind the spatial point process model itself as well as the model selection process which is carried out to arrive at the final model. The removal of outliers is also discussed before moving to the second topic of the two-stage method. Section 2.1.2 discusses the statistical theory behind the unweighted linear mixed model, while Section 2.1.3 discusses the statistical theory behind the weighted linear mixed model. This includes the theory behind both the univariate and multivariate models as well as the weighting method used. Finally, Section 2.2 outlines the methods used to collect data from this experiment and how this translates into the x, y data present for use in this project.

2.1.1 Point process models

Point process models come in many forms, with different statistical models available for varying types of data. If it is appropriate to fit a Poisson process to the data this greatly simplifies the statistical analysis. This is due to the broad range of powerful statistical techniques which can be implemented to these processes (Baddeley et al., 2015). In order to be classed as a Poisson process, the data points must be random and independent. This property is evident in the plant root tip data and allows the exploration of model fitting for Poisson processes in this project.

The simplicity of a Poisson process is due to the fact that it is completely described by the intensity function $\lambda(u)$. That is, Poisson point processes are simply models of intensity, where the model is an equation describing the form of the function $\lambda(u)$ (Baddeley et al., 2015). For this reason, the statistical modelling of Poisson point processes are relatively simple. A random variable X has a Poisson distribution with parameter μ if $R_X = [0, 1, 2, 3, ...]$ and:

$$P_X(k) = \begin{cases} \frac{e^{-\mu}\mu^k}{k!} & k \in R_X \\ 0 & otherwise \end{cases} \tag{2.1}$$

where $P_X(k)$ is the probability of the random variable X occurring k times in this Poisson distribution governed by the parameter μ, which is the mean of the Poisson distribution (Last and Penrose, 2017). The Poisson process has two useful properties. Firstly, if $X{\sim}Poisson(\mu)$, then $E(X) = \mu$ and $Var(X) = \mu$. That is, both the expected value and variance of X are equal to μ. The second property is if $X_i{\sim}Poisson(\mu_i)$, for $i = 1, 2, ..., n$, and the X_i's are independent, then $X_1 + X_2 + ... + X_n{\sim}Poisson(\mu_1 + \mu_2 + ... + \mu_n)$.

Equation 2.1 shows the probability of obtaining k events according to the Poisson distribution. In order to extend this to a Poisson point process, a test region, B, must be present. It is known that the expected number of points in the test region, or spatial window, B is $\mathbb{E}n(X{\cap}B) = \lambda|B|$. As such, it is true that the random number of points $n(X{\cap}B)$ has a Poisson distribution with mean $\mu = \lambda|B|$ (Baddeley et al., 2015). This reiterates the importance the Poisson distribution has when it comes to point processes. The homogeneous Poisson point process with intensity $\lambda > 0$ exhibits the following properties. Firstly, the number of random points $n(X{\cap}B)$ in the spatial window B has the mean value $\mathbb{E}n(X{\cap}B) = \lambda|B|$ defining the property of homogeneity. Secondly, for the spatial windows $B_1, B_2, ..., B_m$ which are not overlapping, the number of random points $n(X{\cap}B_1), ..., n(X{\cap}B_m)$ in each spatial window are independent random variables, defining the property of independence. Finally, the number of random points $n(X{\cap}B)$ in the spatial window B has a Poisson distribution as defined in Equation 2.1.

An inhomogeneous Poisson process exhibits all properties of the homogeneous process, except that the intensity parameter λ changes throughout the spatial window. Suppose that the average intensity of points is defined as a function $\lambda(u)$, where u refers to the spatial location within the spatial window B. Given the intensity is changing throughout the spatial window, the expected total number of points in B is the sum of the values $\lambda(u)\Delta u$, where Δu is the area of a number of segments which make up the spatial window. This can be defined by the integral

$$\int_B \lambda(u)\,du.$$

The inhomogeneous Poisson point process with intensity function $\lambda(u)$ exhibits the following properties. Firstly, the expected number of points in the spatial window B is

defined by the integral $\mu = \int_B \lambda(u)\,du$ of the intensity function $\lambda(u)$ over the window B. Secondly, the property of independence holds in that the random patterns in spatial windows which do not overlap are independent of each other. Finally, the number of points in a given spatial window B has a Poisson probability distribution (Baddeley et al., 2015). In the context of this project, the intensity function will govern the change in intensity of plant root tips according to the spatial (x, y) dimensions of the data. The key decision from this point becomes that of model selection. That is, what model formulation adequately captures the intensity of the plant root tip data throughout the spatial window. Firstly, it must be decided if the intensity is homogeneous or inhomogeneous. As defined above, homogeneous intensity is when the intensity of points is constant throughout the spatial window and inhomogeneous intensity is when the intensity of points is not constant and changes throughout the spatial window.

Inhomogeneous intensity can be modelled in different ways (Baddeley et al., 2015). In a spatial situation such as the dataset used for this project, the x and y Cartesian coordinates can effectively be implemented as spatial covariates. This is particularly useful when it is suspected that the x and y positions of the data may influence the intensity (Baddeley et al., 2015). Equation 2.2 shows one of the most simple inhomogeneous Poisson models which uses the x and y dimensions as spatial covariates.

$$\lambda_\theta(x, y) = \exp(\theta_0 + \theta_1 x + \theta_2 y) \tag{2.2}$$

This first order loglinear model can be extended to various combinations of harmonic and polynomial models. The challenge is to determine a model which effectively uses Cartesian coordinates as spatial covariates without overfitting. Several model selection tools are used to aid in this area.

Three key models were assessed when determining an appropriate Poisson process model to fit to the plant root tip data. The general form of the loglinear model fit when using the *ppm* function in **spatstat** is shown in Equation 2.3. This general form can be adapted to include different terms for spatial covariates, including linear terms (Equation 2.4), harmonic terms (Equation 2.5) and polynomial terms (Equation 2.6).

$$\lambda_\theta(u) = \exp(B(u) + \boldsymbol{\theta}^T \mathbf{Z}(u)) = \exp(B(u) + \theta_1 Z_1(u) + \theta_2 Z_2(u) + ... + \theta_p Z_p(u)) \quad (2.3)$$

where $B(u)$ and $Z_1(u),...,Z_p(u)$ are known functions and $\theta_1,...,\theta_p$ are parameters to be estimated. $\mathbf{Z}(u) = (Z_1(u),..., Z_p(u))$ indicates the vector-valued function and this is termed a modulated process by Cox (Cox, 1972). As defined earlier, u refers to the spatial location within the spatial window. In the case of the plant root tip data, u is a function of the Cartesian coordinates x and y ($u(x, y)$).

The task of selecting an appropriate model for the intensity of plant root tips throughout the spatial window consisted of the comparison of three key models. All of these models can be represented in the general form of the loglinear model fit (Equation 2.3). The simplest of these models was the linear model. The form of this model is:

$$\lambda_\theta(x, y) = \exp(B + \theta_1 abs(x) + \theta_2 y + \theta_3 abs(x)y) \quad (2.4)$$

where $\lambda_\theta(x, y)$ is the intensity as a function of the x and y coordinates in the spatial window. B is the intercept, while $abs(x)$, y and $abs(x)y$ are the known functions which describe the change in intensity. θ_1, θ_2 and θ_3 are the parameters to be estimated.

The implementation of these linear spatial covariates allows for intensity to change in a linear fashion across both the x and y dimensions of the plant. In terms of the plant root system, this corresponds to the width of the plant roots as the x dimension and the depth of the plant roots as the y dimension. The $abs(x)$ function forces the intensity to change in a symmetric manner across the width of the plant roots, emanating out from the central x-axis. The interaction term, $abs(x)y$, allows the change in intensity over root width to vary as the depth of the plant roots change. However, this change can only be linear in the current implementation seen in this model.

A somewhat different approach to modelling the change in intensity was implemented through a second order harmonic model. A second order harmonic model is a

non-linear process which is common place in optics (Yang et al., 2019). It's modelling employs the phenomenon of the two non-linear terms interacting with each other. The specifics of this interaction are evident below. The form of the second order harmonic model is:

$$\lambda_\theta(x, y) = \exp(B + \theta_1 abs(x) + \theta_2 y + \theta_3 abs(x)y + \theta_4(abs(x)^2 - y^2)) \qquad (2.5)$$

where $\lambda_\theta(x, y)$ is the intensity as a function of the x and y coordinates in the spatial window. B is the intercept while $abs(x)$, y, $abs(x)y$ and $abs(x)^2 - y^2$ are the known functions which describe the change in intensity. θ_1, θ_2, θ_3 and θ_4 are the parameters to be estimated.

As was the case for the linear model, the second order harmonic model allows for intensity to change in a linear fashion across both the width (x) and depth (y) of the plant roots. Once again, the $abs(x)y$ function allows the intensity to change in a different manner across the width of the plant roots as the depth of the plant roots change. The addition of the second order harmonic model compared to the linear model is the inclusion of the non-linear spatial covariate. The $abs(x)^2 - y^2$ spatial covariate describes how the non-linear terms $abs(x)^2$ and y^2 interact by taking the difference of the two. Section 3.1 illustrates the effectiveness of this term in capturing the properties of the plant root tip data.

The third term for modelling the change in intensity was implemented through a second order polynomial model. A second order polynomial model is an extension of the linear model which includes second order terms to capture non-linearity. However, unlike the second order harmonic model, the polynomial model implements separate functions for non-linearity in the x and y dimensions rather than the two interacting together. The form of the second order polynomial model is:

$$\lambda_\theta(x, y) = \exp(B + \theta_1 abs(x) + \theta_2 y + \theta_3 abs(x)y + \theta_4 abs(x)^2 + \theta_5 y^2) \qquad (2.6)$$

25

where $\lambda_\theta(x, y)$ is the intensity as a function of the x and y coordinates in the spatial window. B is the intercept while $abs(x)$, y, $abs(x)y$, $abs(x)^2$ and y^2 are the known functions which describe the change in intensity. θ_1, θ_2, θ_3, θ_4 and θ_5 are the parameters to be estimated.

Similar to both the linear and second order harmonic models, the second order polynomial model allows for intensity to change in a linear fashion across both the width (x) and depth (y) of the plant roots. Furthermore, the $abs(x)y$ function allows the intensity to change in a different manner across the width of the plant roots as the depth of the plant roots change. The extension of the second order polynomial model is in the inclusion of both the $abs(x)^2$ and y^2 terms. This allows for intensity to change in a non-linear fashion across both the width and depth of the plant roots. The importance of this model is discussed in Section 3.1, supported by formalised statistical tests.

It is important to note that the absolute value of x has been used in the functionality of all potential models. In the plant root tip data set, the x coordinates range from -1200 to 1500 across the spatial window. These coordinates were implemented so that the x coordinate of 0 is where the growth of the plant roots originate. The decision to take the absolute value of x in the modelling process was based on several key factors. Firstly, the nature of the aeroponic high-throughput phenotyping platforms used allow the plant roots to dangle freely from side to side. Given that multiple images of each plant root system are taken over an 18 day period, varying positions of the plant root tips in the x coordinate dimension are common. For the purposes of this analysis, each plant root system is analysed as a cumulative data set based on all images taken over the 18 day period. That is, time is not being modelled. Further to this, the data set for this analysis is two-dimensional data (x and y dimensions). A plant root system is three-dimensional and through the imaging process implemented to develop this data set, these three-dimensional systems are being transposed into two dimensions. This, coupled with the ability of the roots to dangle freely across the x dimension, could result in misleading interpretations post analysis. As such, the approach of taking the absolute value of the x coordinates in the modelling process has been implemented to mitigate this risk. Taking the absolute value of the x coordinates averages the model fit over the symmetry of the spatial window such that the fitted model is symmetric about the point $x = 0$. Forcing this symmetry in the x dimension allows the vital properties of the data to be accurately investigated.

The model fitting process for a Poisson point process seeks a 'best fit' for the combination of parameters which describe a given point pattern. Poisson point processes are fit using maximum likelihood estimation which seeks to maximise the log-likelihood

of the fitted model by finding the 'most plausible' parameter estimates (Baddeley et al., 2015). Issues arise when using maximum likelihood estimation if the specified model is not true, there are multiple parameters for few observations or model assumptions are not met. As such, model selection is vital in order to efficiently implement the fitting of Poisson point processes. For the plant root tip dataset, the intensity is modelled as a loglinear function of the parameters, with this general form given in Equation 2.3. In this generalised form, the functions which govern the model could be spatially variant in any fashion. This infers the flexibility of this model specification (Baddeley et al., 2015). For such a model, the log-likelihood of the loglinear intensity takes the form:

$$logL(\theta) = \sum_{i=1}^{n} B(x_i) + \boldsymbol{\theta}^T \sum_{i=1}^{n} \mathbf{Z}(x_i) - \int_W \exp(B(u) + \boldsymbol{\theta}^T \mathbf{Z}(u))du \qquad (2.7)$$

where all terms in Equation 2.7 are defined in the same manner as Equation 2.3. Given the data is such that $\sum_i Z_j(x_i) \neq 0$ for all j, the maximum likelihood estimator (MLE) exists and is unique (Baddeley et al., 2015). In this case, the MLE is the solution of the score equations $\boldsymbol{U}(\boldsymbol{\theta}) = 0$, with the score function being:

$$\boldsymbol{U}(\boldsymbol{\theta}) = \boldsymbol{U}(\boldsymbol{\theta}; x) = \sum_{i=1}^{n(x)} \mathbf{Z}(x_i) - \int_W \mathbf{Z}(u)\lambda_\theta(u)du \qquad (2.8)$$

where the score is the vector $\boldsymbol{U}(\boldsymbol{\theta}; x) = (U_1(\boldsymbol{\theta}; x), ..., U_p(\boldsymbol{\theta}; x))$ with components:

$$\boldsymbol{U}_j(\boldsymbol{\theta}; x) = \sum_{i=1}^{n(x)} Z_j(x_i) - \int_W Z_j(u)\lambda_\theta(u)du \qquad (2.9)$$

for $j = 1, ..., p$, where p is the number of parameters. This explains the process being completed using maximum likelihood estimation each time a Poisson point process is fit for the loglinear model of intensity. These score equations cannot be solved analytically. Therefore, numerical approximation is required to obtain the maximum likelihood estimates.

When modelling point processes Baddeley et al. (2015) use residual diagnostics as the key tool for model selection. The *diagnose.ppm* function in the **spatstat** package provides the user with four plots in the one window, and an example of this is shown in Figure 2.1. These plots examine different aspects of the model fit and show whether the model fit is adequate or not. The top left plot presents the fitted model overlapped with the raw data points. This provides a visualisation of how well the fitted model mirrors the raw data or whether it is clearly not appropriate. The top right and bottom left plots display line graphs of the cumulative sum of raw residuals against the *x* and *y* coordinates. For an appropriate model fit, the cumulative sum of raw residuals should remain close to 0 for all coordinates. Where this is not the case, it is likely that a key element of the data has not been captured in the model fit. The bottom right plot displays the spatial window highlighting the positions within the window where the model fit does not match the residuals as closely. The visual nature of this allows the user to clearly see where trends have not been appropriately accounted for in the spatial window. The use of these four plots in unison allows for a comprehensive visualisation of the effectiveness of the model fit using residual diagnostics. Examples of this are presented in Section 3.1. The limitation of residual diagnostics is the visual subjectivity and as such, two users may reach different conclusions about the same model fit. To help guard against this, several other model selection tools are also used.

The formalised statistical test used in **spatstat** for the comparison of two Poisson point process models is an analysis of deviance. The use of a chi-squared test provides a two-sided *P*-value for this analysis of deviance to indicate whether one fitted model is an improvement over the other. If the *P*-value is less than 0.05, the chi-squared test has concluded that the model is a significant improvement on that to which it has been compared to. The Akaike Information Criteria (AIC) is also useful in the model selection process. It ultimately compares the quality of statistical models to each other (Burnham and Anderson, 2004). The AIC statistic is computed using the maximum log-likelihood with an adjustment for the number of parameters estimated in the model. As such, the AIC is calculated as:

$$AIC = 2k - 2logL(\theta)$$

where *k* is the number of parameters in the model and $logL(\theta)$ is the maximum log-likelihood value. A high log-likelihood and small number of model parameters aid to minimise the AIC.

The final tool used for model selection is displayed in the output of a fitted point process model in **spatstat**. In the output, a *Z*-value and corresponding significance

level are presented for each fitted parameter. This reflects a simple Z test for each parameter estimate which tests whether it is significantly different from zero. If this is the case, it indicates that this parameter is important to the model fit and should remain in the model. The important aspect to note from these Z tests are that they should only be used to examine parameters within the model fit. That is, they cannot be used for any kind of comparison between fitted models. The results of these model selection tools are all presented in Section 3.1.

After carrying out the model selection process and determining an appropriate point process model to fit to the plant root tip data set, 923 point process models were fit for each plant root system in the data set. The experiment consisted of 990 plants, however, 67 of these were not included in the data set due to lack of growth. Once the 923 point process models were fit, the estimated parameters were examined for outliers. This was done in two sections. Firstly, a visual assessment was completed on all plants with a maximum *y* coordinate less than 4000. This point was chosen as plants with a maximum *y* coordinate less than 4000 were potential plants which had not grown satisfactorily in the experiment. These plants were compared to the other replicate(s) of that genotype to determine whether they should remain in the analysis
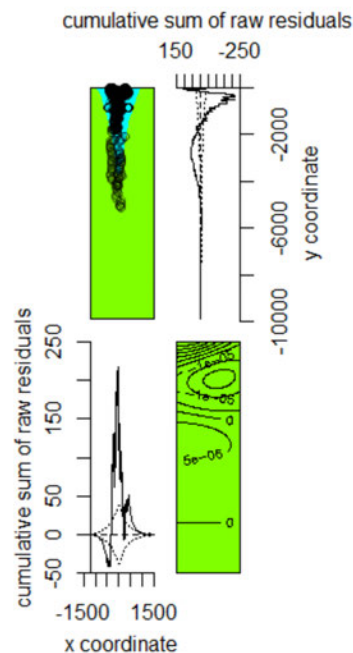
Figure 2.1: An example of the visual residual diagnostic tool available in the **spatstat** package. For each sub-figure, the top left plot shows how well the fitted model mirrors the raw data, the top right plot shows the cumulative sum of raw residuals for the *y* coordinate, the bottom left plot shows the cumulative sum of raw residuals for the *x* coordinate and the bottom right plot shows any trends across the spatial window which the fitted model is not accounting for.

as legitimate plants or not. The 37 plant root systems which were deemed to have not grown satisfactorily are displayed in Appendix A.1. As such, after completing the visual assessments these 37 plants were removed from the analysis. The second stage of outlier detection was implemented using the alternate outlier method (Gogel et al., 2001) in stage two of the analysis using the linear mixed model. This was completed by investigating the distributions of each of the estimated parameters, namely *intercept*, *abs(x)*, *y*, *abs(x)y*, *abs(x)^2* and *y^2*. The standardised conditional residual was used to determine which estimated parameters were outliers along with investigating the plots of the raw data. Conditional residuals take into account both the fixed and random effects of the model. To standardise the conditional residuals, each residual is divided by its standard deviation. All plants with a standardised conditional residual greater than 4 or less than -4 were removed for that parameter. The estimated parameters which were found to be outliers and not belong in their respective distributions are presented in Tables 2.1, 2.2, 2.3, 2.4, 2.5 and 2.6.

The second stage of the analysis was completed with these outliers removed. The *x, y* plant root tip data plots of these outliers can be found in Appendix A.2.

Table 2.1: The experimental details of the plants which have been removed from the analysis based on the estimate of the *intercept* parameter after the fitting of the point process models. *scres* represents the standardised conditional residual.

Plant	platform	strip	position	genotype	scres	*Intercept*
525	2	14	1	SUNTOP_RIL114_316	-14.80	-17.05
719	2	56	4	SUNTOP_SERI M82_264	-4.82	-9.63
702	2	52	3	SUNTOP_ZWW10-128_434	-4.69	-8.93
809	2	76	3	SUNTOP_DHARWAH DRY_33	-4.42	-8.80

Table 2.2: The experimental details of the plants which have been removed from the analysis based on the estimate of the *abs(x)* parameter after the fitting of the point process models. *scres* represents the standardised conditional residual.

Plant	platform	strip	position	genotype	scres	*abs(x)*
525	2	14	1	SUNTOP_RIL114_316	9.75	4.84e-02
719	2	56	4	SUNTOP_SERI M82_264	4.24	2.04e-02
520	2	12	5	SUNTOP_FAC10-16_180	4.11	1.98e-02

Table 2.3: The experimental details of the plants which have been removed from the analysis based on the estimate of the y parameter after the fitting of the point process models. *scres* represents the standardised conditional residual.

Plant	platform	strip	position	genotype	scres	y
20	1	5	1	SUNTOP_WYLIE_350	-4.08	-2.34e-03

Table 2.4: The experimental details of the plants which have been removed from the analysis based on the estimate of the $abs(x)^2$ parameter after the fitting of the point process models. *scres* represents the standardised conditional residual.

Plant	platform	strip	position	genotype	scres	$abs(x)^2$
74	1	16	5	SUNTOP_SERI M82_296	-5.11	-6.96e-05
895	2	94	2	SUNTOP_DRYSDALE_57	-4.69	-6.43e-05
525	2	14	1	SUNTOP_RIL114_316	-4.24	-6.09e-05
807	2	76	1	SPITFIRE-P9	-4.20	-6.00e-05

Table 2.5: The experimental details of the plants which have been removed from the analysis based on the estimate of the $abs(x)y$ parameter after the fitting of the point process models. *scres* represents the standardised conditional residual.

Plant	platform	strip	position	genotype	scres	$abs(x)y$
453	1	98	2	SERI M82_PP	-5.57	-9.36e-06
198	1	44	3	SUNTOP_ZWB10-37_412	-4.44	-7.55e-06
446	1	96	5	SERI M82_PP	4.13	6.16e-06
787	2	71	4	SUNTOP_DHARWAH DRY_22	-4.09	-6.73e-06
382	1	83	3	SUNTOP_FAC10-16_175	4.01	5.74e-06

Table 2.6: The experimental details of the plants which have been removed from the analysis based on the estimate of the y^2 parameter after the fitting of the point process models. *scres* represents the standardised conditional residual.

Plant	platform	strip	position	genotype	scres	y^2
198	1	44	3	SUNTOP_ZWB10-37_412	-9.18	-1.25e-06
868	2	88	4	SUNTOP_ZWB10-37_413	-5.62	-8.70e-07
20	1	5	1	SUNTOP_WYLIE_350	-5.32	-8.27e-07
163	1	37	3	ZWB10-37_P1	-4.99	-8.54e-07
453	1	98	2	SERI M82_PP	-4.89	-8.05e-07
875	2	90	1	SUNTOP_DRYSDALE_64	-4.81	-7.68e-07
11	1	3	1	SUNTOP_SERI M82_252	-4.74	-7.49e-07
851	2	85	2	SUNTOP_DHARWAH DRY_16	-4.63	-7.61e-07
575	2	25	4	SUNTOP_WYLIE_376	-4.70	-6.71e-07
336	1	74	1	SUNTOP_FAC10-16_158	-4.46	6.35e-07
674	2	46	3	SUNTOP_FAC10-16_188	-4.38	6.53e-07
601	2	31	1	SUNTOP_DRYSDALE_58	-4.19	6.26e-07

2.1.2 The linear mixed model

The linear mixed model is implemented in stage two of this two-stage analysis. The first approach considered for stage two of the analysis is an unweighted analysis, which considers a single trait as the response variable for the model. The appropriate linear mixed model to implement to model this data is shown in Equation 2.10. The linear mixed model for each estimated parameter from the spatial point process models can be written as:

$$y = X\tau + Z_p u_p + Z_g u_g + e \tag{2.10}$$

where y is an $n \times 1$ vector of the estimated spatial point process parameters fit to each of n experimental units in the dataset, τ is the $l \times 1$ vector of fixed effects with corresponding $n \times l$ design matrix X, u_p is the $q \times 1$ vector of non-genetic random effects (including structural effects relating to the experimental design) with corresponding $n \times q$ design matrix Z_p, u_g is the $m \times 1$ vector of genotype random effects where m is the number of genotypes in the experiment with corresponding $n \times m$ design matrix Z_g, and e is the $n \times 1$ vector of residual errors for the estimated parameters.

The random effects within the linear mixed model are assumed to follow a Gaussian distribution where the mean is equal to zero and the variance matrix is as below:

$$var \begin{pmatrix} u_p \\ u_g \\ e \end{pmatrix} = \begin{bmatrix} G_p & 0 & 0 \\ 0 & G_g & 0 \\ 0 & 0 & R \end{bmatrix}$$

As such, the variance of u_p is G_p and this relates to the trial specific effects, the variance of u_g is G_g and this relates to the genetic effects, while the variance of e is R and this relates to the residual errors. The residual structure can take several different forms and the simplest of these is $R = \sigma^2 I_n$, where it is assumed that each experimental unit is independent of one another. In the root tip dataset, this independence between experimental units holds true.

The second unweighted analysis approach considers multiple traits in a single model. The appropriate linear mixed model to model this data is shown in Equation 2.11. The multivariate linear mixed model for the estimated parameters from the spatial point process models can be written as:

$$y_j^* = X\tau_j^* + Z_p u_{pj}^* + Z_g u_{gj}^* + e_j^* \tag{2.11}$$

where $(j = 1, ..., t)$, where t is the number of traits in the multivariate model. y_j remains an $n \times 1$ vector of estimated parameters fit to each of n experimental units, however now this is the case for each of t traits in the dataset. The same specification remains for the fixed, random and residual effects as in Equation 2.10, although defined for all t traits. The multivariate model can then be defined as a direct extension of Equation 2.11 (Butler et al., 2018):

$$y^* = (I_t \otimes X)\tau^* + (I_t \otimes Z_p)u_p^* + (I_t \otimes Z_g)u_g^* + e^* \tag{2.12}$$

where $y^* = (y_1', ..., y_t')', \tau^* = (\tau_1', ..., \tau_t')', u_p^* = (u_{p_1}', ..., u_{p_t}')', u_g^* = (u_{g_1}', ..., u_{g_t}')', e^* = (e_1', ..., e_t')'$

The random effects follow a Gaussian distribution with mean 0 and variance matrices G_p^*, G_g^* and R^* as below:

$$var \begin{pmatrix} u_p^* \\ u_g^* \\ e^* \end{pmatrix} = \begin{bmatrix} G_p^* & 0 & 0 \\ 0 & G_g^* & 0 \\ 0 & 0 & R^* \end{bmatrix}$$

As such, the variance of u_p^* is G_p^* and this relates to the trial specific effects for each trait, the variance of u_g^* is G_g^* and this relates to the genotype by trait effects, while the variance of e^* is R^* and this relates to the residual errors for each trait. These matrices are formed for each trait in the multivariate model as defined in Equation 2.12. That is, there is now trial specific, genetic and residual variance for each trait. The structure of these variance matrices will be discussed below.

For this analysis, interest is in modelling both residual and genetic correlations between traits. As such, two variance structures will be tested at the random and residual levels of the model to determine the most appropriate. An independent, or 'diag' model in **ASReml-R**, allows for heterogeneous trial specific and genetic variance to be fit for each trait but no correlations between traits. The dependent, or 'corgh' structure in **ASReml-R**, allows for heterogeneous trial specific and genetic variance to be fit for each trait as well as correlations to be fit between traits. The genetic variance

matrix for the multivariate model can be represented as:

$$G_g^* = G_t \otimes I_m$$

where t is the number of traits and m is the number of genotypes. For the independent variance structure G_t takes the form:

$$G_t = \begin{bmatrix} \sigma_{g_1}^2 & & & \\ 0 & \sigma_{g_2}^2 & & \\ \vdots & & \ddots & \\ 0 & 0 & \cdots & \sigma_{g_i}^2 \end{bmatrix}$$

And for the fully unstructured, or dependent variance structure, G_t takes the form:

$$G_t = \begin{bmatrix} \sigma_{g_1}^2 & & & \\ \rho_{12} & \sigma_{g_2}^2 & & \\ \vdots & & \ddots & \\ \rho_{1j} & \rho_{2j} & \cdots & \sigma_{g_i}^2 \end{bmatrix}$$

where $\sigma_{g_i}^2$ is the genetic variance and $i = 1, .., t$, and ρ_{ij} is the genetic correlation between trait i and trait j where $j = 1, .., t$.

The same definition of variance holds true for the trial specific effects. For this experiment, this applies to the platform variance, as well as the strip and position variances where necessary. As mentioned, modelling correlations between traits at the residual level is of key interest in this analysis. This is to be done at the residual level given that each of the traits taken to the linear mixed model from the spatial point process models, have been measured on the same experimental unit. As such, it is appropriate to model correlations between traits at the residual level.

In the model selection process for the unweighted multivariate linear mixed model, two residual variance structures were investigated. The first of these was the independent, or 'diag' structure, while the second was the dependent, or 'corgh' structure. The residual variance can be represented as:

$$R^* = R_t \otimes I_n$$

Where t is the number of traits and n is the number of experimental units. For the independent variance structure R_t takes the form:

$$R_t = \begin{bmatrix} \sigma_{r_1}^2 & & & \\ 0 & \sigma_{r_2}^2 & & \\ \vdots & & \ddots & \\ 0 & 0 & \cdots & \sigma_{r_i}^2 \end{bmatrix}$$

And for the fully unstructured, or dependent variance structure, R_t takes the form:

$$R_t = \begin{bmatrix} \sigma_{r_1}^2 & & & \\ \rho_{12} & \sigma_{r_2}^2 & & \\ \vdots & & \ddots & \\ \rho_{1j} & \rho_{2j} & \cdots & \sigma_{r_i}^2 \end{bmatrix}$$

where $\sigma_{r_i}^2$ is the residual variance and $i = 1,..,t$, and ρ_{ij} is the genetic correlation between trait i and trait j where $j = 1,..,t$.

The dependent variance structure is the least restrictive of all possible structures, however, it is not always possible to fit in **ASReml-R**. Issues can arise in the fitting of this model when a large number of traits are present in the residual structure. The benefit of the dependent structure is that in addition to heterogeneous residual variances for each trait, heterogeneous correlations between traits are fit for every pairwise combination.

Once determining an appropriate residual variance structure, an identical process is completed for the random structure, and more specifically, the genetic variance structure. Both the independent ('diag') and dependent ('corgh') variance structures were investigated to model the genetic variance and their specification is presented above. Once again, the dependent structure is far less restrictive than the independent structure and will enable the modelling of genetic correlations between traits.

The variance structures of the linear mixed model tested in this analysis have now been explored. The next key part of the linear mixed model is the estimation process. The variance parameters are estimated using residual maximum likelihood (REML) as discussed in section 1.3.2. This discusses the computational engine of Gilmour et al. (1995) behind the use of REML in **ASReml-R** as well as the average information (AI) algorithm used. The fixed effects of the linear mixed model are estimated as best linear unbiased estimators (BLUEs) while the random effects are estimated as best linear unbiased predictors (BLUPs).

The linear mixed model can be generalised to the form:

$$y = X\tau + Zu + e \tag{2.13}$$

where u is a vector of the random effects such that $u = (u'_p, u'_g)'$ with corresponding design matrix $Z = [Z_p \ Z_g]$.

This allows a clear interpretation of the estimates of each respective part of the model. From equation 2.13 the random effects have a mean of zero and a variance matrix as given below:

$$var\begin{pmatrix} u \\ e \end{pmatrix} = \begin{bmatrix} G(\gamma) & 0 \\ 0 & R(\phi) \end{bmatrix}$$

where γ is the vector of variance parameters relating to u and ϕ is the vector of variance parameters relating to e.

The estimation of the linear mixed model requires the solution of the mixed model equations. The mixed model equations are:

$$\begin{bmatrix} X'R^{-1}X & X'R^{-1}Z \\ Z'R^{-1}X & Z'R^{-1}Z + G^{-1} \end{bmatrix}\begin{bmatrix} \tau \\ u \end{bmatrix} = \begin{bmatrix} X'R^{-1}y \\ Z'R^{-1}y \end{bmatrix} \tag{2.14}$$

where the solution of these equations require the REML estimates of γ and ϕ.

The log-likelihood equation for REML can be defined as (Gilmour et al., 1995):

$$l = -\frac{1}{2}(\log|X'H^{-1}X| + \log|H| + v \log \sigma^2 + y'Py/\sigma^2) \tag{2.15}$$

$$= -\frac{1}{2}(\log|C| + \log|R| + \log|G| + v \log \sigma^2 + y'Py/\sigma^2). \tag{2.16}$$

where $v = n - t, H = ZGZ' + R, C$ is the coefficient matrix in Equation 2.14 and P is defined as below:

$$P = H^{-1} - H^{-1}X(X'H^{-1}X)^{-1}X'H^{-1}$$

If K is defined as $K = (\gamma, \phi)$, the REML estimates of σ^2 and K will satisfy the following equations:

$$\frac{\partial l}{\partial \sigma^2} = -\frac{1}{2}(v/\sigma^2 - y'Py/\sigma^4) = 0 \tag{2.17}$$

$$\frac{\partial l}{\partial K_i} = -\frac{1}{2}[tr(PH_i) - y'PH_iPy/\sigma^2] = 0 \tag{2.18}$$

The restricted maximum likelihood estimator is favourable due to its unbiased nature. The solution of the score equations in Equations 2.17 and 2.18 allows for the fixed and random effects of the linear mixed model to be estimated. The fixed effects τ of the linear mixed model are estimated by:

$$\hat{\tau} = (X'H^{-1}X)^{-1}X'H^{-1}y \tag{2.19}$$

and the random effects u of the linear mixed model are estimated by:

$$\tilde{u} = GZ'Py \tag{2.20}$$

The parameter vectors to be used in these calculations are those which maximise Equation 2.16.

This section has detailed both the structure and estimation of the linear mixed model. The practicality of this is evident in Section 3.2 where the results of the unweighted linear mixed model fits are presented. The core attributes of the linear mixed model remain true for the weighted models, however, some differences are present as discussed in Section 2.1.3.

2.1.3 *Weighted linear mixed models*

Like the unweighted approach, the weighted approach to the second stage of the analysis takes two forms. The first of these is the fitting of univariate linear mixed models for each of the estimated parameters from the first stage of analysis, that is, the spatial point process models. In this instance, however, a weighted method is implemented in the fitting of these models. This is also the case for the second approach in this section, the weighted multivariate linear mixed model.

For both approaches, the weights used are calculated in the same fashion. The calculation itself is simple, as given below:

$$w = \frac{1}{se(y)} \tag{2.21}$$

where w is the $n \times 1$ vector of weights and $se(y)$ is the $n \times 1$ vector of standard errors of the estimated spatial point process parameters from the spatial point process models.

As such, the weight for any given parameter estimate is simply the inverse of its standard error from the spatial point process model. The goal of a weighted analysis is to allow for data points with different variances, and respect this when it comes to analysis. An estimate with a large standard error will be weighted low, and this is particularly important in circumstances where that estimate causes misleading results in an unweighted setting.

In **ASReml-R**, there are two ways to apply weights in the linear mixed model. This depends on whether the weights are relative or absolute. Absolute weights are defined as the reciprocal of known variances while relative weights are to be scaled by the residual variance (Butler et al., 2018). In **ASReml-R**, the argument *family* = *asr_gaussian*(*dispersion* = 1) is used in the case of absolute weights. This will fix all residual variances to 1. However, in this experiment, interest is in the differences between residual variances and the ability to model correlations between traits using them in the multivariate model. Respecting the variability in the residual variances of this experiment is critical to the analysis. There are replicated values due to the nature of the experiment and this allows the estimation of residual variances. The weights are then used to account for the differences in precision surrounding the spatial point process parameter estimates. As such, for this experiment it is ideal that the weights are scaled by the residual variance. Therefore, the argument presented above is not necessary.

The formulation of the univariate weighted linear mixed model can once again be represented by equation 2.10. The difference comes in the calculation of the residual or R structure of the model. If a structure is present in the residuals of the model, the weights are applied as a matrix product. The inverse of the residual structure is calculated as below (Butler et al., 2018):

$$R^{-1} = WS^{-1}W \tag{2.22}$$

where W is an $n \times n$ diagonal matrix constructed from the square root of the values in the weight variate w:

$$W = \begin{bmatrix} w_1 & & & \\ 0 & w_2 & & \\ \vdots & & \ddots & \\ 0 & 0 & \cdots & w_n \end{bmatrix}$$

where n is the number of experimental units. S is the $n \times n$ residual structure prior to the impact of weights. After this matrix product, the residual structure is treated as it would be in any other linear mixed model. As such, the estimation equations 2.19 and 2.20 both hold true, although the result will change due to the difference in calculation of the R matrix.

The calculation of the R matrix changes again for the weighted multivariate linear mixed model. The difference stems from the fact that in the multivariate setting the matrix of weights must be applied to a set of response variables, or traits. In this case, the residual or R structure is calculated as below:

$$R^{-1*} = W^* S^{-1*} W^* \tag{2.23}$$

where W is an $nt \times nt$ diagonal matrix of weights constructed from the square root of the values in the weight variate w:

$$W^* = \begin{bmatrix} w_1 & & & \\ 0 & w_2 & & \\ \vdots & & \ddots & \\ 0 & 0 & \cdots & w_{nt} \end{bmatrix}$$

where n is the number of experimental units and t is the number of traits. R^* is an $nt \times nt$ matrix as is S^*. Once the R^* structure has been calculated, the remainder of the estimation process is as stated previously in this section.

The decision on the most appropriate linear mixed model to implement was made using two key model selection tools. These were the log-likelihood ratio test (LRT) and Akaike Information Criteria (AIC). The LRT uses a chi-squared test to determine whether the log-likelihood of one model is a significant improvement on the log-likelihood of another model given the difference in the number of parameters. The

AIC provides an overall measure of parsimony where this value is sought to be minimised.

ASReml-R sometimes has issues with numerical estimation when dealing with numbers of either a very small or very large scale in the response variable. To guard against this, a number of the spatial point process estimated parameters are rescaled before being used as the response variables in the linear mixed model. Table 2.7 shows the transformation applied to each estimated parameter in this rescaling process. The theory presented throughout this section will be implemented in a practical sense in this project using the motivating data set provided by the Catholic University of Louvain.

Table 2.7: The transformation applied to each spatial point process estimated parameter. These transformations rescaled the estimates to an appropriate magnitude for **ASReml-R** to deal with.

Parameter	Transformation
Intercept	None
$abs(x)$	x100
y	x1000
$abs(x)^2$	x100000
$abs(x)y$	x1000000
y^2	x10000000

2.2 Development of data set

The data set used for all analyses conducted in this project was supplied by an experiment conducted at the Catholic University of Louvain in Belgium. Extensive preparation went into the design, implementation and development of data for this experiment. This section will detail the key aspects of this and ultimately explain how the data set in use has come about.

The experiment was conducted on two aeroponic high-throughput phenotyping platforms. Each of these platforms consisted of 99 strips where each strip had 5 plant positions. Figure 2.2 displays the layout of one of these platforms. As such, 495 plants were grown on each platform. The experiment in this project was conducted over two platforms giving a total of 990 plants in the data set. The purpose of this experiment was to investigate the plant root architecture of different wheat genotypes. A partially replicated design was implemented for this experiment as there were 520 different wheat genotypes used. This resulted in an average replication value of 1.9034 for the experiment. That is, on average each wheat genotype occurs 1.9034 times across

the two platforms. The implementation of aeroponic high-throughput phenotyping platforms has made experiments with large numbers of genotypes more viable in recent years, particularly with the development of imaging and robotics to allow for the capture of intricate details of plant roots. The plant roots can be accessed in a non-invasive manner while growing unimpeded (Draye et al., 2018). Currently, Draye et al. (2018) state that the aeroponics platform at the Catholic University of Louvain can assess the following root traits:

- Maximum root length (cm)
- Primary root elongation rate (cm.day-1)
- Embryonic roots number (nb of tips)
- Lateral root density (nb of lateral.cm-1 of branched embryonic root)
- Root angle between 2 first pair of seminals (° or rad)
- Mean/mode/median diameter (embryonic roots, lateral roots all roots, cm)
- Convex hull area (cm2)

This illustrates the usefulness of the aeroponic setup and the many types of analysis which can be conducted from the resulting data.

The development of the data set begins with the imaging process. The first stage of the process is the detection of the plant root tips. The initial image naturally includes seed and shoot-borne roots which are not of interest in this analysis. These are filtered out and the plant is reconstructed through the use of machine learning techniques.

The machine learning techniques used to reconstruct the plant root system have been trained on simulated plant root systems (Draye et al., 2018). This aids in determining the nature of the plant root system being dealt with and yields appropriate parameters which describe this system. The implementation of these techniques post root tip detection allow for the image to be reconstructed as purely plant root tips. An example of what this reconstruction looks like in this experiment is shown in Figure 2.3.

After the reconstruction process is complete, the data set of x, y data points is ready for analysis. In this format, the data follows a spatial point pattern. Ultimately, without the reconstruction of the data set into x, y data, the spatial point process component of this analysis could not be completed.
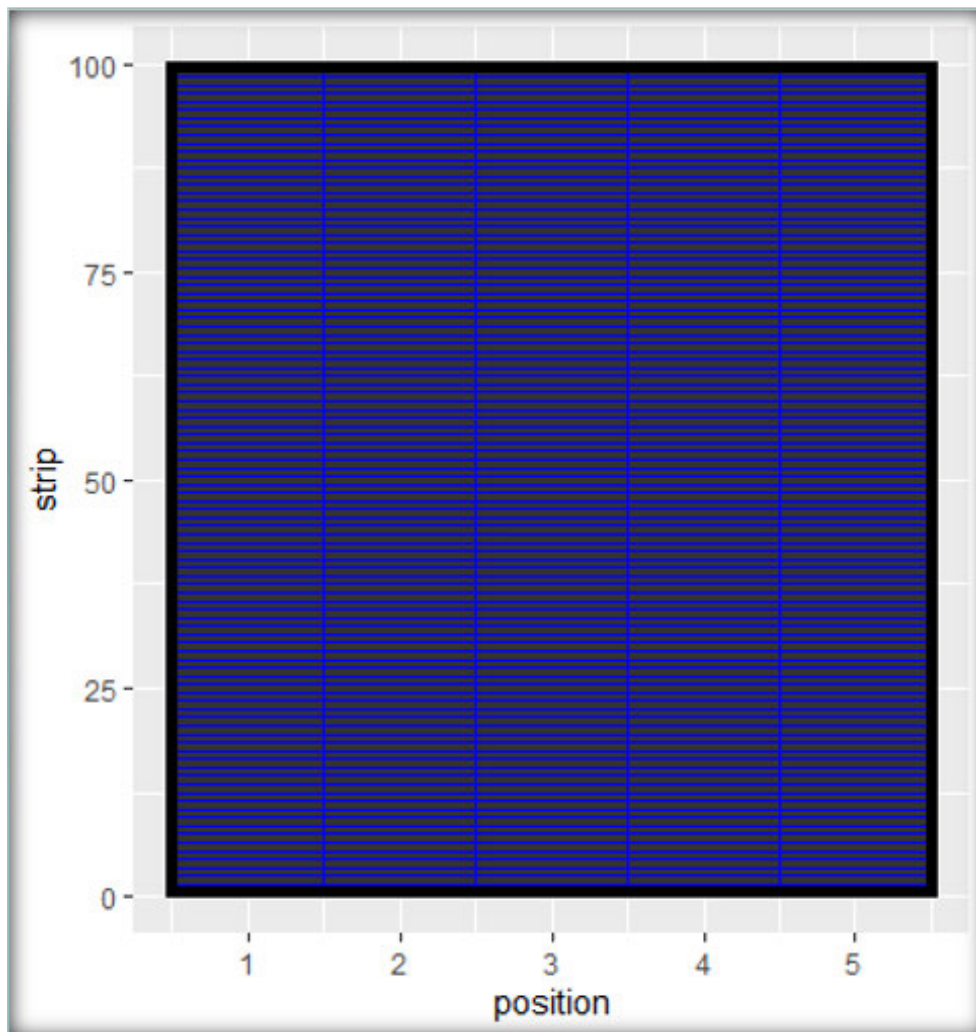
Figure 2.2: Experimental layout of one aeroponic high-throughput phenotyping platform at the Catholic University of Louvain. Each platform consists of 99 strips where each strip has 5 positions.
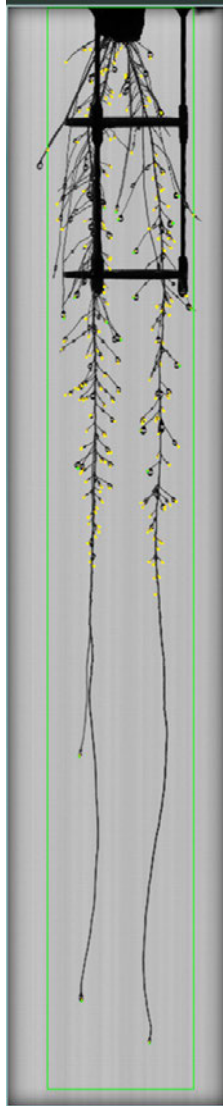
Figure 2.3: The reconstruction of a plant root tip system from the motivating data set. The dots show the plant root tips coming off each of the plant roots. The final data set is developed from the (x,y) coordinates of all plant root tips.

CHAPTER 3

Results

This chapter provides the key results from the analysis of root tip data collected from wheat genotypes grown in the replicated experiment on the aeroponic platforms. Firstly, Section 3.1 shows the results of the model selection process and summaries of the estimated parameters from the fitted point process models. This includes the distributions of the estimated parameters in addition to x, y data point plots of plants which span the range of the estimated parameters. Section 3.2 shows the results of the unweighted univariate and multivariate linear mixed models. Section 3.3 shows the results of the weighted univariate and multivariate linear mixed models. Both Sections 3.2 and 3.3 include summaries of variance components for the respective models as well as predictions of genotype effects. Furthermore, the residual and genetic correlations between estimated parameters are provided from the multivariate models. This will allow the unweighted and weighted methods to be compared, assisting in the determination of differences between methods for this analysis.

3.1 Point process models

The results of the model selection process for the case of plant 90 in the experiment is presented here in detail as an exemplar case. This plant has the maximum parameter estimate of y^2. Figure 3.1 contains three sub figures displaying the residual diagnostics for the three respective point process models (linear, second order harmonic and second order polynomial). Figure 3.1 shows a reduction in the cumulative sum of raw residuals for the x coordinates (bottom left plot of each sub figure) for the second order polynomial model (right) in comparison to the linear model (left) and second order harmonic model (middle). This indicates that the second order polynomial model is accounting for the properties of the raw data more effectively in the x dimension. The top left plot of each sub-figure in Figure 3.1 shows that the second order polynomial (right sub figure) mirrors the raw data points more closely than the linear and second order harmonic models. This is to be expected given that the cumulative sum of raw residuals in the x dimension is smaller for the second order polynomial model. The cumulative sum of raw residuals for the y coordinate are reduced for the second order
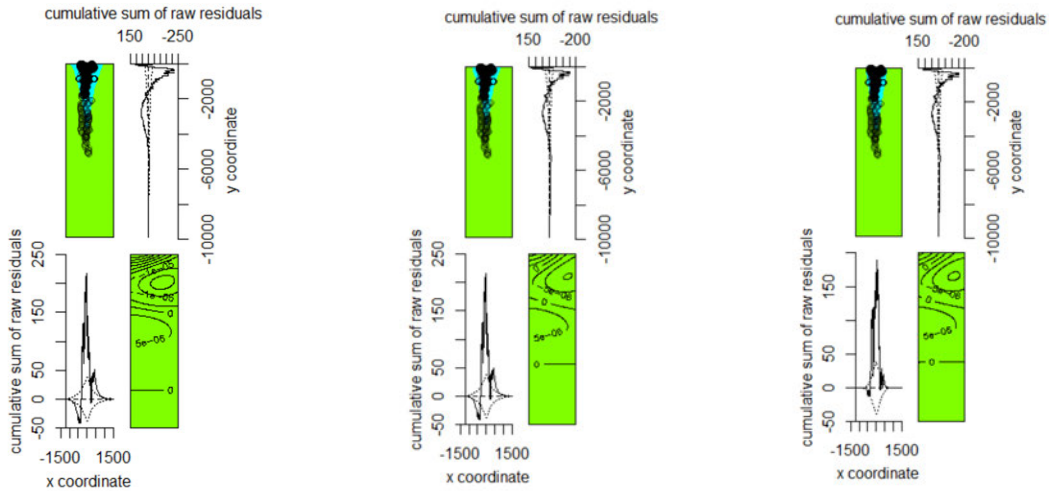
Figure 3.1: The residual diagnostics for plant 90 for all three models tested in the model selection process. From left to right there is the linear model, second order harmonic model and second order polynomial model. Each of these models are attempting to appropriately model the change in intensity of plant root tips throughout the spatial window. For each sub-figure, the top left plot shows how well the fitted model mirrors the raw data, the top right plot shows the cumulative sum of raw residuals for the y coordinate, the bottom left plot shows the cumulative sum of raw residuals for the x coordinate and the bottom right plot shows any trends across the spatial window which the fitted model is not accounting for.

harmonic and polynomial models compared to the linear model (Figure 3.1).

The Akaike Information Criteria (AIC) was also a key tool to determine the most appropriate point process model. The AIC for each of the fitted point process models are presented in Table 3.1. In addition to the AIC values, Table 3.1 presents the results of an analysis of deviance between the linear model and both the second order harmonic model and the second order polynomial model. The AIC values and analyses of deviance indicate that the second order polynomial model is the superior model of the three. The second order harmonic model reduces the AIC by 80.83 from the linear model. The second order polynomial model then reduces the AIC by a further 169.3 from the second order harmonic model. The analyses of deviance support the AIC values in concluding the second order polynomial model should be selected. The probability values from the analyses of deviance are calculated using a chi-squared test. Table 3.1 shows the second order harmonic model to be a significant improvement on the linear model as reflected by the P-value of <0.001. It is also evident that the second order polynomial model has an even larger deviance (254.13) than that for the second order harmonic model (82.831). The final point to note in Table 3.1 is that the second order polynomial model has an extra degree of freedom compared to the second order harmonic model due to the extra parameter in the model. The linear

Table 3.1: The results of two analyses of deviance as well as the AIC for each model for plant 90. A P-value is presented for each analysis of deviance using a chi-squared test. The analysis of deviance between the linear and second order harmonic models can be investigated by only looking at the first and second rows of the table. The analysis of deviance between the linear and second order polynomial model can be viewed by looking at the first and third rows of the table. *Npar* is the number of parameters, *Df* is the degrees of freedom, *Pr(>Chi)* is the P-value where a value less than 0.05 indicates a significant improvement and *AIC* represents the Akaike Information Criteria, where the minimum *AIC* is bolded.

Model	Npar	Df	Deviance	Pr(>Chi)	AIC
Linear	4				23806
Second order harmonic	5	1	82.831	<0.001	23725
Second order polynomial	6	2	254.13	<0.001	**23556**

model is shown to have four parameters which creates the difference in degrees of freedom between the successive models to be one and two respectively in the analyses of deviance. Ultimately, both the AIC and analyses of deviance are indicating the second order polynomial model should be the final model selected. These model selection results presented relate strictly to plant 90, the maximum y^2 estimated parameter. This identical process was conducted for all plants which span the range of each estimated parameter (Table 3.2) to ensure the final model selected was appropriate for all types of point processes in the dataset.

After conducting the model selection process, the second order polynomial model was selected as the final model to fit the spatial point processes. As such, this model was fit to each plant in the *R* package **spatstat**. Each of the estimated parameters were then examined for outliers which were removed as necessary (see Section 2.1.1). The summary of each of the estimated parameters distributions after the removal of outliers are presented in Table 3.2. These distributions are displayed visually in the form of histograms in Figure 3.2.

The summaries for each estimated parameter presented in Table 3.2 show the range of the model fits. These are presented in Figures 3.3, 3.4, 3.5, 3.6, 3.7 and 3.8 in the form of the x, y plant root tip data points for the specific plants which exhibit these estimated parameters. Each figure displays the minimum, mean and maximum values for that respective parameter. These figures provide an insight into the different types of plant root systems which have been detected through the second order polynomial point process model fit. Further to this, these figures display the characteristics of the

Table 3.2: The summaries of each of the estimated parameters from the fitting of 923 point process models with outliers removed. For each parameter there is a six figure summary consisting of the minimum, first quartile, median, mean, third quartile and maximum estimated parameters. The *NA's* reflect the number of missing values for that parameter.

Parameter	Minimum	1st Qu.	Median	Mean	3rd Qu.	Maximum	NA's
Intercept	-8.51	-6.33	-5.89	-5.95	-5.51	-4.02	41
abs(x)	-1.69e-02	-1.98e-03	5.50e-04	8.60e-04	3.56e-03	1.84e-02	40
y	-2.07e-03	-6.10e-04	-3.60e-04	-3.20e-04	-2.00e-05	1.61e-03	38
abs(x)y	-6.38e-06	-1.31e-06	-4.00e-07	-4.40e-07	4.70e-07	4.51e-06	42
abs(x)^2	-5.44e-05	-1.99e-05	-1.33e-05	-1.51e-05	-8.00e-06	3.80e-06	41
y^2	-5.65e-07	-2.65e-07	-2.07e-07	-2.19e-07	-1.60e-07	1.06e-07	49

spatial point pattern which are being captured by each parameter.

The *intercept* parameter is indicating the average log-intensity of the spatial point pattern. Figure 3.3 shows the plant root systems which exhibit the minimum, mean and maximum *intercept* estimated parameters. At first glance, the mean plant root system may appear to have a larger average intensity than the maximum, however this is not the case. The concentration of the plant root tips near the top of the spatial window for the plant root system with the maximum estimated parameter is far greater, resulting in a larger average intensity. The *abs(x)* parameter describes the linear change in intensity of plant root tips across the *x* dimension of the spatial window, or width of the plant root system. Figure 3.4 shows a thin plant root system for the minimum parameter which naturally exhibits little change in intensity across the *x* dimension. The mean and maximum parameter plant root systems require a closer investigation. It is vital to remember the absolute value of *x* has been taken in this analysis. The mean parameter plant root system in Figure 3.4 is symmetric in places about the point $x = 0$ which influences the fitting of the *abs(x)* parameter. In contrast, the maximum parameter plant root system is not symmetric about the point $x = 0$ and shows a linear change in intensity across the *x* dimension. The *y* parameter describes the linear change in intensity over the *y* dimension, or depth of the plant root system. In Figure 3.5 it is clear that there is little change in intensity over the depth of the minimum parameter plant root system. The mean parameter plant root system exhibits a gradual change in intensity of plant root tips over the depth while the maximum parameter plant root system shows a sharper change in intensity. Figure 3.6 displays the plant root systems for the minimum, mean and maximum *abs(x)y* estimated parameter values. This parameter describes the change in intensity of plant root tips over the width of the plant root system, as the depth of the plant root system changes. As such, it is
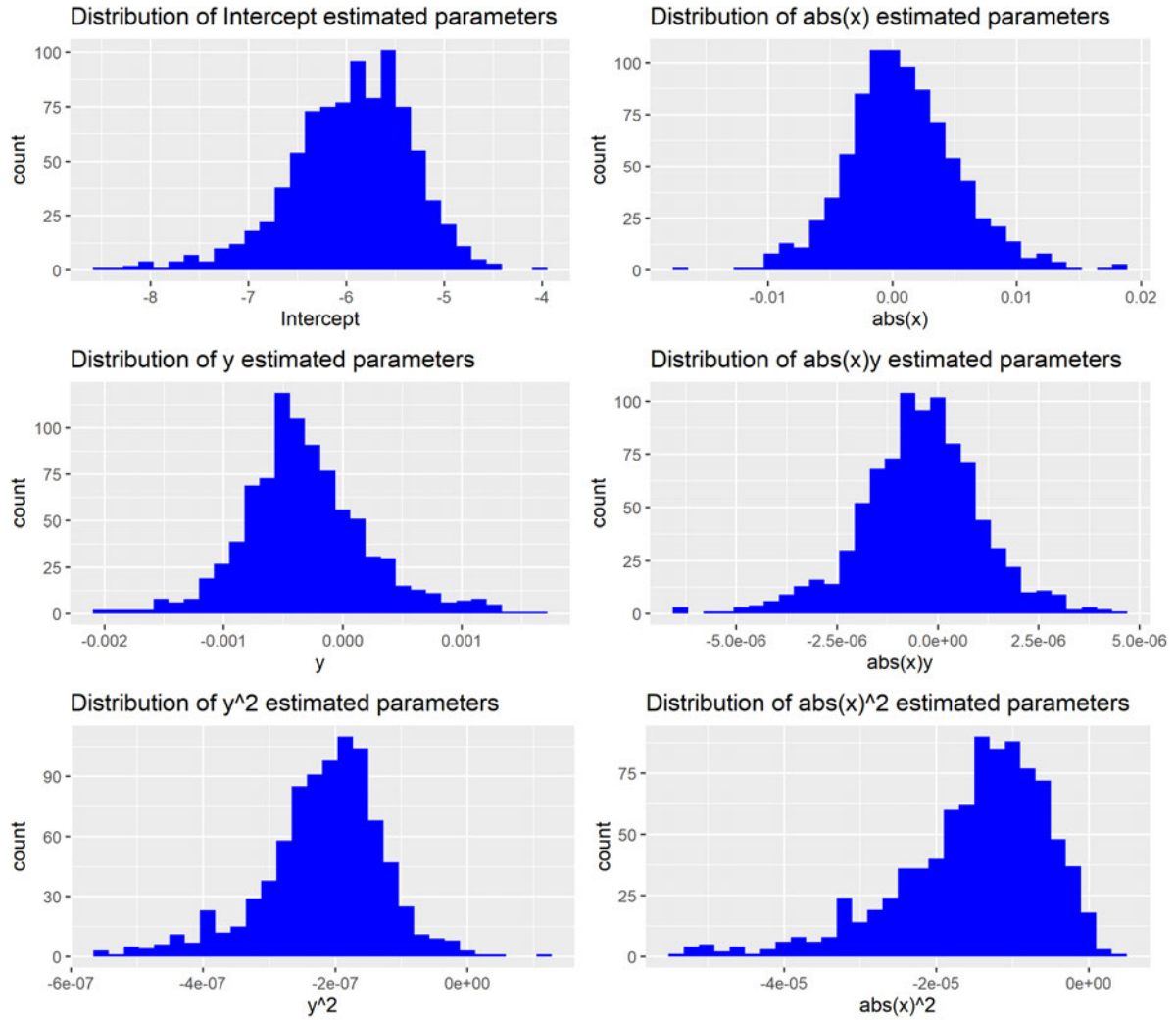
Figure 3.2: The distributions of each estimated parameter from the 923 point process models fitted to the plant root tip data. The *intercept*, *abs(x)*, *y* and *abs(x)y* estimated parameters resemble a normal distribution, while the $abs(x)^2$ and to a lesser extent y^2 parameters, display a left-skew.

evident in Figure 3.6 that the plant root system with the minimum *abs(x)y* parameter is reasonably uniform over both dimensions in complete contrast to the plant root system with the maximum *abs(x)y* parameter. In the maximum parameter plant root system, the intensity of the plant root tips change considerably over the width of the plant root system as the depth of the plant root system changes. The mean parameter plant root system exhibits some change over the width of the system as the depth changes but not to the extent of the maximum parameter plant root system. Figure 3.7 shows the minimum, mean and maximum parameter plant root systems for the $abs(x)^2$ estimated parameter. The $abs(x)^2$ estimated parameter describes the non-linear change in intensity of the plant root tips across the width of the plant root system. The minimum parameter plant root system in Figure 3.7 displays very little change

in intensity across the width of the plant root system while the maximum parameter plant root system does. Not only does it exhibit change across the x dimension, but this change is non-linear. The mean parameter plant root system also has this property to a lesser extent but in both plant root systems, the curvature indicates the need for this non-linear estimated parameter. Finally, Figure 3.8 displays the minimum, mean and maximum parameter plant root systems for the y^2 estimated parameter. The y^2 estimated parameter is essential for modelling the non-linear change in intensity of plant root tips over the depth of the plant root system. The minimum and maximum parameter plant root systems in Figure 3.8 both show a change in intensity of plant root tips over the depth of the system. Despite this, the maximum parameter plant root system exhibits a non-linear change, while the change in the minimum parameter plant root system has been captured in the y parameter.

Given the model fit to each plant root system has all six estimated parameters, they work together to provide an overall model fit which is appropriate. For example, this means that the plant root system with the greatest average intensity does not strictly have the largest *intercept* estimated parameter. The same can be said for the other estimated parameters. Despite this, the estimated parameters give a strong indication of the characteristics described which relate to each of the estimated parameters.
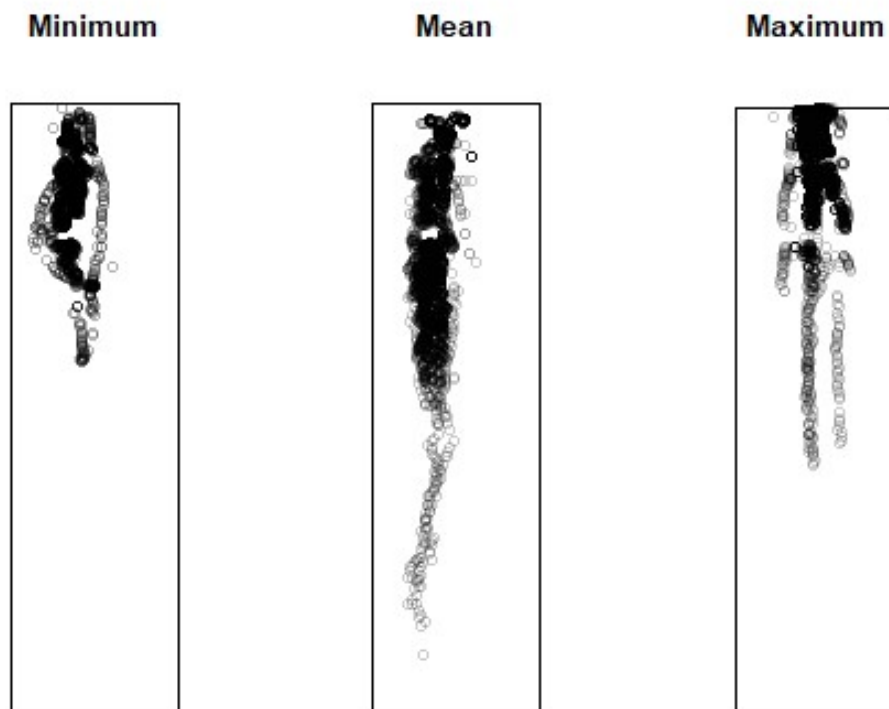
Figure 3.3: Three plots of the x, y root tip data points for the plant root systems with the minimum, mean and maximum estimated *intercept* parameter.
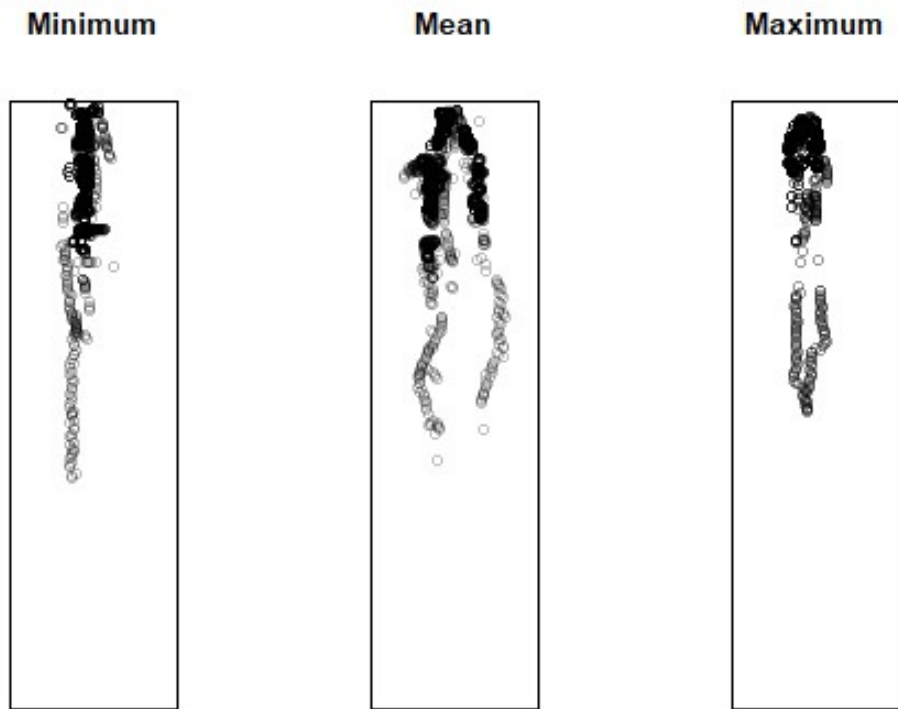
Figure 3.4: Three plots of the x, y root tip data points for the plant root systems with the minimum, mean and maximum estimated $abs(x)$ parameter.
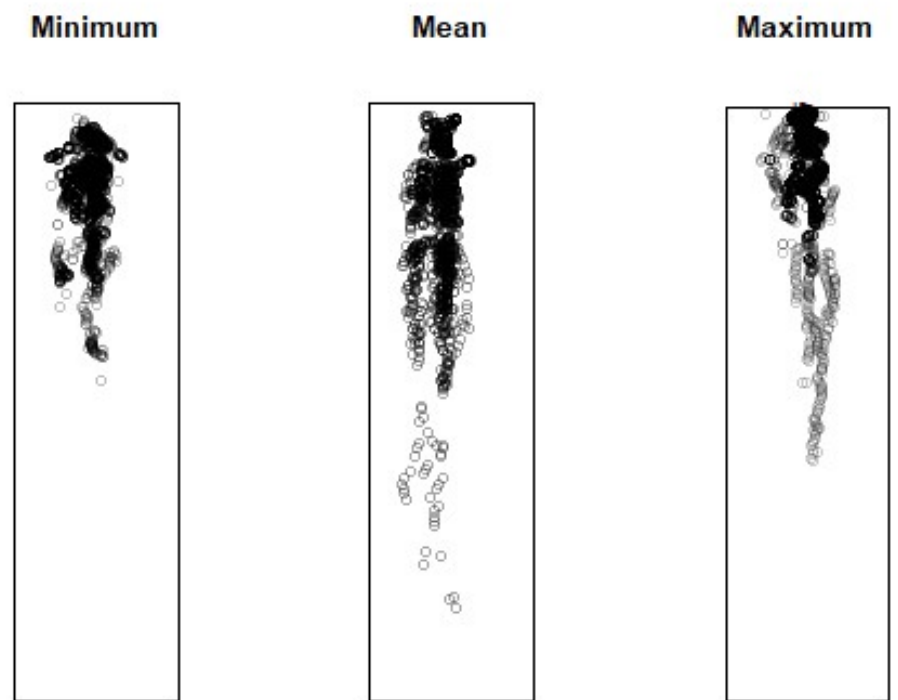
Figure 3.5: Three plots of the x, y root tip data points for the plant root systems with the minimum, mean and maximum estimated y parameter.
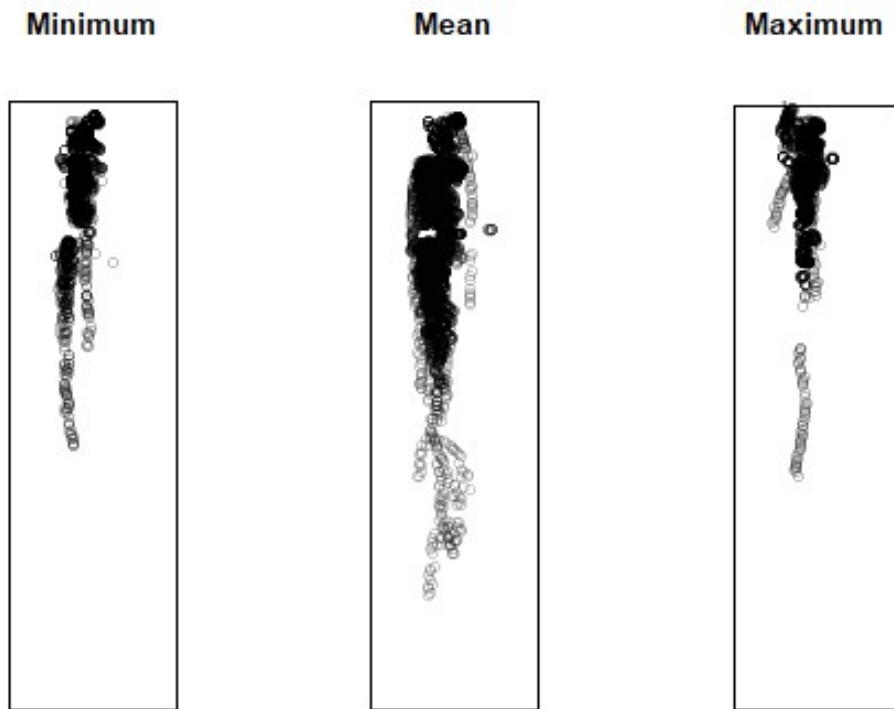
Figure 3.6: Three plots of the x, y root tip data points for the plant root systems with the minimum, mean and maximum estimated $abs(x)y$ parameter.
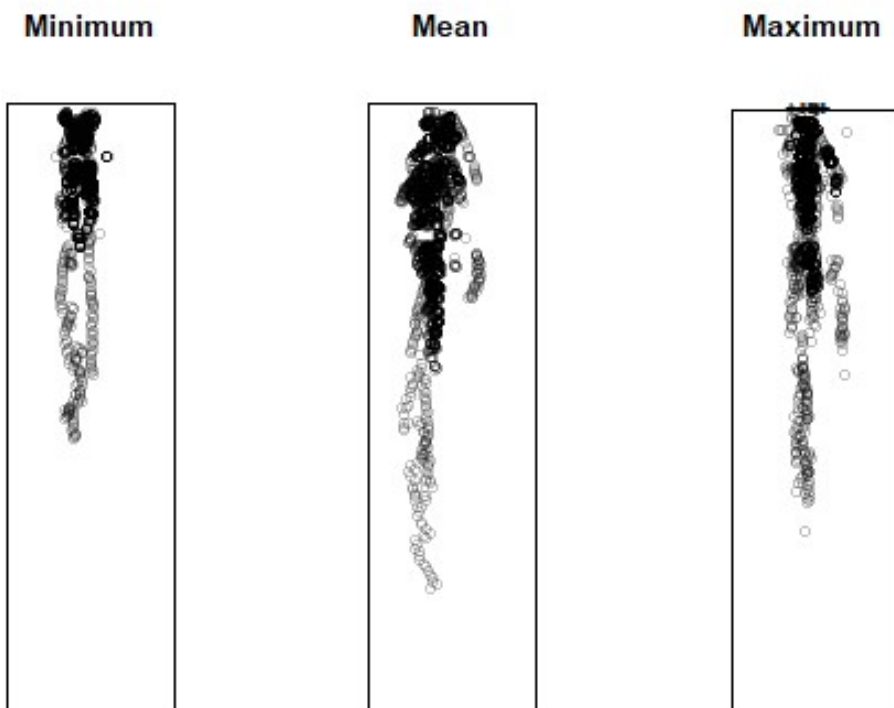
Figure 3.7: Three plots of the x, y root tip data points for the plant root systems with the minimum, mean and maximum estimated $abs(x)^2$ parameter.
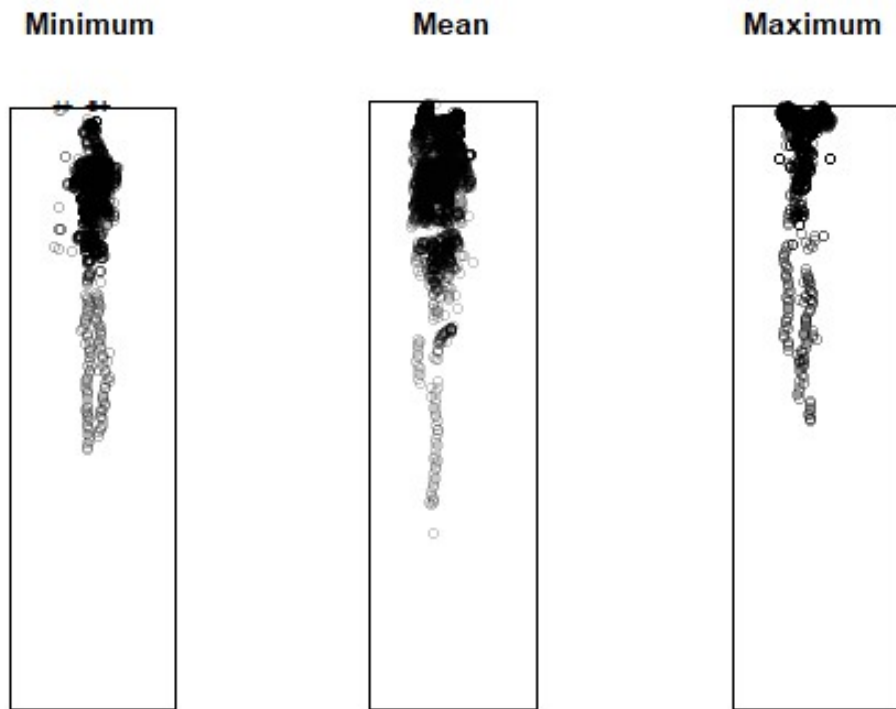
Figure 3.8: Three plots of the x, y root tip data points for the plant root systems with the minimum, mean and maximum estimated y^2 parameter.

3.2 Unweighted linear mixed models

3.2.1 Univariate unweighted linear mixed models

The second stage of analysis involves taking the estimated parameters from the 923 spatial point process models into a linear mixed model framework. Firstly, this was investigated in a univariate unweighted setting, where each estimated parameter was analysed in a separate linear mixed model. The difference between this and a spatial point process model is that all 923 plant root systems are included in one linear mixed model. The variance components for each term in the unweighted univariate linear mixed models are presented in Table 3.3.

Table 3.3 shows four different sources of variance from the experiment. The platform variance comes from the differences between the two aeroponic platforms in the experiment. The position component is only included where it was significant in the linear mixed model by way of a log-likelihood ratio test. If present, the position component relates to the differences between positions in the experimental layout. The genotype variance component captures the differences between genotypes in the experiment, while the residual variance component captures the differences between each experimental unit (each plant). Table 3.3 shows the $abs(x)y$ and $abs(x)^2$ estimated

52

Table 3.3: The variance components of each term in the unweighted univariate linear mixed model. The position term was only included where significant by way of a log-likelihood ratio test. The residual variance relates to each plant root system in the experiment. This experimental unit is identified as *ID* in the plant root tip dataset. The value of each variance component is the amount of variance in the estimated parameter which can be attributed to that factor. Note that B indicates this variance component is approaching the boundary of the parameter space and is constrained to be approximately equal to 0.

Variance Component	*Intercept*	*abs(x)*	*y*	*abs(x)y*	*abs(x)*^{2}	*y*^{2}
platform	0.0067	B	0.0095	0.0018	0.0343	B
position			0.0054			0.0103
genotype	0.0553	B	0.0157	0.0072	0.0002	0.1130
residual	0.3359	0.2037	0.2562	2.2836	0.9898	0.7192

parameters to have a large residual variance relative to their genetic variance. The genetic variance of the *y* estimated parameter is higher relative to its residual variance, while this ratio is higher again for the *Intercept* and *y*^{2} estimated parameters. The *abs(x)* parameter has gone to the boundary of the parameter space which indicates the genetic variance is constrained to be approximately 0. The platform variance components are minimal for all estimated parameters except *abs(x)*^{2}. The *abs(x)* and *y*^{2} platform variance components are boundary. Finally, the two estimated parameters which required a position variance component were the *y* and *y*^{2} estimated parameters. This indicates that the change in intensity of plant root tips over the depth of the plant root systems was affected in some way by it's position on the aeroponic platform.

For each of the unweighted univariate linear mixed models, the *predict* function in **ASReml-R** was used to predict the estimated parameters for each genotype. That is, six sets of predictions were calculated for the genotype effects, with one for each estimated parameter. The full sets of predictions can be found in Appendix B.1, however, a subset of genotype predictions are presented in Table 3.4. It is evident in Table 3.4 that the genotype predictions for the *abs(x)*, *abs(x)y* and *abs(x)*^{2} parameters have little variation and this is to be expected given the minimal genetic variance for these parameters (Table 3.3).

Table 3.4: The genotype predictions for each unweighted univariate linear mixed model, where each estimated parameter has its own model. A subset of 10 genotypes are presented here, and it is important to note that these predictions are on the transformed data scale with the exception of *Intercept* which did not require transforming.

Genotype	*Intercept*	*abs(x)*	*y*	*abs(x)y*	*abs(x)²*	*y²*
SUNTOP_RIL114_319	-6.212	0.086	-0.385	-0.432	-1.520	-2.642
SUNTOP_WYLIE_350	-6.193	0.086	-0.311	-0.435	-1.520	-2.187
SUNTOP_EGA GREGORY_130	-6.214	0.086	-0.289	-0.443	-1.520	-2.287
SUNTOP_DRYSDALE_54	-5.700	0.086	-0.310	-0.434	-1.519	-2.184
SUNTOP_SPITFIRE_52	-5.810	0.086	-0.336	-0.440	-1.519	-2.372
SUNTOP_EGA GREGORY_135	-6.004	0.086	-0.309	-0.427	-1.520	-2.037
SUNTOP_RIL114_336	-5.931	0.086	-0.314	-0.432	-1.519	-2.051
SPITFIRE-P9	-5.785	0.086	-0.172	-0.469	-1.520	-2.207
SUNTOP_SB062_239	-5.923	0.086	-0.219	-0.455	-1.520	-2.372
SUNTOP_SPITFIRE_48	-6.140	0.086	-0.367	-0.438	-1.519	-2.647

3.2.2 *Multivariate unweighted linear mixed models*

After fitting the six unweighted univariate models and producing genetic predictions, the fitting of an unweighted multivariate linear mixed model was conducted. In this analysis, each estimated parameter is treated as a trait such that trait is a factor with six levels. The response variable includes all estimated parameter values and as such, the multivariate model allows investigation of relationships between these parameters. This can be investigated in different manners depending on the residual and random variance structures implemented.

Firstly, the residual variance structure must be chosen with any genetic variances which are boundary removed from the model. This ensures the correct number of parameters are used in the model for traits which are actually contributing genetic variance. After fitting the multivariate model with an independent ('diag') residual variance structure, the *abs(x)* trait was removed due to its genetic variance being boundary. The genetic variance components of the model with an independent ('diag') residual structure are shown in the first row of Table 3.5. The dependent ('corgh') residual structure was then fit which initially resulted in two further traits having boundary terms for their genetic variance (second row of Table 3.5). After removing these two traits and fitting the same model, one further trait went boundary as seen in the third row of Table 3.5. As such, after settling on a dependent ('corgh') residual variance structure only two traits, the *Intercept* and y^2 estimated parameters, remained in the model.

Table 3.5: The genetic variance components for each trait in the unweighted multivariate model. The 'Residual' column reflects the residual variance structure fit while the 'Genetic' column reflects the genetic variance structure fit in the model. A 'B' corresponds to a boundary term which has approximately 0 variance. The following row will see these boundary terms removed until the final model is arrived at in the final row.

Residual	Genetic	*Intercept*	*abs(x)*	*y*	*abs(x)y*	*abs(x)²*	*y²*
diag	diag	0.0553	B	0.0002	0.0072	0.0157	0.1130
corgh	diag	0.0260		0.0129	B	B	0.0368
corgh	diag	0.0351		B			0.0873
corgh	corgh	0.0556					0.1217

The same structures were fit at the random level to model the genetic correlations between traits. Given only two traits remain in the model, the dependent ('corgh') structure is only fitting one correlation between traits. Table 3.6 uses the model selection tools of the log-likelihood ratio test and AIC to determine the final unweighted multivariate model. After removing the boundary genetic variance parameters as seen in Table 3.5, the independent ('diag') model is fit again with only the two remaining traits. This model is then compared to the dependent ('corgh') structure for both the residual and genetic variance structures. The dependent ('corgh') residual structure is a significant improvement on the independent ('diag') residual structure (Pr<0.001). It also shows a large reduction in the AIC. The dependent ('corgh') genetic variance structure is also shown to be a significant improvement on the independent ('diag') genetic variance structure with a probability of 0.01.

As such, the unweighted multivariate model was fit with the dependent ('corgh') residual variance structure and dependent ('corgh') genetic variance structure. This

Table 3.6: The model selection criteria used to determine the most appropriate residual and genetic variance structure for the unweighted multivariate model. A *P*-value is presented for each comparison of models. This *P*-value is generated from a log-likelihood ratio test which uses a chi-squared test. *Pr(>Chi)* is the *P*-value where a value less than 0.05 indicates a significant improvement and *AIC* represents the Akaike Information Criteria, where the minimum *AIC* is bolded.

Genetic structure	Residual structure	LogLik	Pr(>Chi)	AIC
diag	diag	-384.77		784
diag	corgh	-356.18	<0.001	728
corgh	corgh	-352.89	0.01	**724**

fits correlations between traits at both the residual and genetic levels in addition to variance components for the design, genotype and residual terms for each trait. Table 3.7 shows the variance components from the fitted model. Table 3.7 indicates that the ratio of genetic to residual variance for the y^2 parameter is similar to the *Intercept* parameter. The platform variance is minimal for the *Intercept* parameter and boundary for the y^2 parameter. The position variance component is only necessary for the y^2 parameter. The residual correlation between the estimated parameters are low from the fitted unweighted multivariate model at 0.21. Conversely, the genetic correlation between the two estimated parameters is moderately high at 0.65.

As was done for the unweighted univariate linear mixed models, the *predict* function in **ASReml-R** was used to predict the estimated parameters for each genotype from the unweighted multivariate linear mixed model. In this case, all predictions are provided in one set, given the nature of the multivariate model. The full set of predictions from the multivariate model can be viewed in Appendix B.3, however, Table 3.8 presents a subset of 10 genotypes. Variation is evident in these predictions for both the *Intercept* and y^2 parameters. A larger *Intercept* prediction indicates a higher average intensity of plant root tips for that genotype, while a higher y^2 prediction indicates a larger non-linear change in intensity over the depth of the plant root for that genotype.

Table 3.7: The variance components of each term in the final unweighted multivariate linear mixed model. The position term was only included where significant by way of a log-likelihood ratio test. The residual variance relates to each plant root system in the experiment. The experimental unit is identified as *ID* in the plant root tip dataset. The value of each variance component is the amount of variance in the estimated parameter which can be attributed to that factor. Any variance components with a 'B' indicate this term has gone boundary and is approximately 0.

Variance Component	*Intercept*	y^2
platform	0.0067	B
position		0.0063
genotype	0.0556	0.1217
residual	0.3354	0.7157

Table 3.8: The genotype predictions for the unweighted multivariate linear mixed model, where each estimated parameter is incorporated in one model. A subset of 10 genotypes are presented here, and it is important to note that these predictions are on the transformed data scale with the exception of *intercept* which did not require transforming.

Genotype	*Intercept*	y^2
SUNTOP_RIL114_319	-6.318	-2.783
SUNTOP_WYLIE_350	-6.195	-2.426
SUNTOP_EGA GREGORY_130	-6.215	-2.445
SUNTOP_DRYSDALE_54	-5.727	-2.054
SUNTOP_SPITFIRE_52	-5.874	-2.292
SUNTOP_EGA GREGORY_135	-5.953	-2.077
SUNTOP_RIL114_336	-5.899	-2.059
SPITFIRE-P9	-5.806	-2.134
SUNTOP_SB062_239	-5.976	-2.357
SUNTOP_SPITFIRE_48	-6.254	-2.742

3.3 Weighted linear mixed models

3.3.1 *Univariate weighted linear mixed models*

The second approach taken to stage two of the analysis involved the implementation of weights within the linear mixed model. As was the case for the unweighted models, the weighted models were investigated in both a univariate and multivariate sense. The weights were calculated as the inverse of the standard errors from the spatial point process models such that a plant root system with greater uncertainty is assigned a lower weight. Figure 3.9 shows the scatter plots of the weights against each transformed estimated parameter. The relationship between the estimated parameter and weight appears completely random for *Intercept*, $abs(x)$, y, $abs(x)y$ and y^2, however, for the $abs(x)^2$ parameter there is an inclination for the weights to be larger as the estimated parameter is larger. This indicates greater certainty around the larger parameter estimates as opposed to the smaller estimates.

Table 3.9 presents the variance components for each term in the weighted univariate linear mixed models. The ratio of genetic variance to residual variance is smallest for the $abs(x)$ and y parameters. This ratio is largest for the $abs(x)^2$ and y^2 parameters, indicating that there is higher genetic variance for these non-linear parameter estimates. The position term is once again necessary for the y and y^2 parameters and the platform variance component is greatest for *Intercept*. The remaining platform terms show minimal variance with $abs(x)^2$ being boundary.
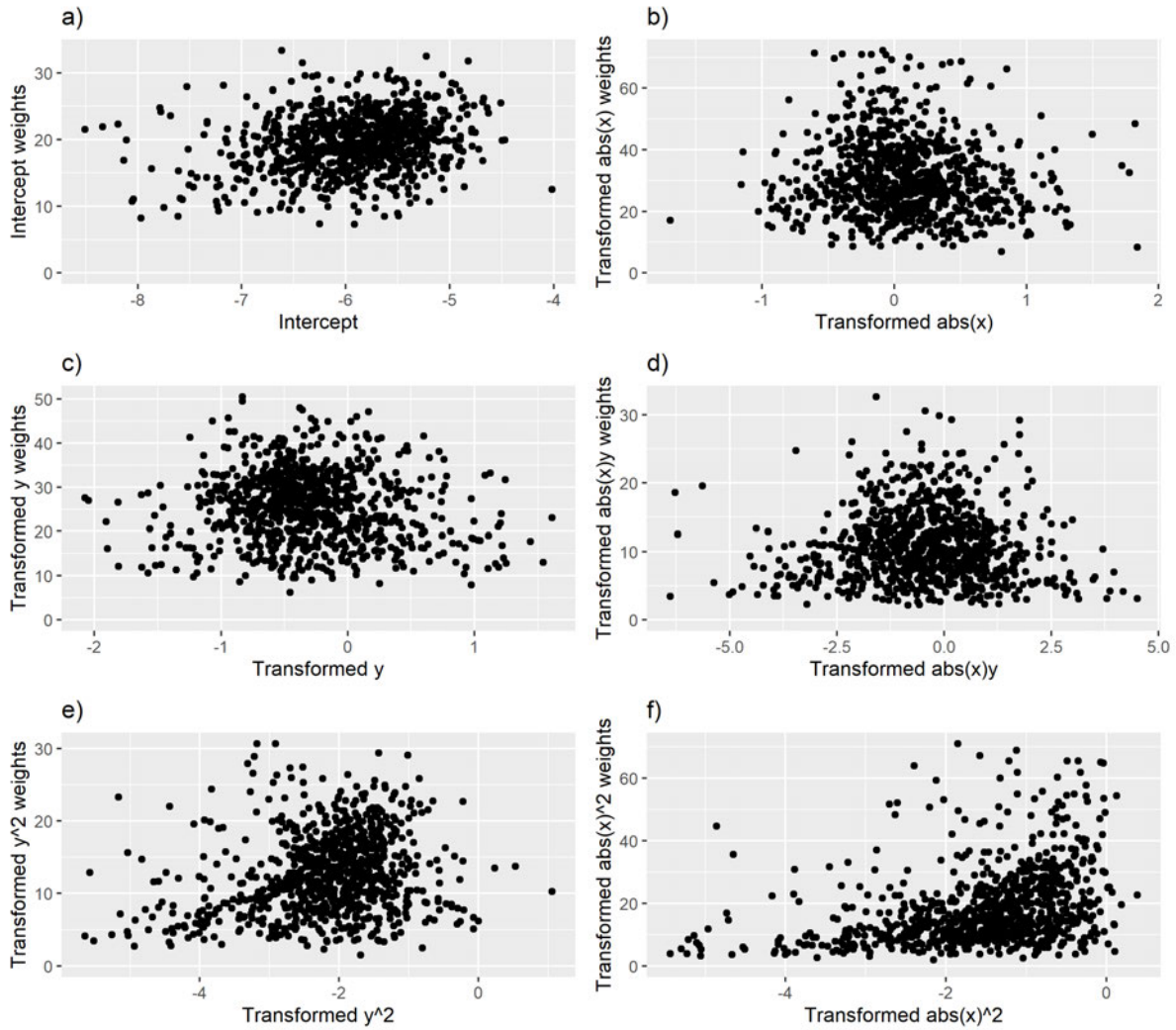
Figure 3.9: Scatter plots of each estimated parameter from the 923 point process models against their respective weights. The weights have been calculated as $1/se$ of each transformed estimated parameter where se is the standard error. The estimated parameters have been transformed so that they are all on a similar data scale. a) shows the *Intercept* parameter, b) shows the $abs(x)$ parameter, c) shows the y parameter, d) shows the $abs(x)y$ parameter, e) shows the y^2 parameter and f) shows the $abs(x)^2$ parameter.

The *predict* function in **ASReml-R** was used to predict the estimated parameters for each genotype. This was done for each of the weighted models to provide six sets of genotype predictions and these are presented in Table 3.10. These predictions consider the weights applied in the fitting of the model, and subsequently provide different predictions to those seen in Table 3.4. The subset of 10 genotypes show a range of predicted values for all estimated parameters in contrast to Table 3.4, which showed minimal genetic variation for the $abs(x)$, $abs(x)y$ and $abs(x)^2$ parameters. The full set of genotype predictions are provided in Appendix B.2.

Table 3.9: The variance components of each term in the weighted univariate linear mixed models. The position term was only included where significant by way of a log-likelihood ratio test. The residual variance relates to each plant root system in the experiment. This experimental unit is identified as *ID* in the plant root tip dataset. The value of each variance component is the amount of variance in the estimated parameter which can be attributed to that factor. Any terms denoted by 'B' indicate this term has gone boundary and is approximately 0.

Variance Component	*Intercept*	*abs(x)*	*y*	*abs(x)y*	*abs(x)^2*	*y^2*
platform	0.0144	0.0003	0.0072	0.0073	B	0.0070
position			0.0031			0.0073
genotype	0.0563	0.0105	0.0176	0.1355	0.1449	0.1340
residual	6.1578	5.4504	5.8360	19.2291	12.6142	7.1219

Table 3.10: The genotype predictions for the weighted univariate linear mixed models, where each estimated parameter has its own model. A subset of 10 genotypes are presented here, and it is important to note that these predictions are on the transformed data scale with the exception of *Intercept* which did not require transforming.

Genotype	*Intercept*	*abs(x)*	*y*	*abs(x)y*	*abs(x)^2*	*y^2*
SUNTOP_RIL114_319	-6.075	0.087	-0.361	-0.405	-1.381	-2.361
SUNTOP_WYLIE_350	-6.045	0.067	-0.321	-0.441	-1.365	-2.109
SUNTOP_EGA GREGORY_130	-6.151	0.134	-0.293	-0.618	-1.553	-2.259
SUNTOP_DRYSDALE_54	-5.640	-0.030	-0.318	-0.430	-0.952	-2.102
SUNTOP_SPITFIRE_52	-5.762	-0.017	-0.352	-0.580	-1.079	-2.338
SUNTOP_EGA GREGORY_135	-5.981	0.164	-0.318	-0.185	-2.529	-1.951
SUNTOP_RIL114_336	-5.910	0.024	-0.328	-0.389	-0.831	-1.930
SPITFIRE-P9	-5.773	0.087	-0.137	-1.190	-1.522	-2.094
SUNTOP_SB062_239	-5.894	0.126	-0.176	-1.090	-1.946	-2.622
SUNTOP_SPITFIRE_48	-6.036	0.064	-0.348	-0.465	-1.295	-2.321

3.3.2 *Multivariate weighted linear mixed models*

The final phase of the analysis was to conduct the fitting of the weighted multivariate linear mixed model. This model incorporates the weights while also analysing all estimated parameters in one model. That is, all estimated parameter values are included in one response variable, with a 'trait' factor distinguishing which value belongs to which estimated parameter. As was the case for the unweighted multivariate model, an appropriate residual and genetic variance structure must be determined. Any genetic variances which are boundary must be removed from the model. The independent ('diag') residual variance structure did not show any boundary genetic variances as seen in the first row of Table 3.11. When moving to a dependent ('corgh') residual variance structure the *abs(x)*, *abs(x)y* and *y* estimated parameters all show boundary

Table 3.11: The genetic variance components for each trait in the weighted multivariate model. The 'Residual' column reflects the residual variance structure fit while the 'Genetic' column reflects the genetic variance structure fit in the model. A 'B' corresponds to a boundary term which has approximately 0 variance. The following row will see these boundary terms removed until the final model is arrived at in the final row.

Residual	Genetic	*Intercept*	*abs(x)*	*y*	*abs(x)y*	*abs(x)²*	*y²*
diag	diag	0.0718	0.0191	0.1710	0.1981	0.0255	0.1636
corgh	diag	0.0132	B	B	B	0.0704	0.0639
corgh	corgh	0.0751				0.1789	0.1729

genetic variances and as such, were removed from the model. The dependent ('corgh') structure was then also fit at the random level to model genetic correlations and this provides the final weighted multivariate model. The genetic variance components for this model are shown in the final row of Table 3.11.

Table 3.12 shows the results of the model selection process to select the most appropriate residual and genetic variance structures for the weighted multivariate model. After removing the boundary genetic variance parameters from Table 3.11, the independent ('diag') model is fit again with the three remaining traits. This model is then compared to the dependent ('corgh') structure for both the residual and genetic variance structures. The dependent ('corgh') residual structure is a significant improvement on the independent ('diag') residual structure (Pr<0.001). It also shows a large reduction in the AIC. The dependent ('corgh') genetic variance structure is shown to be a significant improvement on the independent ('diag') genetic variance structure with a probability of 0.002.

Table 3.12: The model selection criteria used to determine the most appropriate residual and genetic variance structure for the weighted multivariate model. A *P*-value is presented for each comparison of models. This *P*-value is generated from a log-likelihood ratio test which uses a chi-squared test. *Pr(>Chi)* is the *P*-value where a value less than 0.05 indicates a significant improvement and *AIC* represents the Akaike Information Criteria, where the minimum *AIC* is bolded.

Genetic structure	Residual structure	LogLik	Pr(>Chi)	AIC
diag	diag	-901.30		1823
diag	corgh	-851.82	<0.001	1730
corgh	corgh	-844.16	0.002	**1720**

Based on this model selection criteria, the dependent ('corgh') variance structure was once again selected to model both the residual and genetic variance structures. The variance components for the final weighted multivariate model are presented in Table 3.13. The y^2 parameter has the largest genetic variance relative to its residual variance, with this ratio being similar for the $abs(x)^2$ and *Intercept* parameters. The platform and position variance components for y^2 are small relative to the other variance components while the platform variance component for $abs(x)^2$ is boundary. Table 3.14 illustrates the residual correlations between parameters for the weighted multivariate model. All residual correlations are low with the strongest correlation being between *Intercept* and y^2 (0.15). Table 3.15 shows moderately high genetic correlations between the *Intercept* and $abs(x)^2$ parameters (0.63) and the *Intercept* and y^2 parameters (0.70). The genetic correlation between y^2 and $abs(x)^2$ is much lower at 0.14.

Finally, genotype predictions were produced from the weighted multivariate model. These predictions are produced as one set given the nature of the multivariate model. The full set of weighted multivariate predictions can be found in Appendix B.4, however, Table 3.16 presents a subset of 10 genotypes. Variation in the genotype predictions are evident for all three parameters. A larger *Intercept* prediction indicates a greater average intensity of plant root tips for that genotype, a larger $abs(x)^2$ prediction indicates a greater non-linear change in intensity across the width of the plant roots and a larger y^2 prediction indicates a greater non-linear change in intensity over the depth of the plant roots.

After conducting both the unweighted and weighted linear mixed model analyses, the results can be compared. Figure 3.10 shows the weighted and unweighted BLUPs plotted against each other for each estimated parameter from the univariate analyses.

Table 3.13: The variance components of each term in the final weighted multivariate linear mixed model. The position term was only included where significant by way of a log-likelihood ratio test. The residual variance relates to each plant root system in the experiment. This experimental unit is identified as *ID* in the plant root tip dataset. The value of each variance component is the amount of variance in the estimated parameter which can be attributed to that factor. A 'B' indicates any variance components which are boundary meaning approximately 0.

Variance Component	*Intercept*	$abs(x)^2$	y^2
platform	0.0152	B	0.0076
position			0.0032
genotype	0.0751	0.1789	0.1729
residual	5.5189	11.4816	6.2542

Table 3.14: The residual correlations between the three estimated parameters in the weighted multivariate linear mixed model.

	Intercept	$abs(x)^2$	y^2
Intercept	1		
$abs(x)^2$	0.06	1	
y^2	0.15	0.002	1

Table 3.15: The genetic correlations between the three estimated parameters in the weighted multivariate linear mixed model.

	Intercept	$abs(x)^2$	y^2
Intercept	1		
$abs(x)^2$	0.63	1	
y^2	0.70	0.14	1

Table 3.16: The genotype predictions for the weighted multivariate linear mixed model, where all estimated parameters are analysed in a single model. A subset of 10 genotypes are presented here, and it is important to note that these predictions are on the transformed data scale with the exception of *Intercept* which did not require transforming.

Genotype	Intercept	$abs(x)^2$	y^2
SUNTOP_RIL114_319	-6.243	-1.571	-2.610
SUNTOP_WYLIE_350	-6.108	-1.530	-2.308
SUNTOP_EGA GREGORY_130	-6.317	-1.818	-2.509
SUNTOP_DRYSDALE_54	-5.515	-0.680	-1.884
SUNTOP_SPITFIRE_52	-5.777	-0.946	-2.263
SUNTOP_EGA GREGORY_135	-6.374	-2.743	-2.031
SUNTOP_RIL114_336	-5.684	-0.794	-1.920
SPITFIRE-P9	-5.819	-1.398	-1.989
SUNTOP_SB062_239	-6.299	-1.969	-2.690
SUNTOP_SPITFIRE_48	-6.137	-1.418	-2.508

The shrinkage of the unweighted BLUPs for the $abs(x)$, $abs(x)y$ and $abs(x)^2$ estimated parameters is evident in sub-figures b), d) and f) of Figure 3.10. The minimal change in these BLUPs reflect the small, or boundary, genetic variance components for these parameters. The weighted BLUPs show more variance for the univariate analyses, most noticeably for the $abs(x)$, $abs(x)y$ and $abs(x)^2$ estimated parameters.

The results of the weighted and unweighted multivariate analyses can be compared for the traits in common between the final two models. As such, Figure 3.11 shows two plots, the weighted BLUPs against the unweighted BLUPs for the *Intercept* and y^2 estimated parameters. The *Intercept* parameter shows a lower correlation between the weighted and unweighted BLUPs than the y^2 parameter, although both are still highly correlated. For both parameters, there is greater disparity between the weighted and unweighted BLUPs for lower parameter estimates. As the parameter estimates increase, the two sets of BLUPs come closer together.
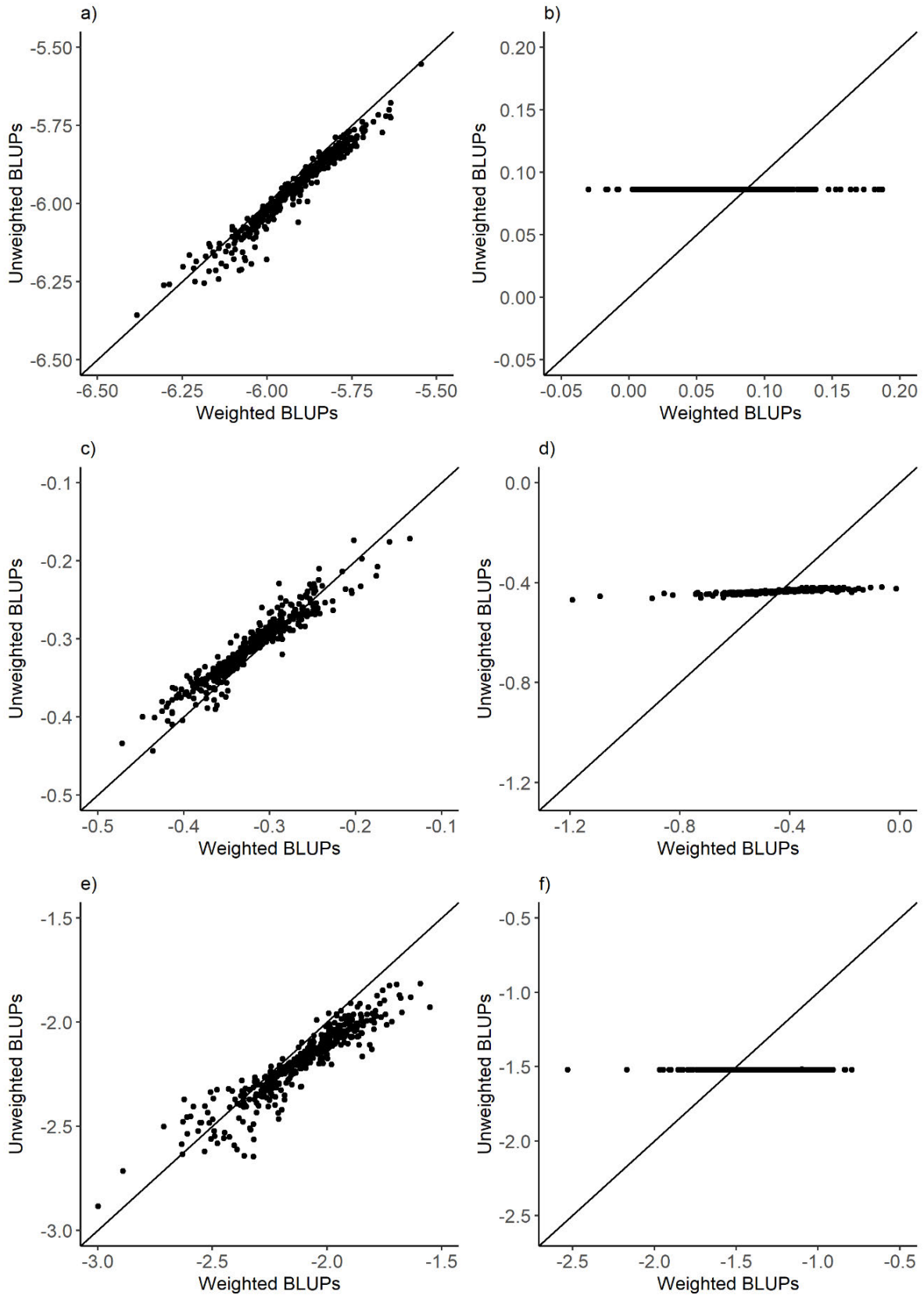
Figure 3.10: Plots of the weighted vs unweighted Best Linear Unbiased Predictors (BLUPs) of the genetic effects for all estimated parameters from the univariate linear mixed models analyses. a) shows the *Intercept* parameter, b) shows the *abs(x)* parameter, c) shows the y parameter, d) shows the *abs(x)y* parameter, e) shows the y^2 parameter and f) shows the *abs(x)²* parameter.
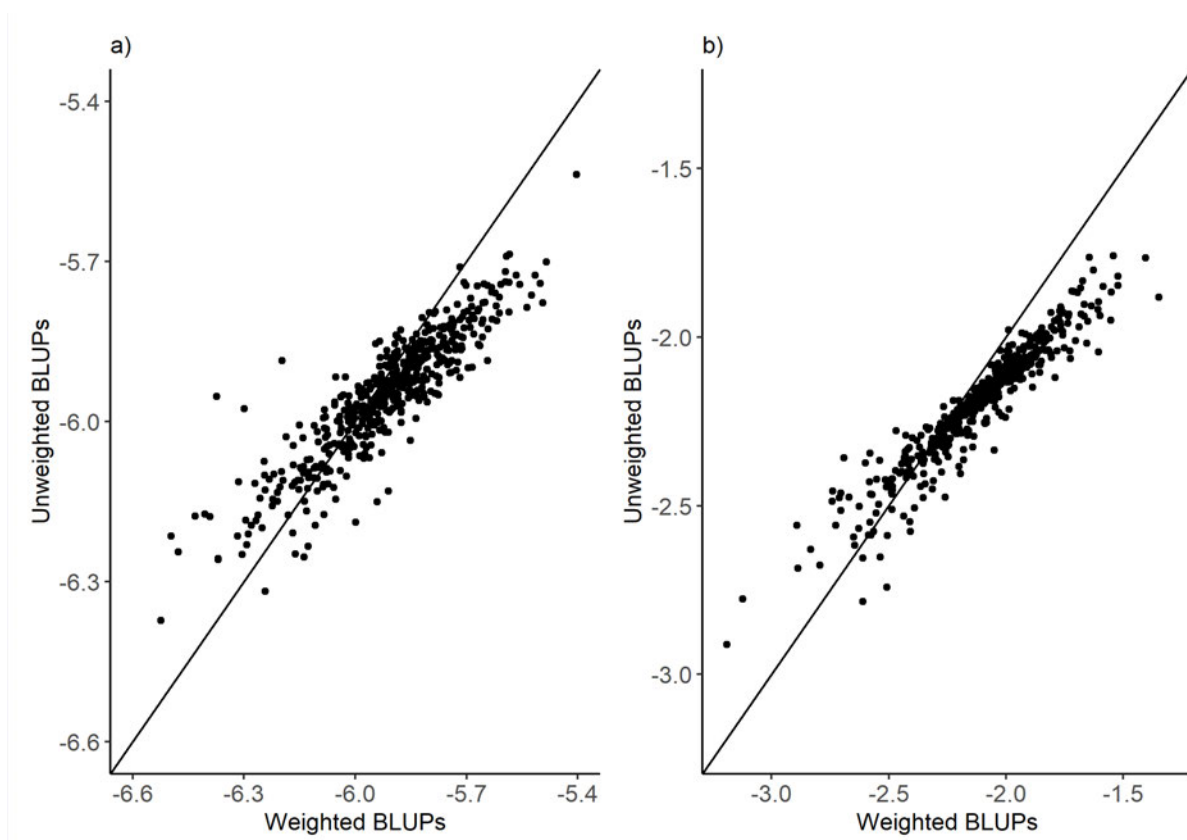
Figure 3.11: Plots of the weighted vs unweighted Best Linear Unbiased Predictors (BLUPs) of the genetic effects for the two estimated parameters in common from the multivariate linear mixed models analyses. a) shows the *Intercept* parameter while b) shows the y^2 parameter.

CHAPTER 4

Discussion and Conclusions

The analysis of point pattern data is conducted using the methodology of spatial point processes. This methodology allows for statistical models to be fit which describe the spatial point patterns in the data set. In the case of the plant root tip data, this means that the spatial locations of plant root tips are modelled in an attempt to describe plant root architecture. When applying spatial point processes to large, replicated experiments often the analysis is computationally difficult and limited by the large number of individual spatial point patterns that need to be modelled simultaneously. In comparative experiments, the primary research aim is generally to detect differences between genotypes. The computational difficulties in the fitting of spatial point processes for large, replicated experiments compromise their ability to compare genotypes. As such, it is necessary to investigate the use of other methodology to ensure the research aims of the experiment are met. This led to the realisation of a two-stage method using linear mixed models.

The linear mixed model's ability to model replicated experimental data including design parameters, allow the aims of this comparative experiment to be met. This is achieved through including all experimental information, such as platform, strip, position and genotype in one model, as opposed to multiple spatial point processes. Further to this, the modelling of genetic and residual correlations between traits is an additional strength of the linear mixed model. The primary aim of this study is to determine whether differences are evident in the results of the two-stage method when a weighted method is applied as opposed to an unweighted method. This has been investigated in both a univariate and multivariate setting where the difference in results are compared. There is limited research linking the two methodologies of spatial point processes and linear mixed models. Therefore, the findings from this study will show the capabilities of such an analysis, and seek to determine an appropriate analysis approach moving forward.

4.1 Point process models

The spatial point processes fit to the plant root tip data compared three different models. The linear, second order harmonic and second order polynomial models were all tested in an attempt to most effectively account for the change in intensity of plant root tips throughout the spatial window. The second order polynomial model most effectively accounts for the change in intensity of plant root tips for the plant root systems. It was found that the linear model was not appropriate given the non-linear change in intensity of plant root tips across both the width and depth of the plant root systems. Fitting a linear model assumes that the intensity of plant root tips changes at a constant rate across both dimensions. The description of plant root architecture provided by Hodge et al. (2009) indicates that non-linearity in plant root systems is expected, and this is created by the far denser base of the plant roots as opposed to the peripheries of the system which exhibit far fewer plant root tips (Hodge et al., 2009). The second order harmonic model accounts for non-linearity through an interaction term (x^2 - y^2), however, it does not fit a parameter for each of these terms individually. In this study, the individual x^2 and y^2 parameters have shown to be critical in modelling the inhomogeneous intensity of plant root systems. Due to the non-linearity of plant root systems (Hodge et al., 2009), the modelling of plant root tips using x^2 and y^2 spatial covariates is critical. In summary, the results of the spatial point processes strongly indicate that there is significant non-linearity in the intensity of plant root tips, and furthermore, the modelling of spatial covariates in both dimensions (x and y) is key to capturing the change in intensity of plant root systems.

4.2 Two-stage method

Two-stage analyses can be applied in many contexts including those described by Möhring and Piepho (2009), Welham et al. (2010), Damesa et al. (2017) and Gogel et al. (2018). Regardless of the situation, the estimates from stage one are treated as true values in stage two (Kackar and Harville, 1981). The application of this methodology is not new, however, the linking of spatial point processes and linear mixed models is. In many contexts, the implementation of a weighted method is beneficial in two-stage analyses (Möhring and Piepho, 2009). Weighting ensures that the uncertainty in stage one of the analysis is respected in stage two and depending on the characteristics of the data this can be vital. As such, the primary investigation in this study was determining the difference between weighted and unweighted methods in the context of plant root tip data. The results of this study show differences between the weighted and unweighted two-stage methods and the reasoning behind this will be explained.

The spatial point process analysis (stage one) provided a useful insight into what was occurring in each plant root system, but this stage of the analysis was limited to evaluation of each plant individually. While spatial point processes have the ability to include multiple point patterns in one model, for large replicated experiments, such as the plant root tip data set, this is computationally difficult. In this study, computation was an issue and the reason for a separate spatial point process being fit to each plant root system. Additionally, the spatial point process model for replicated experiments is limited in the types of treatment and design terms that can be included in the model. For this reason, the ability to model genetic relationships within the experiment was restricted. The combination of these factors led to the implementation of a two-stage method, with the second stage using the linear mixed model framework.

In this study, the implementation of a two-stage method greatly expanded the conclusions which could be drawn from the analysis. In the univariate analyses, the linear mixed model allowed for all plant systems in the experiment to be included in one model, as well as effectively including design parameters (Butler et al., 2018). This provides a more complete analysis of the plant root tip data than the spatial point processes do alone. This is achieved through the estimation of variance components as evident in the results which allows predictions to be calculated for all genotypes in the experiment from one model. In the univariate analyses, this is done for each estimated parameter from the spatial point processes. The benefits of the two-stage method are increased when the multivariate model is implemented through the ability of the linear mixed model to model correlations between traits at both the residual and genetic levels. This allowed both the residual and genetic correlations between the estimated parameters from the spatial point processes to be calculated for both the weighted and unweighted multivariate models. As such, the implementation of a two-stage method using linear mixed models was particularly advantageous for the multivariate analyses, where residual and genetic correlations between the estimated parameters were investigated. Although correlations between estimated parameters do not apply in the univariate analyses, the two-stage method is still advantageous in its ability to incorporate point processes from all plant root systems in the experiment into one model.

4.3   Linear mixed models

In this study, four types of linear mixed model were fit. These were the univariate unweighted, multivariate unweighted, univariate weighted and multivariate weighted models. The results generated from each of these models showed differences in the estimation of variance components in stage two of the analysis.

There was minimal genetic variation for some spatial parameters, and these were mostly those associated with the x-dimension of the data, namely the $abs(x)$, $abs(x)y$ and $abs(x)^2$ parameters. This result shows that there was little discrimination in plant root width between the genotypes. The results from the unweighted univariate models are contrasted with those from the weighted univariate models, estimating genetic variation for all spatial parameters. The weights are accounting for uncertainty in this x dimension which subsequently results in genetic variance increasing in these weighted models. In this data set, the three-dimensional object of the plant root system is transposed into two dimensions. The absolute value of x was implemented in the model fitting process to force symmetry in this dimension about the point $x = 0$. The implementation of weighting has improved the results of the univariate analyses in detecting genetic variances which could not be estimated in the unweighted models. This is especially true for the $abs(x)$, $abs(x)y$ and $abs(x)^2$ parameters. The remaining three parameters show less shrinkage in the unweighted BLUPs relative to weighted BLUPs, indicating that weights are not as important in the y dimension. Damesa et al. (2017) state that weighting is vital when heterogeneity is present in the data. For the plant root data, the use of weights is key in accounting for both the uncertainty and heterogeneity in the x dimension.

The next component of the study was the fitting of weighted and unweighted multivariate linear mixed models. The implementation of the dependent variance structure at both the residual and genetic levels is essential to model correlations between traits (Butler et al., 2018). The dependent variance structure as specified in **ASReml-R** is fully unstructured in that it does not impose any restrictions. That is, all variances and covariances between traits can be modelled. Through the iterative process of implementing the variance structures tested (Table 3.5), a number of genetic variances are estimated to be boundary, that is, have approximately 0 variance. This indicates that when all estimated parameters are fit in one multivariate model, and the residual covariance between the parameters is modelled, there is no additional genetic information. The results highlight the importance of respecting the residual variance induced in the experiment. Two key estimated parameters emerge as characterising the genetic variation in the plant root tip data for the unweighted multivariate model. These parameters are *Intercept* and y^2. In practice, this means that the experiment detected changes in spatial intensity of roots near the surface and in plant root depth. This result is consistent with that seen for the univariate models. For the weighted analysis, the $abs(x)^2$ estimated parameter remains in the final weighted multivariate model along with *Intercept* and y^2. It is evident for the $abs(x)^2$ parameter that estimates closer to 0 are weighted higher, reflecting the greater confidence in these estimates. This changes the manner in which this parameter is treated in the multivariate model and the outcome

is that genetic variance can be estimated when weighting the spatial parameters. As such, the weights once again account for the uncertainty in the x dimension as was the case in the univariate analyses, and this ensures the non-linearity evident across the width of the plant root system is respected. Plant root architecture is known to vary across the width of a plant root system (Hodge et al., 2009), demonstrating the importance of using weights for this plant root tip data set. Without the use of weights, the $abs(x)^2$ parameter would not be present in the final multivariate model causing a key aspect of plant root architecture to be overlooked.

The model selection process for both the weighted and unweighted multivariate models showed the dependent variance structure to be necessary at the residual and genetic levels. Tables 3.6 and 3.12 show the log-likelihood ratio tests and AIC values for the multivariate models fit in the model fitting process. The independent ('diag') variance structure does not model any correlations between traits, therefore it is not surprising that the dependent structure shows significant improvement. Given investigating genetic relationships was a key research aim of the experiment, the fitting of the dependent variance structure at both the residual and genetic levels was ideal. This allowed correlations between the estimated parameters to be calculated which were found to be 0.21 at the residual level and 0.65 at the genetic level for the unweighted multivariate model. Both the weighted and unweighted models exhibit low residual correlations between all traits which is to be expected given the inherent variation in plant root architecture (Hodge et al., 2009). That is to say, just because a plant root system has a large change in intensity for the non-linear root depth parameter does not mean it will have a large change in intensity for the non-linear root width parameter. Nonetheless, it is important to respect this residual relationship between traits in the fitted model before investigating genetic correlations. Given only two estimated parameters were present in the final unweighted multivariate model, only one genetic correlation was fit. The correlation between surface intensity and non-linear root depth of 0.65 is similar to the correlation between these two parameters for the weighted model (0.70). The correlation between surface intensity and non-linear root width is also moderately strong at 0.63, however, the correlation of 0.14 between non-linear root depth and non-linear root width is low. This suggests that genotypes with a large non-linear root depth parameter estimate often have a low non-linear root width parameter estimate. Given the *Intercept* parameter estimates the average log-intensity of the plant root tips, it is expected that this parameter is moderately to strongly positively correlated to the y^2 and $abs(x)^2$ parameters. That is, if the non-linear root depth or non-linear root width parameter is large, the average log-intensity will also be somewhat similar.

The BLUPs for the weighted and unweighted methods are generally well correlated. This is true for the non-linear root depth parameter, however, more spread is evident between the BLUPs for the surface intensity. This relates to the inclusion of the $abs(x)^2$ parameter in the weighted multivariate model. The inclusion of this parameter influences the impact of the *Intercept* parameter given it represents the average log-intensity. There are some particularly notable points in Figure 3.11 which are distanced from the main grouping. The three clearest points in sub Figure a) have an unweighted BLUP of approximately -5.9 but a weighted BLUP of approximately -6.3. This indicates a large amount of uncertainty in the *Intercept* estimated parameter for these points, resulting in the weights having a large influence on the prediction of BLUPs. The weights are therefore important in accounting for the uncertainty in these particular estimates which are distanced from the main grouping.

Both the univariate and multivariate analyses have shown the weighted method to account for the uncertainty in the plant root width dimension of the root tip data more effectively than the unweighted models. The multivariate analysis has demonstrated that the modelling of plant root tip data can be characterised by a handful of key parameters.

4.4   Limitations of the data

The plant root tip data set consists of 923 plant root systems across two aeroponic platforms. The primary limitation of the data set is the minimal replication of genotypes within the experiment. When it comes to the modelling phase, conclusions regarding genotypes and their plant root architecture could be made with greater confidence if replication was increased. Given the average replication value of 1.90, some genotypes are only present once, and this makes it difficult to determine the accuracy of these plant root tip data points. Further to this, the low heritability of most plant root traits means that increased replication is highly beneficial. The trade-off to increasing replication for such a large genotype trial comes with experimental resources and computational power when it comes to analysis. Nonetheless, increased replication of genotypes would lead to a more comprehensive analysis of plant root architecture in this case.

Another key limitation of the plant root tip data set is the reduction in dimensionality. The transposing of three-dimensional plant root systems into two dimensions limits the conclusions which can be made regarding certain aspects of the plant. It is possible that some important aspects of plant root architecture have been overlooked due to this. The spatial point process methodology used in this study could handle

three-dimensional data through the incorporation of a *z* covariate for the third dimension. Currently, the barrier to this lies in the practicalities of collecting the data. The method of collecting the images as described by Draye et al. (2018) would need to be modified to capture the appropriate three-dimensional data. If this technology can be employed, it would improve the overall analysis conducted in studies such as this.

Finally, the outliers detected in this study have raised the issue of poor plant growth in this experiment. Appendix A.1 displays the plant root tip data plots of 37 plant root systems which were removed from the analysis due to lack of growth. Of these 37 plant root systems, 35 were located on platform one of the experiment. This indicates an issue relating to this aeroponic platform which prevented adequate growth. Research into why this may have occurred and how to prevent it in the future is important to similar experiments moving forward. Appendix A.2 shows the plant root systems which were detected as outliers by way of the alternate outlier method for the various estimated parameters. It is evident in a number of these plots that an issue has occurred in the development of the point pattern. This is seen in the form of centering issues and the occurrence of random or spasmodic points throughout the spatial window. As such, improvement in the data generating process is critical to future experiments. Despite these limitations in the plant root tip data set, the conclusions drawn from this study remain informative and beneficial.

4.5   Practical outcomes

The inherent variation in plant root architecture is evident in the plant root tip data set. Given all genotypes in the data set were the wheat crop type, the findings of this study support the claims of Cannon (1949), Kutschera (1960) and Weaver and Bruner (1926) that plant root architecture varies significantly, even within species. This is evident in the range of estimated parameters fit in the spatial point process models, which indicate the different characteristics of genotypes within the wheat species. The difficulty in phenotyping plant root systems has been a major hurdle to accurate analyses of plant root traits. The use of aeroponic high-throughput phenotyping platforms is key to the production of accurate data in this study. The non-destructive manner in which cameras can access the plant root systems ensures the experimental material is not compromised while allowing for quality data to be collected. This study has highlighted the use of aeroponic high-throughput phenotyping platforms as an ideal source of plant root system data for high level statistical analysis..

A number of outliers were identified in the conduct of this study. Nine hundred and ninety plant root systems were present in the initial experimental design, with 67 of these initially removed due to the plant root systems not growing appropriately. On

inspection of the plant root tip data set, a further 37 plant root systems were identified as not growing in a healthy way and these plants were removed from the dataset. There are two likely causes of lack of growth in this experiment, namely poor seed germination and difficulty growing on an aeroponic platform. The plant root tip data plots of these outliers, along with those removed using the alternate outlier method are shown in appendices A.1 and A.2. It is apparent when examining these plots, that some plant root systems have been detected as outliers through the inability of the data generating process to accurately capture the plant root architecture. That is, the detection and positioning of some plant root tips appear to be inaccurate. There may be several factors involved with this inaccuracy including the cameras themselves, the transposing of three-dimensional objects into two dimensions and the machine learning techniques used to develop the images into plant root tip data. Given the variability intrinsic to plant root architecture, inducing further variability through the data generating process is going to impact on the accuracy of analyses such as this. This plant root tip study has highlighted this issue and illustrated that continued improvement in the accuracy of data generation is necessary for the evolution of spatial point pattern analyses.

The inherent variation within the wheat genotypes in the plant root tip data is reflected through the high error variance compared to genetic variance in the results. The residual variance is much greater than the genetic variance for all estimated parameters, in both the univariate and multivariate models. The size of the error variances in this study demonstrate the importance of collecting data which is as accurate as possible to ensure valid conclusions can be drawn from analysis. Further to this, increasing replication of genotypes would aid in reducing error variance through enhancing the information collected for each genotype. As stated by Hodge et al. (2009), the variation in plant root architecture is unavoidable and as such, planning experiments in a manner which will allow this variation to be captured is vital to accuracy.

4.6 Theoretical outcomes

The linking of spatial point processes and linear mixed models using a two-stage approach has proven to be a viable method for the analysis of plant root tip data. The **spatstat** R-package is purpose designed for the analysis of spatial point patterns, however, there are limitations to this (Baddeley and Turner, 2004). The fitting of spatial point processes in this study brought the issue of computational power to the fore illustrating the difficulty **spatstat** has in modelling spatial point patterns for large, replicated experiments. This, coupled with the ability of linear mixed models to include both design parameters as well as complex covariance structures in the model,

led to the implementation of a two-stage method. Often, the fitting of two-stage methods is not ideal, however, in the case of the plant root tip data this methodology enhances the analysis. This is achieved through the linear mixed model's ability to include all experimental information in one fitted model as well as model correlations between traits. Including all experimental information in a single model increases the accuracy of the analysis by borrowing strength through correlated data, and therefore strengthens the conclusions which can be made in a comparative experiment.

Once determining that the two-stage method applied was feasible, the weighted and unweighted models were compared. This study found differences in the results of the weighted and unweighted models, particularly in terms of the influence weighting had on the plant root width dimension. Respecting the uncertainty in an analysis is key to producing valid results. Due to the high residual variation in plant root architecture, accounting for uncertainty is especially important to provide informative results. As such, the weighted method appears to be the preferred method to use for analyses involving plant root architecture.

While the univariate linear mixed models provide useful results for each estimated parameter individually, the multivariate models provide the complete picture. Interest in plant root architecture involves how the different dimensions relate to each other (Hodge et al., 2009). Therefore, the results from the multivariate model provide the most information in this study. The weighted multivariate model determined that the genetic variation in the spatial point patterns in the plant root tip data set can be characterised by three key estimated parameters; surface intensity, non-linear plant root depth and non-linear plant root width. This practical outcome of the weighted multivariate model was reached through the modelling of dependent variance structures at the residual and genetic levels. It was through this that it was found that three of the estimated parameters showed no additional genetic variance once the dependent residual variance structure was modelled. Although research aims vary between experiments, the theoretical findings of this study indicate that the implementation of a two-stage method where the second stage is a weighted multivariate linear mixed model provide the most comprehensive analysis of spatial point pattern data for plant root systems.

4.7 Conclusions and Future work

This study has provided key insight into the viability of a two-stage method linking spatial point processes and linear mixed models. Through addressing the three research questions, potential for future work to improve similar analyses has been

identified.

The first stage of this study showed the second order polynomial spatial point process model to most effectively model the inhomogeneous intensity of the plant root systems (Research Question 1). The linear model did not account for the non-linear change in intensity present while the second order harmonic model was not as appropriate as the second order polynomial model. The fitting of this model provided the estimated parameters for the second stage of the analysis. The implementation of the linear mixed model was found to be a viable method to complete the two-stage analysis (Research Question 2). It effectively models the design parameters of the experiment and also provided the option to model residual and genetic correlations between the estimated parameters in a multivariate model. There was found to be a difference in accuracy between the weighted and unweighted methods in the second stage of the analysis (Research Question 3). This was clear in the comparison of multivariate models where the non-linear root width parameter exhibited genetic variance for the weighted method but not the unweighted method. As such, the weights played a key role in accounting for the uncertainty in the plant root width dimension of the plant root systems. Given the inherent variation across both dimensions of plant root systems, this indicated that the weighted method provided more accurate results than the unweighted method.

An important potential future improvement in this analysis is the ability to evaluate the performance of the two-stage method by computing the results from a one-stage method. This will rely on an increase in computing resources and the **spatstat** package to handle such a data set. Through this, further information would be gathered to compare the weighted and unweighted methods. As mentioned, continued improvement in the data generation phase is vital to the achievement of reliable results. This will naturally progress in the future as camera technology and machine learning techniques evolve further. Future work in this area can further investigate the relationship between the estimated parameters fit in the models and various aspects of plant root behaviour. In this analysis, residual and genetic correlations were modelled between traits with the conclusions drawn primarily relating to these results. In future studies, this research can be taken a step further by investigating what the estimated parameters may actually mean in terms of plant root function. If such links were found, this may allow certain plant root architectures to be identified for a specific purpose.

References

Akaike, H. (1973), 'Maximum likelihood identification of gaussian autoregressive moving average models', *Biometrika* **60**(2), 255–265.

Atkinson, D. (2000), *Root Characteristics: Why and What to Measure*, Springer Berlin Heidelberg, Berlin, Heidelberg, pp. 1–32.

Baddeley, A., Bárány, I. and Schneider, R. (2007), 'Spatial point processes and their applications', *Stochastic Geometry: Lectures Given at the CIME Summer School Held in Martina Franca, Italy, September 13–18, 2004* pp. 1–75.

Baddeley, A., Rubak, E. and Turner, R. (2015), *Spatial point patterns: methodology and applications with R*, CRC press.

Baddeley, A. and Turner, R. (2000), 'Practical maximum pseudolikelihood for spatial point patterns: (with discussion)', *Australian New Zealand Journal of Statistics* **42**(3), 283–322.

Baddeley, A. and Turner, R. (2004), 'Spatstat: An r package for analyzing spatial point patterns'.

Berman, M. and Turner, T. R. (1992), 'Approximating point process likelihoods with glim', *Journal of the Royal Statistical Society. Series C (Applied Statistics)* **41**(1), 31–38.

Burnham, K. P. and Anderson, D. R. (2004), 'Multimodel inference: understanding aic and bic in model selection', *Sociological methods & research* **33**(2), 261–304.

Butler, D., Cullis, B., Gilmour, A. and Thompson, R. (2018), Asreml version 4, Technical report, Technical report, University of Wollongong.

Cannon, W. A. (1949), 'A tentative classification of root systems', *Ecology* pp. 542–548.

Chang, C.-H. and Schoenberg, F. P. (2011), 'Testing separability in marked multidimensional point processes with covariates', *Annals of the Institute of Statistical Mathematics* **63**(6), 1103–1122.

Cox, D. (1972), 'The statistical analysis of dependencies in point processes', *Stochastic Point Processes. Wiley: New York* pp. 55–66.

Damesa, T. M., Hartung, J., Gowda, M., Beyene, Y., Das, B., Semagn, K. and Piepho, H.-P. (2019), 'Comparison of weighted and unweighted stage-wise analysis for genome-wide association studies and genomic selection', *Crop Science* **59**(6), 2572–2584.

Damesa, T. M., Möhring, J., Worku, M. and Piepho, H. (2017), 'One step at a time: Stage-wise analysis of a series of experiments', *Agronomy Journal* **109**(3), 845–857.

Das, A., Schneider, H., Burridge, J., Ascanio, A. K. M., Wojciechowski, T., Topp, C. N., Lynch, J. P., Weitz, J. S. and Bucksch, A. (2015), 'Digital imaging of root traits (dirt): a high-throughput computing and collaboration platform for field-based root phenomics', *Plant methods* **11**(1), 1–12.

Draye, X., Thaon, P., Ligeza, A., Lobet, B., Lobet, G., Civava, R., Alabart, C. and De Vleeschouwer, C. (2018), High throughput root phenotyping in aeroponics: one step from seed to root growth parameters, *in* 'International Society of Root Research'.

Frensham, A., Cullis, B. and Verbyla, A. (1997), 'Genotype by environment variance heterogeneity in a two-stage analysis', *Biometrics* **53**(4), 1373–1383.

Gilmour, A. R., Thompson, R. and Cullis, B. R. (1995), 'Average information reml: an efficient algorithm for variance parameter estimation in linear mixed models', *Biometrics* pp. 1440–1450.

Gogel, B., Smith, A. and Cullis, B. (2018), 'Comparison of a one- and two-stage mixed model analysis of australia's national variety trial southern region wheat data', *Euphytica* **214**(2), 44.

Gogel, B., Welham, S., Verbyla, A. and Cullis, B. (2001), Outlier detection in linear mixed effects, Technical report, summary of research. report p106. Technical report, University of Adelaide . . . .

Harper, J., Jones, M. and Sackville Hamilton, N. (1991), 'evolution of roots and the problems of analysing their behaviour', *Special publication... of the British Ecological Society* .

Hodge, A. (2004), 'The plastic plant: root responses to heterogeneous supplies of nutrients', *New phytologist* **162**(1), 9–24.

Hodge, A. (2006), 'Plastic plants and patchy soils', *Journal of experimental botany* **57**(2), 401–411.

Hodge, A., Berta, G., Doussan, C., Merchan, F. and Crespi, M. (2009), 'Plant root growth, architecture and function', *Plant and soil* **321**(1), 153–187.

Hodge, A., Robinson, D., Griffiths, B. and Fitter, A. (1999), 'Why plants bother: root proliferation results in increased nitrogen capture from an organic patch when two grasses compete', *Plant, Cell & Environment* **22**(7), 811–820.

Hodge, A., Stewart, J., Robinson, D., Griffiths, B. and Fitter, A. (2000), 'Spatial and physical heterogeneity of n supply from soil does not influence n capture by two grass species', *Functional Ecology* **14**(5), 645–653.

Isham, V. (1981), 'An introduction to spatial point processes and markov random fields', *International Statistical Review / Revue Internationale de Statistique* **49**(1), 21–43.

Kackar, R. N. and Harville, D. A. (1981), 'Unbiasedness of two-stage estimation and prediction procedures for mixed linear models', *Communications in Statistics - Theory and Methods* **10**(13), 1249–1261.

Kutschera, L. (1960), 'Wurzelatlas mitteleuropaischer ackerunkrauter und kulturpflanzen'.

Last, G. and Penrose, M. (2017), *Lectures on the Poisson process*, Vol. 7, Cambridge University Press.

Manschadi, A. M., Christopher, J., deVoil, P. and Hammer, G. L. (2006), 'The role of root architectural traits in adaptation of wheat to water-limited environments', *Functional plant biology* **33**(9), 823–837.

Moller, J. and Waagepetersen, R. P. (2003), *Statistical inference and simulation for spatial point processes*, CRC Press.

Muller, S., Scealy, J. L. and Welsh, A. H. (2013), 'Model selection in linear mixed models', *Statist. Sci.* **28**(2), 135–167.

Möhring, J. and Piepho, H. (2009), 'Comparison of weighting in two-stage analysis of plant breeding trials', *Crop Science* **49**(6), 1977–1988.

Neyman, J. and Scott, E. L. (1972), 'Processes of clustering and applications', *Stochastic Point Processes* pp. 646–681.

Ogata, Y. (1983), 'Estimation of the parameters in the modified omori formula for aftershock frequencies by the maximum likelihood procedure', *Journal of Physics of the Earth* **31**(2), 115–124.

Ogata, Y. and Akaike, H. (1982), On linear intensity models for mixed doubly stochastic poisson and self-exciting point processes, *in* 'Selected Papers of Hirotugu Akaike', Springer, pp. 269–274.

Ogata, Y. and Katsura, K. (1986), 'Point-process models with linearly parametrized intensity for application to earthquake data', *Journal of applied probability* pp. 291–310.

Patterson, H. D. and Thompson, R. (1971), 'Recovery of inter-block information when block sizes are unequal', *Biometrika* **58**(3), 545–554.

R Core Team (2019), *R: A Language and Environment for Statistical Computing*, R Foundation for Statistical Computing, Vienna, Austria.

Richard, C. A., Hickey, L. T., Fletcher, S., Jennings, R., Chenu, K. and Christopher, J. T. (2015), 'High-throughput phenotyping of seminal root traits in wheat', *Plant Methods* **11**(1), 1–11.

Ripley, B. D. (1977), 'Modelling spatial patterns', *Journal of the Royal Statistical Society: Series B (Methodological)* **39**(2), 172–192.

Ripley, B. D. (1979), 'Tests of 'randomness' for spatial point patterns', *Journal of the Royal Statistical Society. Series B (Methodological)* **41**(3), 368–374.

Robinson, D., Hodge, A., Griffiths, B. S. and Fitter, A. H. (1999), 'Plant root proliferation in nitrogen–rich patches confers competitive advantage', *Proceedings of the Royal Society of London. Series B: Biological Sciences* **266**(1418), 431–435.

Robinson, H., Kelly, A., Fox, G., Franckowiak, J., Borrell, A. and Hickey, L. (2018), 'Root architectural traits and yield: exploring the relationship in barley breeding trials', *Euphytica* **214**(9), 1–16.

Schwarz, G. (1978), 'Estimating the dimension of a model', *The annals of statistics* **6**(2), 461–464.

Searle, S. (1971), 'Linear models john wiley & sons', *Inc., New York-London-Sydney-Toronto* .

Sideli, G. M., McAtee, P., Marrano, A., Allen, B. J., Brown, P. J., Butterfield, T. S., Dandekar, A. M., Leslie, C. A. and Neale, D. B. (2020), 'Genetic analysis of walnut (juglans regia l.) pellicle pigment variation through a novel, high-throughput phenotyping platform', *G3: Genes, Genomes, Genetics* **10**(12), 4411–4424.

Smith, A. B., Ganesalingam, A., Kuchel, H. and Cullis, B. R. (2015), 'Factor analytic mixed models for the provision of grower information from national crop variety testing programs', *Theoretical and Applied Genetics* **128**(1), 55–72.

Vere-Jones, D. and Ozaki, T. (1982), 'Some examples of statistical estimation applied to earthquake data', *Annals of the Institute of Statistical Mathematics* **34**(1), 189–207.

Weaver, J. E. and Bruner, W. E. (1926), 'Root development of field crops'.

Welham, S., Cullis, B., Gogel, B., Gilmour, A. and Thompson, R. (2004), 'Prediction in linear mixed models', *Australian & New Zealand Journal of Statistics* **46**(3), 325–347.

Welham, S. J., Gogel, B. J., Smith, A. B., Thompson, R. and Cullis, B. R. (2010), 'A comparison of analysis methods for late-stage variety evaluation trials', *Australian New Zealand Journal of Statistics* **52**(2), 125–149.

Yang, Y., Ng, C.-T. and Kotousov, A. (2019), 'Second-order harmonic generation of lamb wave in prestressed plates', *Journal of Sound and Vibration* **460**, 114903.

Appendix A

Plant root tip data plots of outliers

A.1 This appendix contains 37 plant root tip data plots of the plants which did not grow adequately on the aeroponic platform and were removed from the analysis. These plots are presented as one figure over the following seven pages.

Plant 15
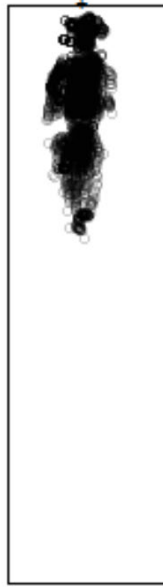
Plant 27

Plant 58

Plant 154

Plant 158
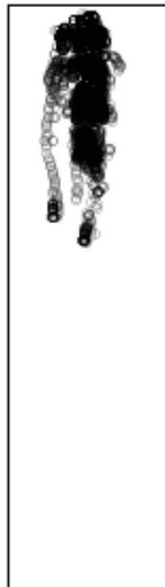
Plant 161
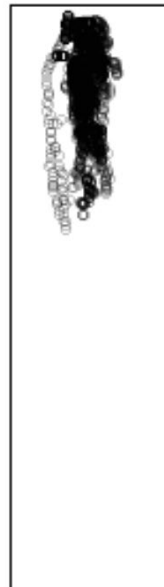
Plant 166
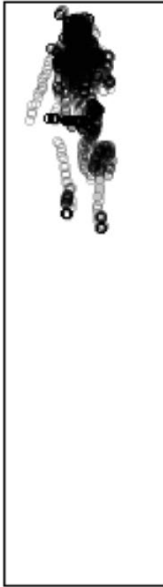
Plant 171

Plant 172
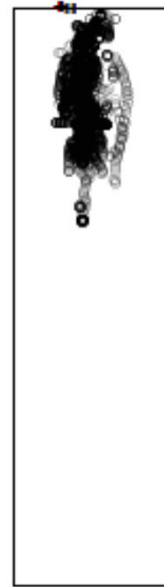
Plant 176

Plant 177

Plant 181
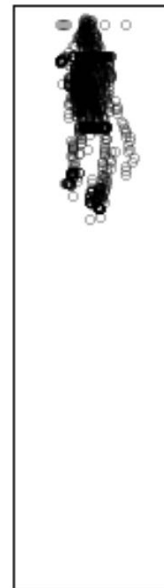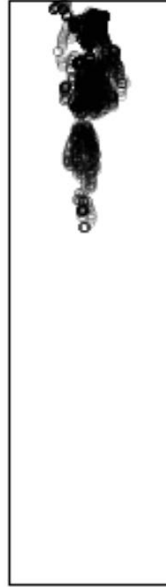
Plant 182   **Plant 186**   **Plant 188**
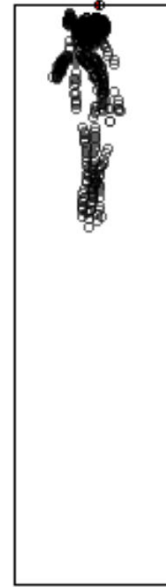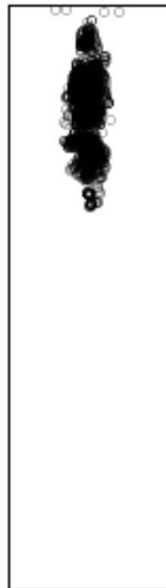
Plant 191   **Plant 200**   **Plant 214**
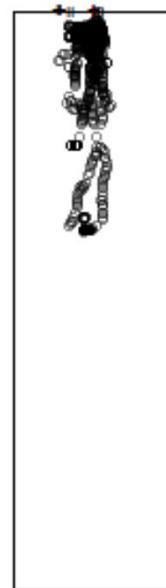
Plant 218

Plant 222

Plant 227

Plant 228

Plant 241
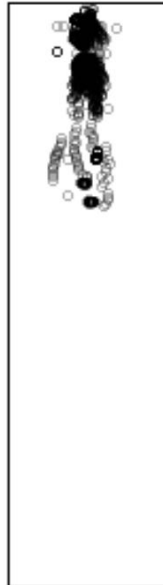
Plant 246

Plant 251

Plant 265

Plant 311
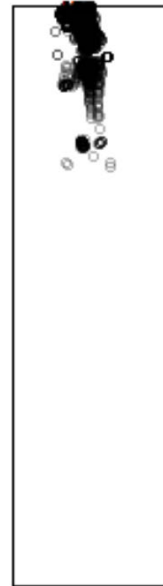
Plant 369

Plant 412

Plant 419

Plant 452

Plant 458

Plant 590

Plant 764
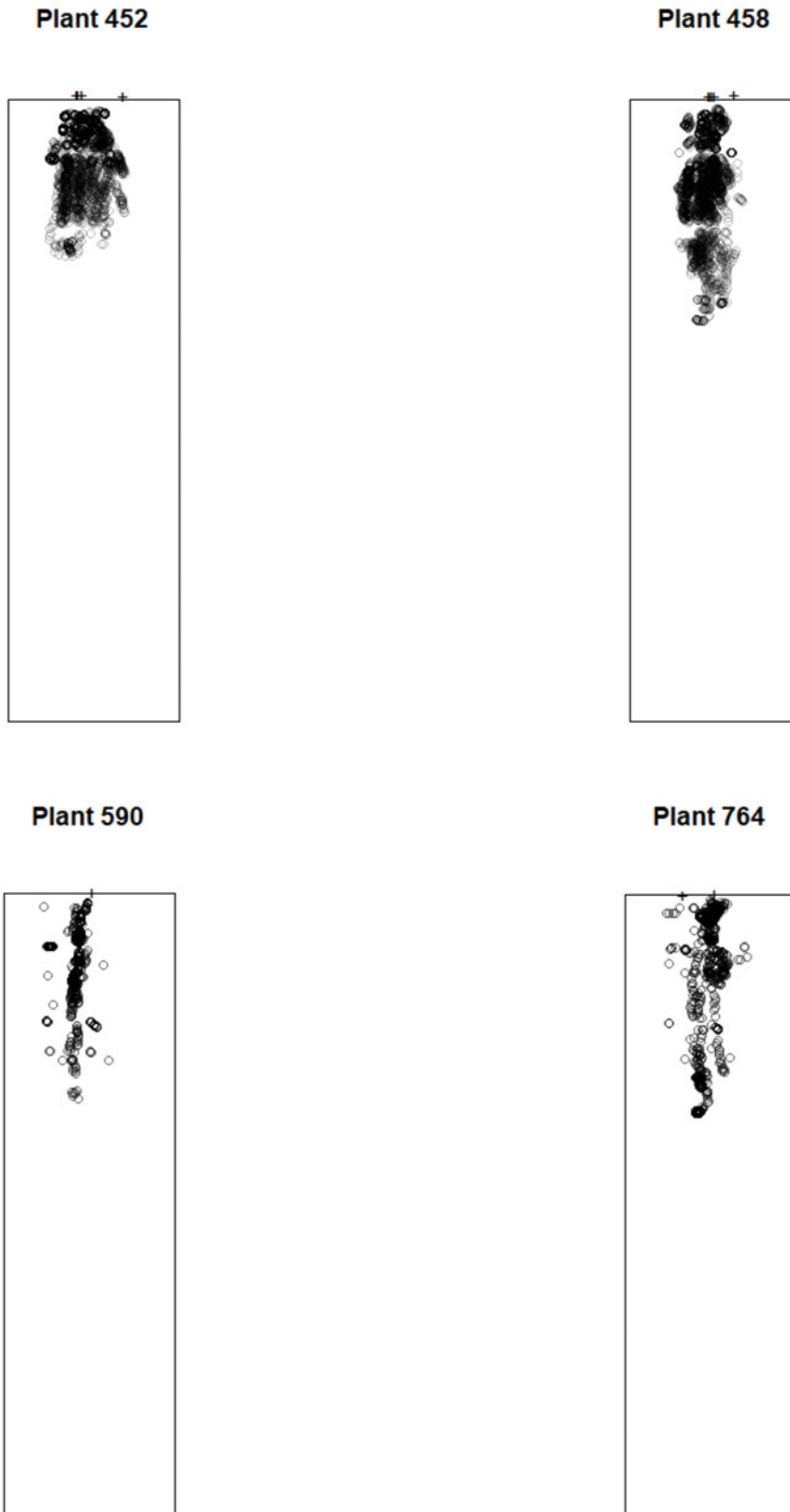
Figure A.1: Plots of the plant root tip data for the 37 plant root systems which were deemed to have not grown in the experiment. Of these 37 plant root systems, 35 were located on platform 1 of the experiment, with plants 590 and 764 the only 2 which were on platform 2.

A.2 Plants which were detected as outliers using the alternate outlier method for each estimated parameter

Plant 525

Plant 719

Plant 702

Plant 809
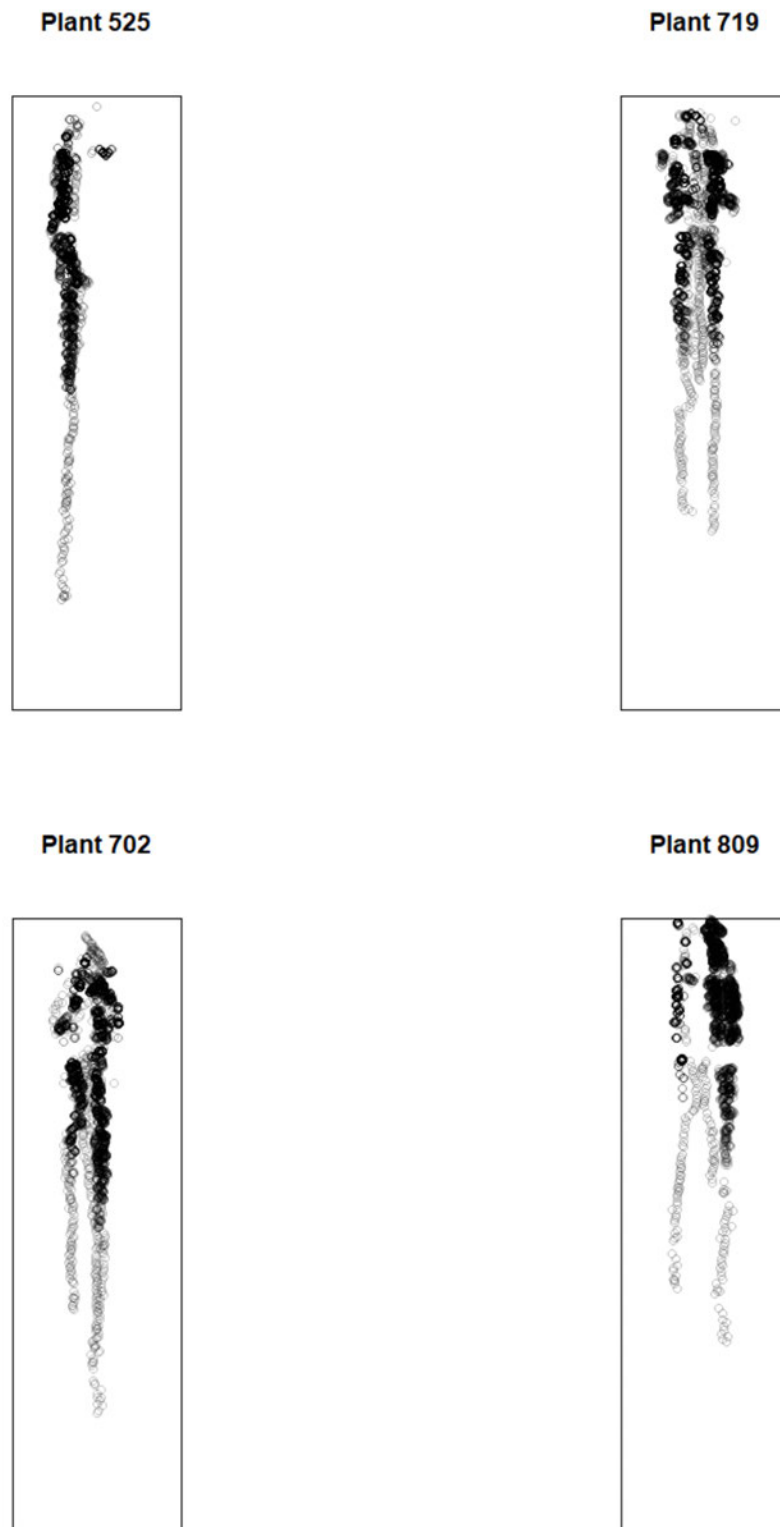
Figure A.2: Plots of the plant root tip data for the 4 plant root systems which were detected as outliers for the *Intercept* estimated parameter.

Plant 525　　　　**Plant 719**　　　　**Plant 520**
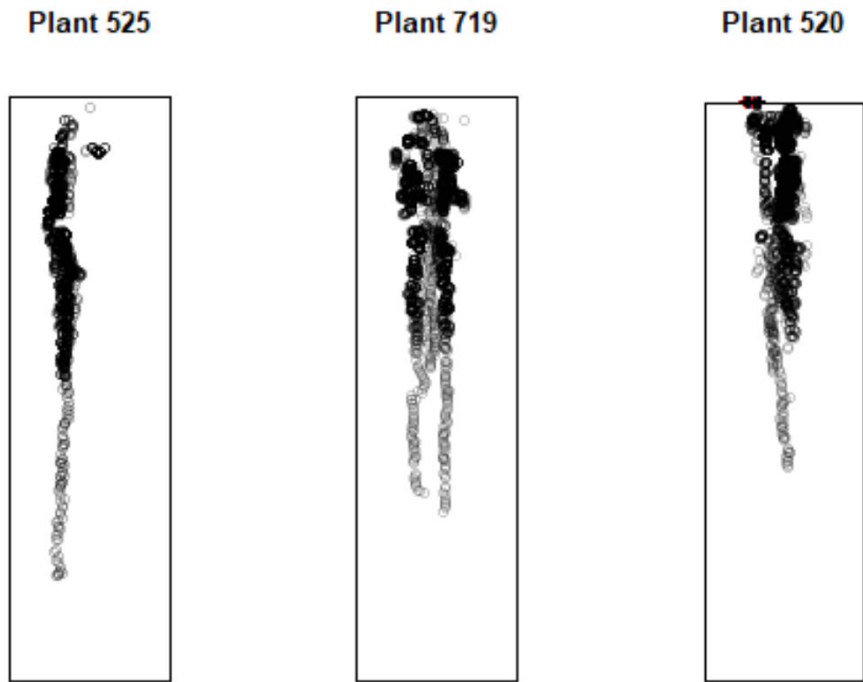
Figure A.3: Plots of the plant root tip data for the 3 plant root systems which were detected as outliers for the *abs(x)* estimated parameter.

Plant 20
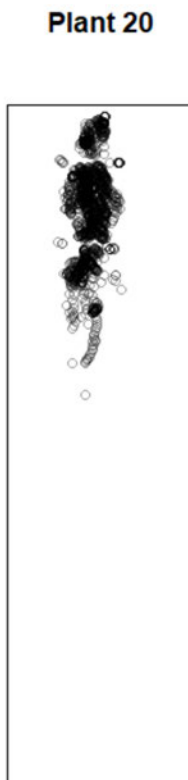
Figure A.4: Plot of the plant root tip data for the 1 plant root system which was detected as an outlier for the *y* estimated parameter.

Plant 74

Plant 895

Plant 525

Plant 807
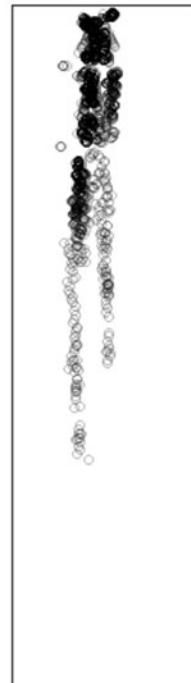
Figure A.5: Plots of the plant root tip data for the 4 plant root systems which were detected as outliers for the $abs(x)^2$ estimated parameter.
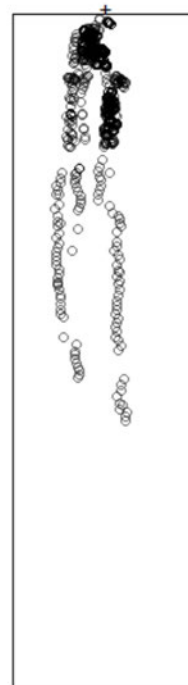
Figure A.6: Plots of the plant root tip data for the 5 plant root systems which were detected as outliers for the $abs(x)y$ estimated parameter.

Plant 198 **Plant 868** **Plant 20**

Plant 163 **Plant 453** **Plant 875**
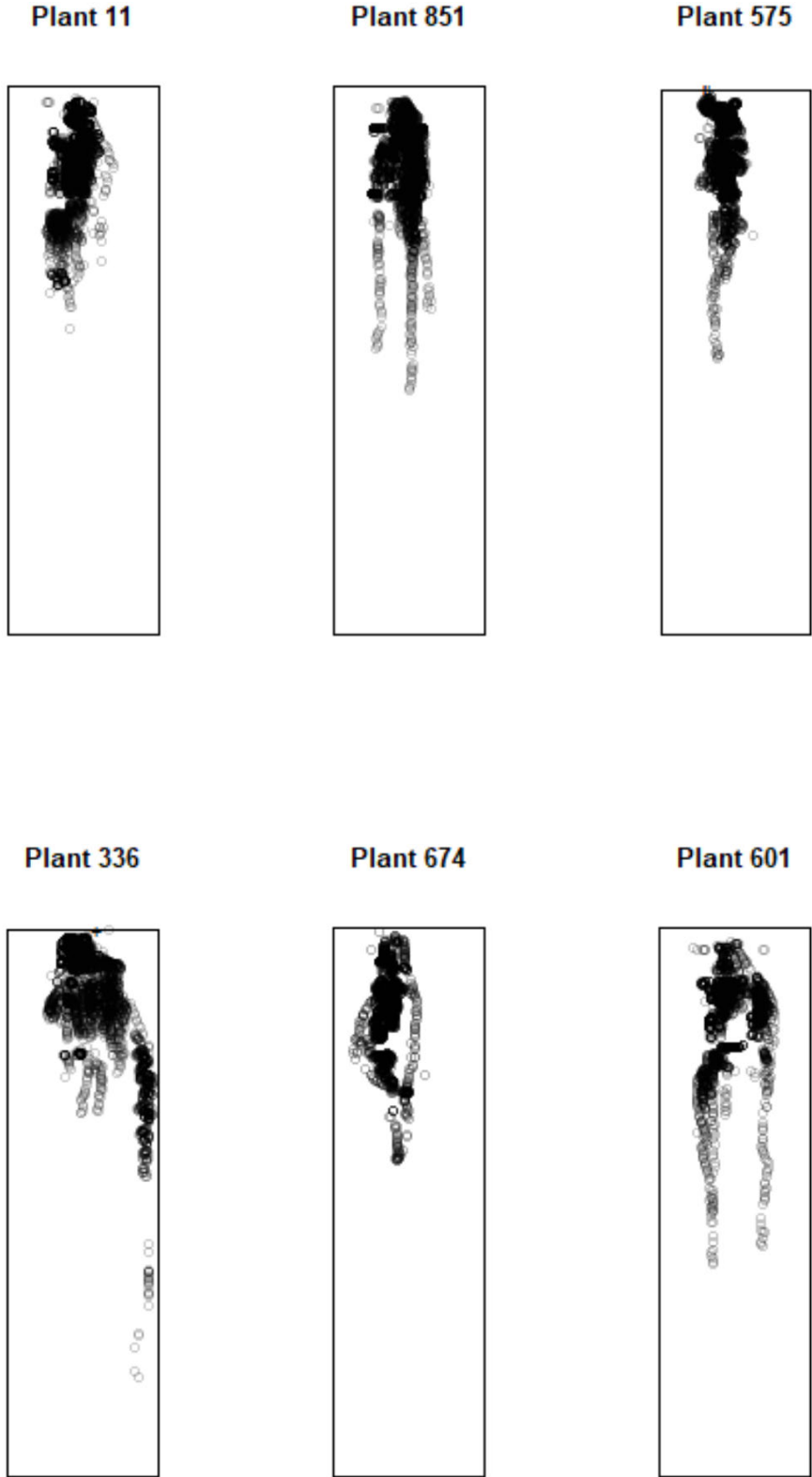
Figure A.7: Plots of the plant root tip data for the 12 plant root systems which were detected as outliers for the y^2 estimated parameter.

Full sets of genotype predictions

B.1   Univariate unweighted genotype predictions

Table B.1: The genotype predictions for each unweighted univariate linear mixed model, where each estimated parameter has its own model. The full set of genotype predictions are presented here, and it is important to note that these predictions are on the transformed data scale with the exception of *intercept* which did not require transforming.

Genotype	*Intercept*	*abs(x)*	*y*	*abs(x)y*	*abs(x)²*	*y²*
DHARWAR DRY_PP	-5.855	0.086	-0.348	-0.433	-1.519	-2.145
DRYSDALE_PP	-5.959	0.086	-0.379	-0.439	-1.520	-2.482
EGA GREGORY_PP	-5.827	0.086	-0.320	-0.430	-1.519	-2.164
EGA WYLIE_PP	-6.109	0.086	-0.434	-0.424	-1.520	-2.524
FAC10-16_P1	-5.721	0.086	-0.275	-0.447	-1.520	-2.176
MACE_PP	-5.758	0.086	-0.208	-0.447	-1.520	-2.008
MACE_SB062_123	-5.739	0.086	-0.256	-0.438	-1.520	-2.076
RIL114_PP	-5.964	0.086	-0.300	-0.438	-1.519	-2.110
SB062_PP	-5.958	0.086	-0.260	-0.424	-1.519	-1.820
SERI M82_PP	-6.100	0.086	-0.444	-0.443	-1.520	-2.549
SPITFIRE-P9	-5.785	0.086	-0.172	-0.469	-1.520	-2.207
SUNTOP_DHARWAH DRY_1	-5.884	0.086	-0.343	-0.433	-1.520	-2.177
SUNTOP_DHARWAH DRY_10	-5.836	0.086	-0.307	-0.431	-1.520	-2.051
SUNTOP_DHARWAH DRY_11	-5.857	0.086	-0.294	-0.428	-1.520	-1.964
SUNTOP_DHARWAH DRY_12	-5.807	0.086	-0.332	-0.436	-1.519	-2.193
SUNTOP_DHARWAH DRY_13	-5.923	0.086	-0.351	-0.425	-1.520	-2.204
SUNTOP_DHARWAH DRY_14	-5.980	0.086	-0.330	-0.431	-1.519	-2.060
SUNTOP_DHARWAH DRY_15	-5.846	0.086	-0.310	-0.440	-1.520	-2.160
SUNTOP_DHARWAH DRY_16	-6.070	0.086	-0.377	-0.441	-1.520	-2.187
SUNTOP_DHARWAH DRY_17	-5.948	0.086	-0.285	-0.429	-1.519	-1.978
SUNTOP_DHARWAH DRY_18	-5.930	0.086	-0.333	-0.434	-1.519	-2.240

Table B.1 – continued from previous page

Genotype	Intercept	abs(x)	y	abs(x)y	abs(x)²	y²
SUNTOP_DHARWAH DRY_19	-6.094	0.086	-0.341	-0.434	-1.519	-2.352
SUNTOP_DHARWAH DRY_2	-6.072	0.086	-0.304	-0.439	-1.520	-2.072
SUNTOP_DHARWAH DRY_20	-6.043	0.086	-0.320	-0.438	-1.520	-2.294
SUNTOP_DHARWAH DRY_21	-5.918	0.086	-0.332	-0.427	-1.520	-2.261
SUNTOP_DHARWAH DRY_22	-6.094	0.086	-0.252	-0.436	-1.520	-2.324
SUNTOP_DHARWAH DRY_23	-5.815	0.086	-0.333	-0.428	-1.519	-2.109
SUNTOP_DHARWAH DRY_24	-6.079	0.086	-0.312	-0.431	-1.519	-2.032
SUNTOP_DHARWAH DRY_25	-5.819	0.086	-0.290	-0.445	-1.520	-2.201
SUNTOP_DHARWAH DRY_26	-6.014	0.086	-0.313	-0.447	-1.519	-2.392
SUNTOP_DHARWAH DRY_27	-6.106	0.086	-0.346	-0.434	-1.519	-2.316
SUNTOP_DHARWAH DRY_28	-6.180	0.086	-0.292	-0.435	-1.519	-2.106
SUNTOP_DHARWAH DRY_29	-5.924	0.086	-0.303	-0.446	-1.520	-2.397
SUNTOP_DHARWAH DRY_3	-5.809	0.086	-0.254	-0.426	-1.519	-1.815
SUNTOP_DHARWAH DRY_30	-6.004	0.086	-0.280	-0.422	-1.520	-1.947
SUNTOP_DHARWAH DRY_31	-5.810	0.086	-0.311	-0.431	-1.519	-2.006
SUNTOP_DHARWAH DRY_32	-5.934	0.086	-0.304	-0.443	-1.520	-2.408
SUNTOP_DHARWAH DRY_33	-5.934	0.086	-0.268	-0.442	-1.520	-2.242
SUNTOP_DHARWAH DRY_34	-5.853	0.086	-0.321	-0.434	-1.519	-2.084
SUNTOP_DHARWAH DRY_35	-5.881	0.086	-0.326	-0.433	-1.520	-2.104
SUNTOP_DHARWAH DRY_36	-5.943	0.086	-0.328	-0.431	-1.519	-2.125
SUNTOP_DHARWAH DRY_37	-5.826	0.086	-0.298	-0.443	-1.520	-2.147
SUNTOP_DHARWAH DRY_38	-6.035	0.086	-0.365	-0.430	-1.519	-2.307
SUNTOP_DHARWAH DRY_39	-5.889	0.086	-0.328	-0.438	-1.520	-2.185
SUNTOP_DHARWAH DRY_4	-5.830	0.086	-0.301	-0.434	-1.519	-2.005
SUNTOP_DHARWAH DRY_40	-5.763	0.086	-0.275	-0.441	-1.519	-2.110
SUNTOP_DHARWAH DRY_41	-5.964	0.086	-0.339	-0.428	-1.519	-2.140
SUNTOP_DHARWAH DRY_42	-5.849	0.086	-0.284	-0.441	-1.519	-2.405
SUNTOP_DHARWAH DRY_43	-6.136	0.086	-0.343	-0.438	-1.520	-2.307
SUNTOP_DHARWAH DRY_44	-5.857	0.086	-0.305	-0.438	-1.520	-2.222
SUNTOP_DHARWAH DRY_45	-6.012	0.086	-0.263	-0.441	-1.520	-2.065
SUNTOP_DHARWAH DRY_46	-6.074	0.086	-0.296	-0.438	-1.520	-2.385
SUNTOP_DHARWAH DRY_47	-5.907	0.086	-0.292	-0.429	-1.519	-2.076
SUNTOP_DHARWAH DRY_48	-5.850	0.086	-0.329	-0.430	-1.520	-2.055
SUNTOP_DHARWAH DRY_49	-6.049	0.086	-0.355	-0.429	-1.519	-2.116
SUNTOP_DHARWAH DRY_5	-5.935	0.086	-0.321	-0.434	-1.519	-2.234
SUNTOP_DHARWAH DRY_50	-5.834	0.086	-0.308	-0.431	-1.520	-2.045

Table B.1 – continued from previous page

Genotype	Intercept	abs(x)	y	abs(x)y	abs(x)²	y²
SUNTOP_DHARWAH DRY_51	-6.129	0.086	-0.306	-0.453	-1.520	-2.715
SUNTOP_DHARWAH DRY_52	-5.900	0.086	-0.294	-0.442	-1.520	-2.188
SUNTOP_DHARWAH DRY_6	-5.857	0.086	-0.271	-0.443	-1.520	-2.018
SUNTOP_DHARWAH DRY_7	-6.018	0.086	-0.261	-0.451	-1.519	-2.456
SUNTOP_DHARWAH DRY_8	-5.789	0.086	-0.310	-0.436	-1.520	-2.166
SUNTOP_DHARWAH DRY_9	-5.857	0.086	-0.317	-0.432	-1.520	-2.135
SUNTOP_DRYSDALE_100	-5.891	0.086	-0.324	-0.436	-1.520	-2.204
SUNTOP_DRYSDALE_101	-5.984	0.086	-0.314	-0.429	-1.519	-2.124
SUNTOP_DRYSDALE_102	-5.933	0.086	-0.295	-0.446	-1.520	-2.207
SUNTOP_DRYSDALE_103	-5.924	0.086	-0.300	-0.442	-1.519	-2.323
SUNTOP_DRYSDALE_104	-5.951	0.086	-0.309	-0.436	-1.519	-2.364
SUNTOP_DRYSDALE_53	-6.169	0.086	-0.393	-0.428	-1.519	-2.587
SUNTOP_DRYSDALE_54	-5.700	0.086	-0.310	-0.434	-1.519	-2.184
SUNTOP_DRYSDALE_55	-5.904	0.086	-0.316	-0.448	-1.520	-2.561
SUNTOP_DRYSDALE_56	-6.060	0.086	-0.355	-0.434	-1.519	-2.404
SUNTOP_DRYSDALE_57	-5.854	0.086	-0.242	-0.447	-1.520	-2.120
SUNTOP_DRYSDALE_58	-6.121	0.086	-0.401	-0.438	-1.519	-2.315
SUNTOP_DRYSDALE_59	-6.011	0.086	-0.347	-0.433	-1.519	-2.335
SUNTOP_DRYSDALE_60	-5.864	0.086	-0.292	-0.441	-1.519	-2.340
SUNTOP_DRYSDALE_61	-5.929	0.086	-0.299	-0.438	-1.519	-2.167
SUNTOP_DRYSDALE_62	-5.899	0.086	-0.312	-0.441	-1.519	-2.267
SUNTOP_DRYSDALE_64	-6.255	0.086	-0.400	-0.436	-1.519	-2.237
SUNTOP_DRYSDALE_65	-5.891	0.086	-0.307	-0.434	-1.519	-2.147
SUNTOP_DRYSDALE_66	-5.886	0.086	-0.321	-0.435	-1.519	-2.141
SUNTOP_DRYSDALE_67	-5.891	0.086	-0.326	-0.431	-1.519	-2.102
SUNTOP_DRYSDALE_68	-5.871	0.086	-0.326	-0.430	-1.519	-2.161
SUNTOP_DRYSDALE_69	-5.860	0.086	-0.319	-0.442	-1.519	-2.372
SUNTOP_DRYSDALE_70	-5.988	0.086	-0.326	-0.430	-1.519	-2.086
SUNTOP_DRYSDALE_71	-5.970	0.086	-0.324	-0.429	-1.520	-2.227
SUNTOP_DRYSDALE_72	-6.016	0.086	-0.341	-0.443	-1.520	-2.536
SUNTOP_DRYSDALE_73	-6.108	0.086	-0.352	-0.423	-1.520	-2.170
SUNTOP_DRYSDALE_74	-5.966	0.086	-0.326	-0.437	-1.519	-2.199
SUNTOP_DRYSDALE_75	-5.910	0.086	-0.313	-0.436	-1.519	-2.130
SUNTOP_DRYSDALE_76	-5.950	0.086	-0.343	-0.430	-1.519	-2.169
SUNTOP_DRYSDALE_77	-6.251	0.086	-0.361	-0.431	-1.520	-2.158
SUNTOP_DRYSDALE_78	-5.890	0.086	-0.328	-0.428	-1.520	-2.123

Genotype	Intercept	abs(x)	y	abs(x)y	abs(x)^2	y^2
SUNTOP_DRYSDALE_79	-6.076	0.086	-0.337	-0.440	-1.519	-2.222
SUNTOP_DRYSDALE_80	-6.023	0.086	-0.346	-0.438	-1.519	-2.223
SUNTOP_DRYSDALE_81	-6.157	0.086	-0.307	-0.438	-1.520	-2.109
SUNTOP_DRYSDALE_83	-5.851	0.086	-0.334	-0.435	-1.519	-2.157
SUNTOP_DRYSDALE_84	-5.968	0.086	-0.363	-0.431	-1.520	-2.281
SUNTOP_DRYSDALE_85	-6.022	0.086	-0.343	-0.433	-1.520	-2.243
SUNTOP_DRYSDALE_86	-5.945	0.086	-0.301	-0.439	-1.520	-2.170
SUNTOP_DRYSDALE_87	-6.059	0.086	-0.369	-0.433	-1.519	-2.347
SUNTOP_DRYSDALE_88	-5.876	0.086	-0.197	-0.445	-1.520	-2.032
SUNTOP_DRYSDALE_89	-5.764	0.086	-0.315	-0.437	-1.519	-2.170
SUNTOP_DRYSDALE_90	-6.023	0.086	-0.333	-0.421	-1.521	-2.151
SUNTOP_DRYSDALE_91	-5.786	0.086	-0.292	-0.433	-1.519	-2.017
SUNTOP_DRYSDALE_92	-5.994	0.086	-0.304	-0.439	-1.519	-2.138
SUNTOP_DRYSDALE_93	-6.154	0.086	-0.387	-0.418	-1.519	-2.177
SUNTOP_DRYSDALE_94	-5.973	0.086	-0.332	-0.435	-1.520	-2.230
SUNTOP_DRYSDALE_95	-5.901	0.086	-0.286	-0.448	-1.519	-2.491
SUNTOP_DRYSDALE_96	-5.883	0.086	-0.299	-0.434	-1.520	-2.061
SUNTOP_DRYSDALE_97	-6.007	0.086	-0.308	-0.438	-1.519	-2.229
SUNTOP_DRYSDALE_98	-5.926	0.086	-0.283	-0.440	-1.520	-2.323
SUNTOP_DRYSDALE_99	-5.958	0.086	-0.325	-0.433	-1.520	-2.147
SUNTOP_EGA GREGORY_108	-5.880	0.086	-0.252	-0.436	-1.519	-2.109
SUNTOP_EGA GREGORY_109	-5.913	0.086	-0.316	-0.437	-1.519	-2.292
SUNTOP_EGA GREGORY_110	-6.182	0.086	-0.356	-0.434	-1.519	-2.316
SUNTOP_EGA GREGORY_111	-5.832	0.086	-0.255	-0.448	-1.519	-2.358
SUNTOP_EGA GREGORY_112	-5.795	0.086	-0.233	-0.441	-1.519	-1.927
SUNTOP_EGA GREGORY_113	-6.056	0.086	-0.283	-0.438	-1.520	-2.059
SUNTOP_EGA GREGORY_114	-5.925	0.086	-0.315	-0.437	-1.519	-2.293
SUNTOP_EGA GREGORY_115	-5.911	0.086	-0.296	-0.438	-1.519	-2.044
SUNTOP_EGA GREGORY_116	-6.020	0.086	-0.303	-0.434	-1.519	-2.203
SUNTOP_EGA GREGORY_117	-5.866	0.086	-0.297	-0.448	-1.520	-2.349
SUNTOP_EGA GREGORY_118	-5.940	0.086	-0.320	-0.430	-1.519	-2.200
SUNTOP_EGA GREGORY_119	-5.678	0.086	-0.317	-0.444	-1.519	-2.232
SUNTOP_EGA GREGORY_120	-5.769	0.086	-0.290	-0.444	-1.519	-2.479
SUNTOP_EGA GREGORY_121	-5.925	0.086	-0.322	-0.428	-1.520	-2.178
SUNTOP_EGA GREGORY_122	-5.862	0.086	-0.230	-0.445	-1.520	-2.062
SUNTOP_EGA GREGORY_123	-5.921	0.086	-0.294	-0.437	-1.519	-2.054

Genotype	Intercept	abs(x)	y	abs(x)y	abs(x)²	y²
SUNTOP_EGA GREGORY_124	-5.854	0.086	-0.289	-0.439	-1.519	-2.203
SUNTOP_EGA GREGORY_125	-5.954	0.086	-0.326	-0.438	-1.519	-2.241
SUNTOP_EGA GREGORY_126	-5.890	0.086	-0.326	-0.431	-1.519	-2.244
SUNTOP_EGA GREGORY_127	-5.931	0.086	-0.292	-0.445	-1.520	-2.351
SUNTOP_EGA GREGORY_128	-5.780	0.086	-0.283	-0.430	-1.519	-1.984
SUNTOP_EGA GREGORY_129	-5.791	0.086	-0.300	-0.445	-1.519	-2.246
SUNTOP_EGA GREGORY_130	-6.214	0.086	-0.289	-0.443	-1.520	-2.287
SUNTOP_EGA GREGORY_131	-5.738	0.086	-0.288	-0.437	-1.519	-2.118
SUNTOP_EGA GREGORY_132	-5.986	0.086	-0.301	-0.445	-1.520	-2.245
SUNTOP_EGA GREGORY_133	-6.022	0.086	-0.296	-0.436	-1.519	-2.139
SUNTOP_EGA GREGORY_134	-6.024	0.086	-0.351	-0.432	-1.519	-2.208
SUNTOP_EGA GREGORY_135	-6.004	0.086	-0.309	-0.427	-1.520	-2.037
SUNTOP_EGA GREGORY_136	-6.061	0.086	-0.338	-0.431	-1.520	-2.179
SUNTOP_EGA GREGORY_137	-5.901	0.086	-0.345	-0.434	-1.519	-2.330
SUNTOP_EGA GREGORY_138	-5.896	0.086	-0.290	-0.434	-1.519	-2.197
SUNTOP_EGA GREGORY_139	-5.868	0.086	-0.331	-0.436	-1.519	-2.316
SUNTOP_EGA GREGORY_140	-6.073	0.086	-0.395	-0.432	-1.520	-2.634
SUNTOP_EGA GREGORY_141	-5.942	0.086	-0.325	-0.426	-1.520	-2.095
SUNTOP_EGA GREGORY_142	-5.962	0.086	-0.338	-0.422	-1.520	-2.154
SUNTOP_EGA GREGORY_143	-5.855	0.086	-0.309	-0.445	-1.520	-2.222
SUNTOP_EGA GREGORY_144	-6.096	0.086	-0.321	-0.440	-1.520	-2.211
SUNTOP_EGA GREGORY_145	-6.004	0.086	-0.242	-0.439	-1.519	-2.014
SUNTOP_EGA GREGORY_146	-5.826	0.086	-0.249	-0.441	-1.519	-2.144
SUNTOP_EGA GREGORY_147	-5.974	0.086	-0.353	-0.434	-1.519	-2.402
SUNTOP_EGA GREGORY_148	-5.981	0.086	-0.273	-0.441	-1.520	-2.128
SUNTOP_EGA GREGORY_149	-5.841	0.086	-0.262	-0.436	-1.519	-2.040
SUNTOP_FAC10-16_150	-5.952	0.086	-0.365	-0.431	-1.519	-2.265
SUNTOP_FAC10-16_151	-5.967	0.086	-0.301	-0.430	-1.520	-2.146
SUNTOP_FAC10-16_152	-5.998	0.086	-0.286	-0.432	-1.520	-1.991
SUNTOP_FAC10-16_153	-5.960	0.086	-0.342	-0.436	-1.519	-2.272
SUNTOP_FAC10-16_154	-5.879	0.086	-0.310	-0.437	-1.520	-2.153
SUNTOP_FAC10-16_155	-5.880	0.086	-0.330	-0.430	-1.519	-2.113
SUNTOP_FAC10-16_156	-5.843	0.086	-0.339	-0.434	-1.519	-2.216
SUNTOP_FAC10-16_157	-6.148	0.086	-0.234	-0.445	-1.520	-2.158
SUNTOP_FAC10-16_158	-5.806	0.086	-0.302	-0.442	-1.520	-2.172
SUNTOP_FAC10-16_159	-5.828	0.086	-0.266	-0.440	-1.519	-1.992

Table B.1 – continued from previous page

Genotype	*Intercept*	*abs(x)*	*y*	*abs(x)y*	*abs(x)²*	*y²*
SUNTOP_FAC10-16_160	-6.036	0.086	-0.410	-0.427	-1.519	-2.559
SUNTOP_FAC10-16_161	-6.041	0.086	-0.344	-0.424	-1.520	-2.115
SUNTOP_FAC10-16_162	-5.816	0.086	-0.263	-0.426	-1.520	-1.911
SUNTOP_FAC10-16_163	-6.011	0.086	-0.264	-0.438	-1.520	-2.018
SUNTOP_FAC10-16_164	-5.955	0.086	-0.297	-0.441	-1.519	-2.195
SUNTOP_FAC10-16_165	-5.935	0.086	-0.292	-0.440	-1.519	-2.253
SUNTOP_FAC10-16_166	-5.884	0.086	-0.325	-0.422	-1.519	-2.188
SUNTOP_FAC10-16_167	-6.009	0.086	-0.332	-0.433	-1.520	-2.174
SUNTOP_FAC10-16_168	-5.946	0.086	-0.375	-0.421	-1.519	-2.237
SUNTOP_FAC10-16_169	-5.842	0.086	-0.326	-0.430	-1.520	-2.161
SUNTOP_FAC10-16_170	-6.012	0.086	-0.299	-0.446	-1.520	-2.454
SUNTOP_FAC10-16_171	-6.046	0.086	-0.311	-0.441	-1.520	-2.198
SUNTOP_FAC10-16_172	-6.022	0.086	-0.268	-0.435	-1.520	-2.042
SUNTOP_FAC10-16_173	-5.831	0.086	-0.295	-0.438	-1.519	-2.127
SUNTOP_FAC10-16_174	-5.950	0.086	-0.335	-0.433	-1.520	-2.261
SUNTOP_FAC10-16_175	-5.994	0.086	-0.375	-0.445	-1.520	-2.583
SUNTOP_FAC10-16_176	-5.998	0.086	-0.312	-0.427	-1.520	-2.021
SUNTOP_FAC10-16_177	-5.816	0.086	-0.290	-0.436	-1.519	-2.036
SUNTOP_FAC10-16_178	-6.043	0.086	-0.371	-0.435	-1.519	-2.237
SUNTOP_FAC10-16_179	-6.080	0.086	-0.297	-0.437	-1.520	-2.104
SUNTOP_FAC10-16_180	-6.175	0.086	-0.302	-0.431	-1.520	-2.113
SUNTOP_FAC10-16_181	-5.883	0.086	-0.315	-0.430	-1.520	-2.034
SUNTOP_FAC10-16_182	-6.012	0.086	-0.355	-0.431	-1.519	-2.326
SUNTOP_FAC10-16_183	-5.969	0.086	-0.362	-0.429	-1.520	-2.211
SUNTOP_FAC10-16_184	-5.979	0.086	-0.310	-0.436	-1.520	-2.129
SUNTOP_FAC10-16_185	-6.016	0.086	-0.351	-0.434	-1.520	-2.283
SUNTOP_FAC10-16_186	-5.912	0.086	-0.299	-0.435	-1.520	-2.025
SUNTOP_FAC10-16_187	-5.977	0.086	-0.334	-0.435	-1.520	-2.311
SUNTOP_FAC10-16_188	-6.358	0.086	-0.383	-0.443	-1.520	-2.304
SUNTOP_FAC10-16_189	-5.810	0.086	-0.257	-0.443	-1.519	-2.421
SUNTOP_FAC10-16_190	-6.027	0.086	-0.317	-0.434	-1.519	-2.057
SUNTOP_FAC10-16_191	-6.074	0.086	-0.293	-0.434	-1.520	-2.256
SUNTOP_PP	-6.242	0.086	-0.287	-0.436	-1.519	-2.004
SUNTOP_RIL114_299	-5.866	0.086	-0.287	-0.442	-1.520	-2.124
SUNTOP_RIL114_300	-6.065	0.086	-0.271	-0.440	-1.520	-2.166
SUNTOP_RIL114_301	-6.053	0.086	-0.318	-0.439	-1.520	-2.296

Table B.1 – continued from previous page

Genotype	Intercept	abs(x)	y	abs(x)y	abs(x)²	y²
SUNTOP_RIL114_302	-5.867	0.086	-0.233	-0.441	-1.519	-2.067
SUNTOP_RIL114_303	-5.788	0.086	-0.337	-0.435	-1.519	-2.238
SUNTOP_RIL114_304	-5.910	0.086	-0.305	-0.434	-1.519	-2.118
SUNTOP_RIL114_305	-6.060	0.086	-0.297	-0.433	-1.519	-2.006
SUNTOP_RIL114_306	-5.903	0.086	-0.334	-0.435	-1.519	-2.327
SUNTOP_RIL114_307	-5.945	0.086	-0.313	-0.435	-1.520	-2.166
SUNTOP_RIL114_308	-5.904	0.086	-0.315	-0.430	-1.520	-2.227
SUNTOP_RIL114_309	-6.086	0.086	-0.344	-0.430	-1.519	-2.101
SUNTOP_RIL114_310	-6.082	0.086	-0.287	-0.437	-1.520	-2.295
SUNTOP_RIL114_311	-5.949	0.086	-0.330	-0.437	-1.519	-2.210
SUNTOP_RIL114_312	-5.968	0.086	-0.266	-0.435	-1.520	-1.961
SUNTOP_RIL114_313	-5.873	0.086	-0.271	-0.437	-1.520	-2.008
SUNTOP_RIL114_314	-5.908	0.086	-0.331	-0.433	-1.519	-2.114
SUNTOP_RIL114_315	-5.886	0.086	-0.295	-0.443	-1.520	-2.315
SUNTOP_RIL114_316	-5.884	0.086	-0.381	-0.423	-1.520	-2.179
SUNTOP_RIL114_317	-5.766	0.086	-0.280	-0.440	-1.519	-2.085
SUNTOP_RIL114_318	-5.865	0.086	-0.297	-0.434	-1.519	-2.014
SUNTOP_RIL114_319	-6.212	0.086	-0.385	-0.432	-1.520	-2.642
SUNTOP_RIL114_320	-6.144	0.086	-0.267	-0.443	-1.520	-2.181
SUNTOP_RIL114_321	-6.020	0.086	-0.324	-0.432	-1.519	-2.037
SUNTOP_RIL114_322	-5.957	0.086	-0.283	-0.433	-1.519	-2.010
SUNTOP_RIL114_323	-5.972	0.086	-0.292	-0.434	-1.519	-2.071
SUNTOP_RIL114_324	-5.912	0.086	-0.239	-0.441	-1.520	-1.964
SUNTOP_RIL114_325	-6.262	0.086	-0.296	-0.441	-1.520	-2.131
SUNTOP_RIL114_326	-5.889	0.086	-0.266	-0.430	-1.519	-2.016
SUNTOP_RIL114_327	-5.857	0.086	-0.314	-0.438	-1.519	-2.187
SUNTOP_RIL114_328	-5.951	0.086	-0.311	-0.436	-1.520	-2.187
SUNTOP_RIL114_329	-5.871	0.086	-0.306	-0.441	-1.520	-2.165
SUNTOP_RIL114_330	-6.047	0.086	-0.314	-0.433	-1.520	-2.205
SUNTOP_RIL114_331	-5.870	0.086	-0.310	-0.437	-1.520	-2.113
SUNTOP_RIL114_333	-6.054	0.086	-0.348	-0.432	-1.519	-2.235
SUNTOP_RIL114_334	-5.942	0.086	-0.321	-0.433	-1.519	-2.108
SUNTOP_RIL114_335	-5.877	0.086	-0.314	-0.434	-1.520	-2.119
SUNTOP_RIL114_336	-5.931	0.086	-0.314	-0.432	-1.519	-2.051
SUNTOP_RIL114_337	-6.259	0.086	-0.312	-0.431	-1.520	-2.145
SUNTOP_RIL114_338	-5.882	0.086	-0.314	-0.433	-1.519	-2.072

Genotype	*Intercept*	*abs(x)*	*y*	*abs(x)y*	*abs(x)²*	*y²*
SUNTOP_RIL114_339	-5.772	0.086	-0.286	-0.436	-1.519	-1.989
SUNTOP_RIL114_340	-6.046	0.086	-0.312	-0.433	-1.520	-2.016
SUNTOP_SB062_195	-5.946	0.086	-0.356	-0.432	-1.519	-2.374
SUNTOP_SB062_196	-5.790	0.086	-0.174	-0.441	-1.520	-1.824
SUNTOP_SB062_197	-5.947	0.086	-0.330	-0.432	-1.520	-2.151
SUNTOP_SB062_198	-5.827	0.086	-0.327	-0.433	-1.519	-2.095
SUNTOP_SB062_199	-5.964	0.086	-0.306	-0.435	-1.520	-1.975
SUNTOP_SB062_200	-5.979	0.086	-0.311	-0.437	-1.520	-2.099
SUNTOP_SB062_201	-5.940	0.086	-0.333	-0.438	-1.519	-2.216
SUNTOP_SB062_202	-5.947	0.086	-0.324	-0.441	-1.520	-2.200
SUNTOP_SB062_203	-5.890	0.086	-0.289	-0.436	-1.519	-2.198
SUNTOP_SB062_204	-5.927	0.086	-0.336	-0.425	-1.520	-2.194
SUNTOP_SB062_205	-5.943	0.086	-0.316	-0.430	-1.520	-2.141
SUNTOP_SB062_206	-6.089	0.086	-0.359	-0.428	-1.520	-2.309
SUNTOP_SB062_207	-6.214	0.086	-0.344	-0.431	-1.519	-2.066
SUNTOP_SB062_208	-6.109	0.086	-0.305	-0.434	-1.520	-2.246
SUNTOP_SB062_209	-5.940	0.086	-0.297	-0.430	-1.520	-1.995
SUNTOP_SB062_210	-5.963	0.086	-0.331	-0.438	-1.519	-2.228
SUNTOP_SB062_211	-6.043	0.086	-0.357	-0.432	-1.519	-2.073
SUNTOP_SB062_212	-5.935	0.086	-0.238	-0.439	-1.520	-1.896
SUNTOP_SB062_213	-5.976	0.086	-0.288	-0.442	-1.519	-2.098
SUNTOP_SB062_214	-5.920	0.086	-0.297	-0.440	-1.520	-2.188
SUNTOP_SB062_215	-5.989	0.086	-0.286	-0.421	-1.520	-2.021
SUNTOP_SB062_216	-6.037	0.086	-0.334	-0.434	-1.520	-2.192
SUNTOP_SB062_217	-5.913	0.086	-0.349	-0.442	-1.519	-2.344
SUNTOP_SB062_218	-5.820	0.086	-0.224	-0.460	-1.520	-2.299
SUNTOP_SB062_219	-5.829	0.086	-0.305	-0.442	-1.519	-2.214
SUNTOP_SB062_220	-5.873	0.086	-0.298	-0.439	-1.520	-2.199
SUNTOP_SB062_221	-5.906	0.086	-0.322	-0.429	-1.520	-2.112
SUNTOP_SB062_222	-5.792	0.086	-0.280	-0.433	-1.520	-2.244
SUNTOP_SB062_223	-5.985	0.086	-0.176	-0.448	-1.520	-1.946
SUNTOP_SB062_224	-6.104	0.086	-0.336	-0.434	-1.520	-2.124
SUNTOP_SB062_225	-6.021	0.086	-0.335	-0.420	-1.520	-2.112
SUNTOP_SB062_226	-5.901	0.086	-0.352	-0.443	-1.520	-2.592
SUNTOP_SB062_227	-5.858	0.086	-0.306	-0.443	-1.520	-2.201
SUNTOP_SB062_228	-5.953	0.086	-0.269	-0.440	-1.519	-2.177

Genotype	Intercept	abs(x)	y	abs(x)y	abs(x)^2	y^2
SUNTOP_SB062_229	-5.785	0.086	-0.289	-0.434	-1.520	-2.058
SUNTOP_SB062_230	-6.043	0.086	-0.304	-0.438	-1.519	-2.200
SUNTOP_SB062_231	-6.037	0.086	-0.338	-0.442	-1.520	-2.435
SUNTOP_SB062_232	-5.944	0.086	-0.343	-0.434	-1.519	-2.146
SUNTOP_SB062_233	-5.815	0.086	-0.286	-0.435	-1.519	-2.020
SUNTOP_SB062_234	-5.882	0.086	-0.304	-0.436	-1.520	-2.145
SUNTOP_SB062_235	-5.834	0.086	-0.258	-0.432	-1.519	-1.880
SUNTOP_SB062_236	-5.726	0.086	-0.312	-0.434	-1.520	-2.004
SUNTOP_SB062_237	-6.128	0.086	-0.346	-0.434	-1.520	-2.245
SUNTOP_SB062_238	-5.995	0.086	-0.315	-0.439	-1.520	-2.134
SUNTOP_SB062_239	-5.923	0.086	-0.219	-0.455	-1.520	-2.372
SUNTOP_SB062_240	-6.080	0.086	-0.316	-0.439	-1.520	-2.248
SUNTOP_SB062_241	-5.995	0.086	-0.301	-0.440	-1.520	-2.237
SUNTOP_SB062_242	-5.941	0.086	-0.342	-0.424	-1.519	-2.115
SUNTOP_SB062_243	-5.929	0.086	-0.330	-0.431	-1.519	-2.155
SUNTOP_SB062_244	-5.903	0.086	-0.363	-0.430	-1.520	-2.249
SUNTOP_SB062_245	-6.047	0.086	-0.264	-0.442	-1.520	-2.078
SUNTOP_SB062_246	-5.795	0.086	-0.269	-0.430	-1.519	-1.928
SUNTOP_SERI M82_247	-5.985	0.086	-0.313	-0.432	-1.519	-2.080
SUNTOP_SERI M82_248	-5.969	0.086	-0.269	-0.441	-1.520	-2.015
SUNTOP_SERI M82_249	-6.033	0.086	-0.322	-0.444	-1.520	-2.285
SUNTOP_SERI M82_250	-5.959	0.086	-0.331	-0.434	-1.520	-2.079
SUNTOP_SERI M82_251	-6.129	0.086	-0.301	-0.438	-1.520	-2.279
SUNTOP_SERI M82_252	-5.921	0.086	-0.376	-0.446	-1.520	-2.151
SUNTOP_SERI M82_253	-5.989	0.086	-0.352	-0.425	-1.520	-2.101
SUNTOP_SERI M82_254	-5.865	0.086	-0.244	-0.437	-1.519	-1.873
SUNTOP_SERI M82_255	-5.998	0.086	-0.260	-0.449	-1.519	-2.465
SUNTOP_SERI M82_256	-6.047	0.086	-0.333	-0.437	-1.519	-2.181
SUNTOP_SERI M82_257	-5.884	0.086	-0.307	-0.438	-1.520	-2.103
SUNTOP_SERI M82_258	-5.994	0.086	-0.337	-0.435	-1.519	-2.246
SUNTOP_SERI M82_259	-5.942	0.086	-0.334	-0.432	-1.520	-2.066
SUNTOP_SERI M82_260	-5.984	0.086	-0.326	-0.432	-1.519	-2.143
SUNTOP_SERI M82_261	-5.932	0.086	-0.239	-0.435	-1.520	-1.911
SUNTOP_SERI M82_262	-5.830	0.086	-0.306	-0.436	-1.519	-2.099
SUNTOP_SERI M82_263	-5.832	0.086	-0.308	-0.436	-1.519	-2.060
SUNTOP_SERI M82_264	-5.938	0.086	-0.356	-0.430	-1.520	-2.196

Table B.1 – continued from previous page

Genotype	Intercept	abs(x)	y	abs(x)y	abs(x)²	y²
SUNTOP_SERI M82_265	-5.869	0.086	-0.230	-0.438	-1.520	-2.037
SUNTOP_SERI M82_266	-5.923	0.086	-0.343	-0.431	-1.519	-2.086
SUNTOP_SERI M82_267	-5.932	0.086	-0.301	-0.437	-1.520	-2.021
SUNTOP_SERI M82_268	-5.894	0.086	-0.325	-0.443	-1.520	-2.372
SUNTOP_SERI M82_269	-5.889	0.086	-0.312	-0.432	-1.520	-2.072
SUNTOP_SERI M82_270	-5.844	0.086	-0.306	-0.437	-1.520	-2.144
SUNTOP_SERI M82_271	-5.942	0.086	-0.338	-0.436	-1.519	-2.287
SUNTOP_SERI M82_272	-5.933	0.086	-0.279	-0.438	-1.519	-2.204
SUNTOP_SERI M82_273	-5.960	0.086	-0.308	-0.434	-1.520	-2.088
SUNTOP_SERI M82_274	-6.201	0.086	-0.385	-0.426	-1.520	-2.198
SUNTOP_SERI M82_275	-6.107	0.086	-0.334	-0.439	-1.519	-2.213
SUNTOP_SERI M82_276	-5.932	0.086	-0.322	-0.431	-1.520	-2.195
SUNTOP_SERI M82_277	-5.818	0.086	-0.290	-0.435	-1.519	-2.060
SUNTOP_SERI M82_278	-6.113	0.086	-0.368	-0.427	-1.519	-2.155
SUNTOP_SERI M82_279	-5.982	0.086	-0.340	-0.436	-1.519	-2.435
SUNTOP_SERI M82_280	-5.926	0.086	-0.324	-0.432	-1.519	-2.130
SUNTOP_SERI M82_281	-5.882	0.086	-0.297	-0.436	-1.520	-2.066
SUNTOP_SERI M82_282	-5.996	0.086	-0.311	-0.434	-1.519	-2.083
SUNTOP_SERI M82_283	-6.055	0.086	-0.312	-0.432	-1.520	-2.024
SUNTOP_SERI M82_284	-5.921	0.086	-0.292	-0.434	-1.520	-2.225
SUNTOP_SERI M82_285	-5.885	0.086	-0.254	-0.439	-1.519	-1.992
SUNTOP_SERI M82_286	-5.788	0.086	-0.302	-0.437	-1.519	-2.144
SUNTOP_SERI M82_287	-5.952	0.086	-0.342	-0.439	-1.519	-2.301
SUNTOP_SERI M82_288	-5.881	0.086	-0.307	-0.433	-1.519	-1.955
SUNTOP_SERI M82_289	-5.872	0.086	-0.267	-0.440	-1.519	-2.114
SUNTOP_SERI M82_290	-5.926	0.086	-0.255	-0.445	-1.520	-2.208
SUNTOP_SERI M82_291	-6.087	0.086	-0.356	-0.435	-1.519	-2.172
SUNTOP_SERI M82_292	-5.899	0.086	-0.330	-0.435	-1.519	-2.101
SUNTOP_SERI M82_294	-5.973	0.086	-0.255	-0.437	-1.520	-1.885
SUNTOP_SERI M82_295	-6.186	0.086	-0.324	-0.441	-1.520	-2.242
SUNTOP_SERI M82_296	-6.051	0.086	-0.267	-0.431	-1.519	-1.970
SUNTOP_SERI M82_297	-5.938	0.086	-0.336	-0.439	-1.520	-2.214
SUNTOP_SERI M82_298	-5.894	0.086	-0.287	-0.438	-1.520	-2.035
SUNTOP_SPITFIRE_1	-6.094	0.086	-0.214	-0.441	-1.520	-1.969
SUNTOP_SPITFIRE_10	-5.994	0.086	-0.365	-0.430	-1.519	-2.389
SUNTOP_SPITFIRE_12	-5.955	0.086	-0.345	-0.434	-1.520	-2.364

Table B.1 – continued from previous page

Genotype	*Intercept*	*abs(x)*	*y*	*abs(x)y*	*abs(x)^2*	*y^2*
SUNTOP_SPITFIRE_13	-5.898	0.086	-0.229	-0.439	-1.519	-1.991
SUNTOP_SPITFIRE_14	-5.930	0.086	-0.284	-0.433	-1.520	-2.190
SUNTOP_SPITFIRE_15	-5.791	0.086	-0.247	-0.443	-1.519	-2.141
SUNTOP_SPITFIRE_16	-5.838	0.086	-0.308	-0.444	-1.519	-2.331
SUNTOP_SPITFIRE_17	-5.794	0.086	-0.297	-0.438	-1.519	-2.206
SUNTOP_SPITFIRE_18	-5.964	0.086	-0.264	-0.444	-1.519	-2.172
SUNTOP_SPITFIRE_19	-5.934	0.086	-0.341	-0.429	-1.519	-2.341
SUNTOP_SPITFIRE_2	-5.991	0.086	-0.295	-0.433	-1.520	-2.044
SUNTOP_SPITFIRE_20	-5.974	0.086	-0.351	-0.435	-1.520	-2.268
SUNTOP_SPITFIRE_21	-5.862	0.086	-0.315	-0.439	-1.520	-2.200
SUNTOP_SPITFIRE_22	-5.899	0.086	-0.273	-0.441	-1.519	-2.211
SUNTOP_SPITFIRE_24	-6.007	0.086	-0.332	-0.433	-1.520	-2.509
SUNTOP_SPITFIRE_25	-6.178	0.086	-0.327	-0.436	-1.520	-2.321
SUNTOP_SPITFIRE_26	-5.914	0.086	-0.262	-0.436	-1.519	-1.975
SUNTOP_SPITFIRE_28	-5.905	0.086	-0.295	-0.433	-1.520	-2.195
SUNTOP_SPITFIRE_29	-5.933	0.086	-0.326	-0.443	-1.520	-2.311
SUNTOP_SPITFIRE_3	-5.979	0.086	-0.333	-0.435	-1.520	-2.354
SUNTOP_SPITFIRE_30	-5.853	0.086	-0.257	-0.429	-1.520	-1.962
SUNTOP_SPITFIRE_31	-5.970	0.086	-0.364	-0.435	-1.519	-2.367
SUNTOP_SPITFIRE_32	-6.084	0.086	-0.271	-0.441	-1.519	-2.274
SUNTOP_SPITFIRE_33	-6.193	0.086	-0.335	-0.436	-1.520	-2.257
SUNTOP_SPITFIRE_34	-5.892	0.086	-0.311	-0.436	-1.520	-2.251
SUNTOP_SPITFIRE_35	-6.103	0.086	-0.302	-0.443	-1.520	-2.328
SUNTOP_SPITFIRE_36	-6.014	0.086	-0.373	-0.434	-1.519	-2.345
SUNTOP_SPITFIRE_38	-5.900	0.086	-0.264	-0.438	-1.520	-2.090
SUNTOP_SPITFIRE_39	-5.950	0.086	-0.347	-0.436	-1.519	-2.299
SUNTOP_SPITFIRE_4	-6.049	0.086	-0.282	-0.437	-1.520	-2.150
SUNTOP_SPITFIRE_40	-5.941	0.086	-0.326	-0.426	-1.520	-2.132
SUNTOP_SPITFIRE_41	-6.006	0.086	-0.309	-0.433	-1.520	-2.076
SUNTOP_SPITFIRE_42	-5.938	0.086	-0.304	-0.442	-1.520	-2.485
SUNTOP_SPITFIRE_43	-5.842	0.086	-0.236	-0.461	-1.520	-2.478
SUNTOP_SPITFIRE_44	-5.749	0.086	-0.231	-0.433	-1.520	-1.909
SUNTOP_SPITFIRE_46	-5.932	0.086	-0.282	-0.441	-1.520	-2.278
SUNTOP_SPITFIRE_47	-5.935	0.086	-0.303	-0.434	-1.520	-2.353
SUNTOP_SPITFIRE_48	-6.140	0.086	-0.367	-0.438	-1.519	-2.647
SUNTOP_SPITFIRE_5	-6.021	0.086	-0.284	-0.430	-1.520	-2.052

Table B.1 – continued from previous page

Genotype	*Intercept*	*abs(x)*	*y*	*abs(x)y*	*abs(x)²*	*y²*
SUNTOP_SPITFIRE_50	-5.892	0.086	-0.358	-0.435	-1.519	-2.398
SUNTOP_SPITFIRE_51	-5.836	0.086	-0.317	-0.437	-1.519	-2.195
SUNTOP_SPITFIRE_52	-5.810	0.086	-0.336	-0.440	-1.519	-2.372
SUNTOP_SPITFIRE_53	-5.974	0.086	-0.334	-0.430	-1.520	-2.189
SUNTOP_SPITFIRE_54	-5.939	0.086	-0.347	-0.443	-1.520	-2.620
SUNTOP_SPITFIRE_6	-5.899	0.086	-0.349	-0.433	-1.520	-2.410
SUNTOP_SPITFIRE_7	-5.899	0.086	-0.279	-0.435	-1.520	-2.153
SUNTOP_SPITFIRE_8	-5.962	0.086	-0.246	-0.444	-1.520	-2.169
SUNTOP_SPITFIRE_9	-5.935	0.086	-0.347	-0.432	-1.520	-2.298
SUNTOP_WYLIE_341	-5.867	0.086	-0.324	-0.440	-1.520	-2.241
SUNTOP_WYLIE_342	-5.868	0.086	-0.240	-0.443	-1.520	-2.142
SUNTOP_WYLIE_344	-5.716	0.086	-0.307	-0.429	-1.519	-2.177
SUNTOP_WYLIE_345	-5.990	0.086	-0.344	-0.432	-1.519	-2.314
SUNTOP_WYLIE_346	-5.918	0.086	-0.356	-0.434	-1.520	-2.318
SUNTOP_WYLIE_347	-6.106	0.086	-0.301	-0.437	-1.519	-2.081
SUNTOP_WYLIE_348	-6.014	0.086	-0.371	-0.435	-1.520	-2.484
SUNTOP_WYLIE_349	-5.923	0.086	-0.275	-0.435	-1.520	-2.139
SUNTOP_WYLIE_350	-6.193	0.086	-0.311	-0.435	-1.520	-2.187
SUNTOP_WYLIE_351	-5.930	0.086	-0.318	-0.430	-1.519	-2.128
SUNTOP_WYLIE_352	-5.935	0.086	-0.311	-0.433	-1.519	-2.181
SUNTOP_WYLIE_353	-5.845	0.086	-0.321	-0.434	-1.520	-2.216
SUNTOP_WYLIE_354	-6.086	0.086	-0.367	-0.427	-1.520	-2.248
SUNTOP_WYLIE_355	-6.015	0.086	-0.355	-0.437	-1.520	-2.213
SUNTOP_WYLIE_356	-5.984	0.086	-0.371	-0.420	-1.519	-2.564
SUNTOP_WYLIE_357	-5.879	0.086	-0.304	-0.432	-1.520	-2.167
SUNTOP_WYLIE_358	-5.909	0.086	-0.300	-0.431	-1.520	-2.071
SUNTOP_WYLIE_359	-5.858	0.086	-0.325	-0.438	-1.519	-2.175
SUNTOP_WYLIE_360	-5.851	0.086	-0.247	-0.436	-1.519	-2.138
SUNTOP_WYLIE_361	-5.925	0.086	-0.333	-0.440	-1.520	-2.200
SUNTOP_WYLIE_362	-5.857	0.086	-0.283	-0.428	-1.519	-2.038
SUNTOP_WYLIE_363	-6.056	0.086	-0.405	-0.423	-1.519	-2.462
SUNTOP_WYLIE_364	-6.217	0.086	-0.365	-0.425	-1.520	-2.356
SUNTOP_WYLIE_365	-5.923	0.086	-0.307	-0.438	-1.520	-2.228
SUNTOP_WYLIE_366	-5.918	0.086	-0.278	-0.438	-1.520	-2.083
SUNTOP_WYLIE_367	-5.960	0.086	-0.334	-0.428	-1.520	-2.230
SUNTOP_WYLIE_368	-5.916	0.086	-0.306	-0.420	-1.520	-2.090

Table B.1 – continued from previous page

Genotype	Intercept	$abs(x)$	y	$abs(x)y$	$abs(x)^2$	y^2
SUNTOP_WYLIE_369	-5.843	0.086	-0.320	-0.440	-1.519	-2.226
SUNTOP_WYLIE_371	-5.839	0.086	-0.289	-0.439	-1.520	-2.154
SUNTOP_WYLIE_372	-5.832	0.086	-0.325	-0.435	-1.520	-2.215
SUNTOP_WYLIE_373	-5.871	0.086	-0.308	-0.440	-1.519	-2.324
SUNTOP_WYLIE_374	-5.948	0.086	-0.311	-0.437	-1.519	-2.360
SUNTOP_WYLIE_376	-5.832	0.086	-0.378	-0.441	-1.520	-2.291
SUNTOP_WYLIE_377	-5.819	0.086	-0.333	-0.427	-1.520	-2.375
SUNTOP_WYLIE_378	-5.850	0.086	-0.315	-0.434	-1.519	-2.107
SUNTOP_WYLIE_379	-5.890	0.086	-0.336	-0.436	-1.519	-2.281
SUNTOP_WYLIE_380	-6.105	0.086	-0.338	-0.438	-1.520	-2.283
SUNTOP_WYLIE_381	-6.032	0.086	-0.374	-0.420	-1.519	-2.467
SUNTOP_WYLIE_382	-6.114	0.086	-0.389	-0.421	-1.520	-2.406
SUNTOP_ZWB10-37_383	-5.935	0.086	-0.310	-0.435	-1.519	-2.131
SUNTOP_ZWB10-37_384	-6.170	0.086	-0.344	-0.444	-1.520	-2.321
SUNTOP_ZWB10-37_385	-5.867	0.086	-0.308	-0.440	-1.519	-2.127
SUNTOP_ZWB10-37_386	-5.881	0.086	-0.303	-0.441	-1.520	-2.159
SUNTOP_ZWB10-37_387	-6.107	0.086	-0.371	-0.440	-1.520	-2.523
SUNTOP_ZWB10-37_388	-5.902	0.086	-0.324	-0.438	-1.519	-2.301
SUNTOP_ZWB10-37_389	-6.046	0.086	-0.288	-0.435	-1.520	-2.127
SUNTOP_ZWB10-37_390	-5.952	0.086	-0.320	-0.447	-1.520	-2.346
SUNTOP_ZWB10-37_392	-6.166	0.086	-0.348	-0.437	-1.519	-2.336
SUNTOP_ZWB10-37_393	-6.047	0.086	-0.331	-0.443	-1.520	-2.207
SUNTOP_ZWB10-37_394	-5.895	0.086	-0.327	-0.437	-1.519	-2.197
SUNTOP_ZWB10-37_395	-6.033	0.086	-0.290	-0.439	-1.519	-2.269
SUNTOP_ZWB10-37_396	-5.968	0.086	-0.318	-0.434	-1.519	-2.106
SUNTOP_ZWB10-37_397	-6.078	0.086	-0.376	-0.433	-1.520	-2.354
SUNTOP_ZWB10-37_398	-5.982	0.086	-0.333	-0.435	-1.519	-2.153
SUNTOP_ZWB10-37_400	-5.889	0.086	-0.310	-0.437	-1.519	-2.201
SUNTOP_ZWB10-37_403	-5.832	0.086	-0.274	-0.436	-1.520	-2.104
SUNTOP_ZWB10-37_404	-5.951	0.086	-0.311	-0.436	-1.520	-2.187
SUNTOP_ZWB10-37_405	-5.846	0.086	-0.291	-0.436	-1.519	-1.971
SUNTOP_ZWB10-37_406	-6.014	0.086	-0.309	-0.439	-1.520	-2.191
SUNTOP_ZWB10-37_407	-5.971	0.086	-0.347	-0.429	-1.519	-2.161
SUNTOP_ZWB10-37_408	-6.203	0.086	-0.351	-0.435	-1.519	-2.265
SUNTOP_ZWB10-37_409	-5.975	0.086	-0.353	-0.434	-1.519	-2.187
SUNTOP_ZWB10-37_410	-5.953	0.086	-0.284	-0.437	-1.520	-2.075

Table B.1 – continued from previous page

Genotype	*Intercept*	*abs(x)*	*y*	*abs(x)y*	*abs(x)²*	*y²*
SUNTOP_ZWB10-37_411	-5.956	0.086	-0.274	-0.434	-1.520	-2.036
SUNTOP_ZWB10-37_412	-5.848	0.086	-0.264	-0.441	-1.519	-2.117
SUNTOP_ZWB10-37_413	-6.208	0.086	-0.394	-0.436	-1.520	-2.397
SUNTOP_ZWB10-37_414	-5.982	0.086	-0.299	-0.439	-1.520	-2.180
SUNTOP_ZWB10-37_415	-5.554	0.086	-0.210	-0.441	-1.519	-1.958
SUNTOP_ZWB10-37_416	-5.992	0.086	-0.354	-0.439	-1.520	-2.531
SUNTOP_ZWB10-37_417	-5.851	0.086	-0.268	-0.430	-1.520	-1.929
SUNTOP_ZWB10-37_418	-5.883	0.086	-0.323	-0.440	-1.519	-2.222
SUNTOP_ZWB10-37_419	-5.839	0.086	-0.235	-0.432	-1.520	-1.971
SUNTOP_ZWB10-37_420	-5.946	0.086	-0.339	-0.435	-1.520	-2.518
SUNTOP_ZWB10-37_422	-5.920	0.086	-0.333	-0.437	-1.519	-2.163
SUNTOP_ZWB10-37_423	-5.953	0.086	-0.269	-0.436	-1.519	-2.069
SUNTOP_ZWB10-37_424	-6.160	0.086	-0.405	-0.430	-1.519	-2.553
SUNTOP_ZWW10-128_425	-6.005	0.086	-0.280	-0.438	-1.519	-2.177
SUNTOP_ZWW10-128_426	-6.033	0.086	-0.320	-0.435	-1.520	-2.084
SUNTOP_ZWW10-128_427	-5.957	0.086	-0.308	-0.437	-1.520	-2.242
SUNTOP_ZWW10-128_429	-5.857	0.086	-0.291	-0.430	-1.520	-1.998
SUNTOP_ZWW10-128_430	-6.058	0.086	-0.359	-0.435	-1.519	-2.246
SUNTOP_ZWW10-128_432	-5.919	0.086	-0.319	-0.433	-1.519	-2.171
SUNTOP_ZWW10-128_433	-5.910	0.086	-0.265	-0.448	-1.519	-2.437
SUNTOP_ZWW10-128_434	-5.880	0.086	-0.368	-0.432	-1.520	-2.163
SUNTOP_ZWW10-128_435	-6.086	0.086	-0.311	-0.436	-1.520	-2.160
SUNTOP_ZWW10-128_436	-5.949	0.086	-0.298	-0.431	-1.519	-2.020
SUNTOP_ZWW10-128_437	-6.071	0.086	-0.334	-0.441	-1.519	-2.611
SUNTOP_ZWW10-128_438	-6.074	0.086	-0.336	-0.436	-1.519	-2.503
SUNTOP_ZWW10-128_439	-5.979	0.086	-0.353	-0.432	-1.520	-2.248
SUNTOP_ZWW10-128_440	-6.050	0.086	-0.290	-0.430	-1.520	-1.960
SUNTOP_ZWW10-128_441	-6.085	0.086	-0.363	-0.425	-1.520	-2.406
SUNTOP_ZWW10-128_443	-6.012	0.086	-0.323	-0.434	-1.520	-2.148
SUNTOP_ZWW10-128_444	-5.925	0.086	-0.248	-0.444	-1.520	-2.093
SUNTOP_ZWW10-128_445	-5.808	0.086	-0.236	-0.432	-1.519	-1.870
SUNTOP_ZWW10-128_446	-5.917	0.086	-0.312	-0.438	-1.519	-2.153
SUNTOP_ZWW10-128_448	-6.081	0.086	-0.285	-0.434	-1.520	-2.096
SUNTOP_ZWW10-128_449	-5.899	0.086	-0.292	-0.438	-1.520	-2.046
SUNTOP_ZWW10-128_450	-6.049	0.086	-0.306	-0.437	-1.519	-2.090
SUNTOP_ZWW10-128_451	-6.116	0.086	-0.357	-0.433	-1.520	-2.206

Genotype	*Intercept*	*abs(x)*	*y*	*abs(x)y*	*abs(x)^2*	*y^2*
SUNTOP_ZWW10-128_452	-5.955	0.086	-0.290	-0.442	-1.520	-2.250
SUNTOP_ZWW10-128_453	-6.157	0.086	-0.312	-0.427	-1.519	-2.076
SUNTOP_ZWW10-128_454	-5.897	0.086	-0.276	-0.439	-1.520	-2.063
SUNTOP_ZWW10-128_455	-6.066	0.086	-0.300	-0.437	-1.519	-2.178
SUNTOP_ZWW10-128_456	-5.914	0.086	-0.306	-0.433	-1.519	-2.079
SUNTOP_ZWW10-128_457	-5.775	0.086	-0.275	-0.442	-1.520	-2.137
SUNTOP_ZWW10-128_458	-5.871	0.086	-0.260	-0.425	-1.520	-1.847
SUNTOP_ZWW10-128_459	-5.851	0.086	-0.269	-0.433	-1.519	-1.963
SUNTOP_ZWW10-128_460	-5.894	0.086	-0.323	-0.432	-1.519	-2.142
SUNTOP_ZWW10-128_461	-5.968	0.086	-0.281	-0.437	-1.520	-2.063
SUNTOP_ZWW10-128_462	-5.849	0.086	-0.299	-0.436	-1.520	-2.104
SUNTOP_ZWW10-128_463	-5.773	0.086	-0.275	-0.437	-1.519	-2.130
SUNTOP_ZWW10-128_464	-6.011	0.086	-0.317	-0.432	-1.520	-2.028
SUNTOP_ZWW10-128_465	-5.943	0.086	-0.322	-0.433	-1.519	-2.103
SUNTOP_ZWW10-128_466	-5.722	0.086	-0.266	-0.447	-1.520	-1.976
ZWB10-37_P1	-6.139	0.086	-0.390	-0.463	-1.520	-2.885
ZWW10-128_PP	-5.859	0.086	-0.321	-0.437	-1.520	-1.989

B.2   Univariate weighted genotype predictions

Table B.2: The genotype predictions for each weighted univariate linear mixed model, where each estimated parameter has its own model. The full set of genotype predictions are presented here, and it is important to note that these predictions are on the transformed data scale with the exception of *intercept* which did not require transforming.

Genotype	*Intercept*	*abs(x)*	*y*	*abs(x)y*	*abs(x)^2*	*y^2*
DHARWAR DRY_PP	-5.784	0.032	-0.360	-0.429	-1.144	-2.008
DRYSDALE_PP	-5.939	0.076	-0.414	-0.503	-1.279	-2.553
EGA GREGORY_PP	-5.807	0.026	-0.285	-0.354	-1.099	-1.845
EGA WYLIE_PP	-6.069	0.121	-0.471	-0.204	-1.586	-2.561
FAC10-16_P1	-5.649	0.025	-0.272	-0.599	-1.316	-1.997
MACE_PP	-5.717	0.068	-0.174	-0.629	-1.369	-1.871
MACE_SB062_123	-5.719	0.067	-0.275	-0.421	-1.290	-2.019
RIL114_PP	-5.938	0.075	-0.329	-0.229	-1.224	-1.937

Table B.2 – continued from previous page

Genotype	Intercept	abs(x)	y	abs(x)y	abs(x)^2	y^2
SB062_PP	-5.899	0.093	-0.262	-0.269	-1.009	-1.696
SERI M82_PP	-6.064	0.068	-0.436	-0.565	-1.340	-2.490
SPITFIRE-P9	-5.773	0.087	-0.137	-1.190	-1.522	-2.094
SUNTOP_DHARWAH DRY_1	-5.861	0.066	-0.363	-0.387	-1.237	-2.101
SUNTOP_DHARWAH DRY_10	-5.805	0.054	-0.316	-0.361	-1.309	-1.958
SUNTOP_DHARWAH DRY_11	-5.830	0.078	-0.301	-0.320	-1.356	-1.852
SUNTOP_DHARWAH DRY_12	-5.787	0.029	-0.346	-0.422	-1.187	-2.123
SUNTOP_DHARWAH DRY_13	-5.900	0.088	-0.364	-0.290	-1.434	-2.128
SUNTOP_DHARWAH DRY_14	-5.959	0.054	-0.345	-0.324	-1.039	-1.967
SUNTOP_DHARWAH DRY_15	-5.810	0.090	-0.316	-0.592	-1.720	-2.092
SUNTOP_DHARWAH DRY_16	-6.042	0.087	-0.388	-0.544	-1.454	-2.109
SUNTOP_DHARWAH DRY_17	-5.922	0.063	-0.300	-0.393	-1.325	-1.908
SUNTOP_DHARWAH DRY_18	-5.906	0.027	-0.341	-0.408	-1.035	-2.182
SUNTOP_DHARWAH DRY_19	-6.087	0.091	-0.382	-0.337	-1.186	-2.307
SUNTOP_DHARWAH DRY_2	-6.026	0.107	-0.309	-0.540	-1.413	-1.924
SUNTOP_DHARWAH DRY_20	-5.991	0.082	-0.330	-0.495	-1.293	-2.215
SUNTOP_DHARWAH DRY_21	-5.881	0.089	-0.348	-0.186	-1.320	-2.217
SUNTOP_DHARWAH DRY_22	-6.091	0.105	-0.227	-0.437	-1.824	-2.338
SUNTOP_DHARWAH DRY_23	-5.746	0.046	-0.332	-0.293	-1.238	-1.860
SUNTOP_DHARWAH DRY_24	-6.044	0.059	-0.334	-0.382	-1.261	-1.981
SUNTOP_DHARWAH DRY_25	-5.771	0.063	-0.290	-0.626	-1.482	-2.159
SUNTOP_DHARWAH DRY_26	-5.998	0.067	-0.323	-0.703	-1.270	-2.391
SUNTOP_DHARWAH DRY_27	-6.096	0.053	-0.355	-0.404	-1.163	-2.239
SUNTOP_DHARWAH DRY_28	-6.001	0.075	-0.322	-0.285	-1.241	-1.981
SUNTOP_DHARWAH DRY_29	-5.882	0.082	-0.296	-0.604	-1.462	-2.358
SUNTOP_DHARWAH DRY_3	-5.777	0.069	-0.252	-0.319	-1.306	-1.592
SUNTOP_DHARWAH DRY_30	-5.923	0.084	-0.312	-0.283	-1.472	-1.937
SUNTOP_DHARWAH DRY_31	-5.789	0.037	-0.318	-0.401	-1.157	-1.898
SUNTOP_DHARWAH DRY_32	-5.902	0.078	-0.314	-0.556	-1.355	-2.363
SUNTOP_DHARWAH DRY_33	-5.910	0.156	-0.252	-0.593	-1.557	-2.181
SUNTOP_DHARWAH DRY_34	-5.844	0.040	-0.333	-0.396	-1.150	-2.004
SUNTOP_DHARWAH DRY_35	-5.858	0.064	-0.336	-0.393	-1.354	-2.008
SUNTOP_DHARWAH DRY_36	-5.920	0.060	-0.343	-0.308	-1.177	-2.047
SUNTOP_DHARWAH DRY_37	-5.796	0.081	-0.304	-0.585	-1.614	-2.069
SUNTOP_DHARWAH DRY_38	-6.014	0.061	-0.381	-0.352	-1.210	-2.275
SUNTOP_DHARWAH DRY_39	-5.850	0.036	-0.342	-0.496	-1.424	-2.119

Table B.2 – continued from previous page

Genotype	Intercept	abs(x)	y	abs(x)y	abs(x)²	y²
SUNTOP_DHARWAH DRY_4	-5.783	0.010	-0.306	-0.391	-1.063	-1.841
SUNTOP_DHARWAH DRY_40	-5.720	0.023	-0.263	-0.468	-1.018	-1.812
SUNTOP_DHARWAH DRY_41	-5.953	0.057	-0.361	-0.277	-1.027	-2.095
SUNTOP_DHARWAH DRY_42	-5.824	0.026	-0.301	-0.613	-1.164	-2.583
SUNTOP_DHARWAH DRY_43	-6.115	0.111	-0.359	-0.479	-1.460	-2.283
SUNTOP_DHARWAH DRY_44	-5.865	0.059	-0.315	-0.517	-1.467	-2.113
SUNTOP_DHARWAH DRY_45	-5.981	0.115	-0.270	-0.548	-1.657	-1.974
SUNTOP_DHARWAH DRY_46	-6.030	0.093	-0.338	-0.439	-1.373	-2.362
SUNTOP_DHARWAH DRY_47	-5.888	0.061	-0.304	-0.382	-1.267	-2.019
SUNTOP_DHARWAH DRY_48	-5.812	0.061	-0.332	-0.355	-1.452	-1.938
SUNTOP_DHARWAH DRY_49	-6.037	0.086	-0.383	-0.220	-1.108	-2.017
SUNTOP_DHARWAH DRY_5	-5.910	0.033	-0.331	-0.403	-0.916	-2.180
SUNTOP_DHARWAH DRY_50	-5.800	0.055	-0.315	-0.304	-1.257	-1.935
SUNTOP_DHARWAH DRY_51	-6.140	0.111	-0.328	-0.680	-1.527	-2.890
SUNTOP_DHARWAH DRY_52	-5.877	0.061	-0.300	-0.525	-1.354	-2.138
SUNTOP_DHARWAH DRY_6	-5.808	0.047	-0.263	-0.636	-1.425	-1.867
SUNTOP_DHARWAH DRY_7	-6.013	0.065	-0.244	-0.826	-1.282	-2.611
SUNTOP_DHARWAH DRY_8	-5.797	0.057	-0.320	-0.450	-1.380	-2.093
SUNTOP_DHARWAH DRY_9	-5.829	0.031	-0.332	-0.392	-0.926	-2.030
SUNTOP_DRYSDALE_100	-5.853	0.039	-0.335	-0.442	-1.281	-2.130
SUNTOP_DRYSDALE_101	-5.952	0.056	-0.328	-0.331	-0.962	-2.082
SUNTOP_DRYSDALE_102	-5.896	0.070	-0.296	-0.644	-1.387	-2.150
SUNTOP_DRYSDALE_103	-5.894	0.086	-0.322	-0.523	-1.162	-2.275
SUNTOP_DRYSDALE_104	-5.928	0.076	-0.319	-0.455	-1.202	-2.263
SUNTOP_DRYSDALE_53	-6.153	0.112	-0.425	-0.207	-1.266	-2.633
SUNTOP_DRYSDALE_54	-5.640	-0.030	-0.318	-0.430	-0.952	-2.102
SUNTOP_DRYSDALE_55	-5.896	0.083	-0.331	-0.595	-1.519	-2.507
SUNTOP_DRYSDALE_56	-6.047	0.086	-0.391	-0.407	-1.245	-2.532
SUNTOP_DRYSDALE_57	-5.841	0.135	-0.248	-0.742	-1.432	-2.123
SUNTOP_DRYSDALE_58	-6.094	0.040	-0.434	-0.512	-1.015	-2.254
SUNTOP_DRYSDALE_59	-5.976	0.076	-0.367	-0.398	-1.274	-2.283
SUNTOP_DRYSDALE_60	-5.841	0.065	-0.305	-0.509	-1.249	-2.245
SUNTOP_DRYSDALE_61	-5.896	0.012	-0.303	-0.514	-0.992	-2.066
SUNTOP_DRYSDALE_62	-5.864	0.053	-0.322	-0.566	-1.321	-2.236
SUNTOP_DRYSDALE_64	-6.185	0.043	-0.448	-0.428	-1.132	-2.139
SUNTOP_DRYSDALE_65	-5.849	0.029	-0.317	-0.381	-0.838	-2.064

Table B.2 – continued from previous page

Genotype	Intercept	abs(x)	y	abs(x)y	abs(x)²	y²
SUNTOP_DRYSDALE_66	-5.851	0.068	-0.330	-0.420	-1.242	-2.070
SUNTOP_DRYSDALE_67	-5.851	0.081	-0.342	-0.325	-1.328	-1.977
SUNTOP_DRYSDALE_68	-5.840	0.060	-0.342	-0.334	-1.124	-2.110
SUNTOP_DRYSDALE_69	-5.809	0.013	-0.331	-0.585	-1.156	-2.315
SUNTOP_DRYSDALE_70	-5.954	0.072	-0.338	-0.362	-1.298	-2.003
SUNTOP_DRYSDALE_71	-5.947	0.121	-0.342	-0.133	-1.652	-2.175
SUNTOP_DRYSDALE_72	-6.009	0.065	-0.365	-0.551	-1.531	-2.608
SUNTOP_DRYSDALE_73	-6.087	0.132	-0.378	-0.228	-1.521	-2.103
SUNTOP_DRYSDALE_74	-5.936	0.048	-0.339	-0.480	-1.186	-2.124
SUNTOP_DRYSDALE_75	-5.881	0.063	-0.321	-0.454	-1.326	-2.040
SUNTOP_DRYSDALE_76	-5.913	0.053	-0.356	-0.347	-1.238	-2.129
SUNTOP_DRYSDALE_77	-6.213	0.129	-0.389	-0.300	-1.341	-2.079
SUNTOP_DRYSDALE_78	-5.864	0.108	-0.345	-0.281	-1.497	-2.061
SUNTOP_DRYSDALE_79	-6.070	0.081	-0.351	-0.564	-1.077	-2.181
SUNTOP_DRYSDALE_80	-6.003	0.037	-0.367	-0.525	-1.136	-2.180
SUNTOP_DRYSDALE_81	-6.160	0.173	-0.312	-0.510	-1.556	-2.006
SUNTOP_DRYSDALE_83	-5.847	0.056	-0.353	-0.372	-1.206	-1.999
SUNTOP_DRYSDALE_84	-5.954	0.065	-0.413	-0.228	-1.322	-2.371
SUNTOP_DRYSDALE_85	-5.997	0.097	-0.361	-0.388	-1.451	-2.195
SUNTOP_DRYSDALE_86	-5.921	0.100	-0.305	-0.501	-1.501	-2.103
SUNTOP_DRYSDALE_87	-6.016	0.053	-0.374	-0.413	-1.276	-2.309
SUNTOP_DRYSDALE_88	-5.850	0.106	-0.192	-0.635	-1.609	-1.949
SUNTOP_DRYSDALE_89	-5.743	0.035	-0.324	-0.476	-1.193	-2.088
SUNTOP_DRYSDALE_90	-6.008	0.131	-0.353	-0.269	-1.740	-2.115
SUNTOP_DRYSDALE_91	-5.735	0.058	-0.294	-0.369	-1.238	-1.893
SUNTOP_DRYSDALE_92	-5.906	0.101	-0.304	-0.531	-1.366	-2.056
SUNTOP_DRYSDALE_93	-6.121	0.112	-0.420	-0.066	-1.307	-2.119
SUNTOP_DRYSDALE_94	-5.942	0.077	-0.348	-0.427	-1.339	-2.170
SUNTOP_DRYSDALE_95	-5.877	0.058	-0.305	-0.644	-1.296	-2.320
SUNTOP_DRYSDALE_96	-5.849	0.081	-0.307	-0.420	-1.388	-1.997
SUNTOP_DRYSDALE_97	-5.986	0.077	-0.313	-0.494	-1.258	-2.187
SUNTOP_DRYSDALE_98	-5.901	0.092	-0.296	-0.545	-1.584	-2.270
SUNTOP_DRYSDALE_99	-5.926	0.078	-0.341	-0.376	-1.359	-2.091
SUNTOP_EGA GREGORY_108	-5.860	0.062	-0.281	-0.451	-1.225	-2.074
SUNTOP_EGA GREGORY_109	-5.876	0.047	-0.325	-0.463	-1.132	-2.236
SUNTOP_EGA GREGORY_110	-6.064	0.064	-0.356	-0.407	-1.077	-2.220

Genotype	*Intercept*	*abs(x)*	*y*	*abs(x)y*	*abs(x)^2*	*y^2*
SUNTOP_EGA GREGORY_111	-5.789	0.013	-0.266	-0.607	-1.120	-2.283
SUNTOP_EGA GREGORY_112	-5.751	0.017	-0.239	-0.565	-1.145	-1.867
SUNTOP_EGA GREGORY_113	-6.028	0.112	-0.281	-0.486	-1.490	-1.926
SUNTOP_EGA GREGORY_114	-5.892	0.066	-0.325	-0.461	-1.264	-2.178
SUNTOP_EGA GREGORY_115	-5.867	0.074	-0.287	-0.514	-1.279	-1.879
SUNTOP_EGA GREGORY_116	-6.008	0.093	-0.314	-0.434	-1.324	-2.144
SUNTOP_EGA GREGORY_117	-5.818	0.050	-0.303	-0.634	-1.418	-2.296
SUNTOP_EGA GREGORY_118	-5.905	0.051	-0.336	-0.293	-1.188	-2.134
SUNTOP_EGA GREGORY_119	-5.636	0.008	-0.324	-0.531	-1.163	-2.190
SUNTOP_EGA GREGORY_120	-5.756	0.019	-0.313	-0.672	-1.165	-2.627
SUNTOP_EGA GREGORY_121	-5.902	0.080	-0.331	-0.342	-1.403	-2.117
SUNTOP_EGA GREGORY_122	-5.819	0.079	-0.249	-0.558	-1.458	-2.023
SUNTOP_EGA GREGORY_123	-5.922	0.073	-0.305	-0.427	-1.219	-1.847
SUNTOP_EGA GREGORY_124	-5.821	0.059	-0.304	-0.449	-1.274	-1.981
SUNTOP_EGA GREGORY_125	-5.931	0.062	-0.339	-0.491	-1.281	-2.207
SUNTOP_EGA GREGORY_126	-5.849	0.055	-0.346	-0.343	-1.263	-2.224
SUNTOP_EGA GREGORY_127	-5.912	0.063	-0.311	-0.540	-1.424	-2.184
SUNTOP_EGA GREGORY_128	-5.773	0.052	-0.287	-0.400	-1.268	-1.936
SUNTOP_EGA GREGORY_129	-5.751	-0.008	-0.317	-0.622	-1.193	-2.207
SUNTOP_EGA GREGORY_130	-6.151	0.134	-0.293	-0.618	-1.553	-2.259
SUNTOP_EGA GREGORY_131	-5.686	0.005	-0.293	-0.474	-0.978	-2.059
SUNTOP_EGA GREGORY_132	-5.946	0.077	-0.316	-0.552	-1.531	-2.144
SUNTOP_EGA GREGORY_133	-5.964	0.080	-0.313	-0.445	-1.308	-2.087
SUNTOP_EGA GREGORY_134	-5.988	0.065	-0.363	-0.416	-1.315	-2.134
SUNTOP_EGA GREGORY_135	-5.981	0.164	-0.318	-0.185	-2.529	-1.951
SUNTOP_EGA GREGORY_136	-5.907	0.059	-0.338	-0.177	-1.908	-2.028
SUNTOP_EGA GREGORY_137	-5.853	0.008	-0.383	-0.347	-0.793	-2.412
SUNTOP_EGA GREGORY_138	-5.867	0.046	-0.297	-0.409	-1.211	-2.090
SUNTOP_EGA GREGORY_139	-5.825	0.043	-0.345	-0.462	-1.179	-2.274
SUNTOP_EGA GREGORY_140	-6.036	0.088	-0.414	-0.362	-1.442	-2.630
SUNTOP_EGA GREGORY_141	-5.908	0.068	-0.347	-0.339	-1.379	-2.014
SUNTOP_EGA GREGORY_142	-5.929	0.074	-0.343	-0.356	-1.367	-2.090
SUNTOP_EGA GREGORY_143	-5.798	0.053	-0.311	-0.614	-1.459	-2.116
SUNTOP_EGA GREGORY_144	-6.049	0.080	-0.329	-0.519	-1.384	-2.153
SUNTOP_EGA GREGORY_145	-5.983	0.046	-0.204	-0.580	-1.228	-1.738
SUNTOP_EGA GREGORY_146	-5.792	0.056	-0.253	-0.507	-1.227	-2.055

Table B.2 – continued from previous page

Genotype	Intercept	abs(x)	y	abs(x)y	abs(x)²	y²
SUNTOP_EGA GREGORY_147	-5.956	0.068	-0.360	-0.410	-1.243	-2.298
SUNTOP_EGA GREGORY_148	-5.923	0.084	-0.272	-0.564	-1.284	-2.066
SUNTOP_EGA GREGORY_149	-5.794	0.056	-0.270	-0.452	-1.263	-1.977
SUNTOP_FAC10-16_150	-5.917	0.056	-0.403	-0.379	-1.356	-2.314
SUNTOP_FAC10-16_151	-5.937	0.076	-0.311	-0.403	-1.379	-2.074
SUNTOP_FAC10-16_152	-5.972	0.117	-0.287	-0.402	-1.522	-1.913
SUNTOP_FAC10-16_153	-5.938	0.059	-0.357	-0.438	-1.224	-2.242
SUNTOP_FAC10-16_154	-5.842	0.062	-0.322	-0.466	-1.498	-2.064
SUNTOP_FAC10-16_155	-5.847	0.038	-0.340	-0.235	-1.087	-2.006
SUNTOP_FAC10-16_156	-5.797	0.015	-0.356	-0.394	-0.984	-2.155
SUNTOP_FAC10-16_157	-6.095	0.168	-0.248	-0.588	-1.842	-2.109
SUNTOP_FAC10-16_158	-5.740	0.021	-0.317	-0.568	-1.145	-2.099
SUNTOP_FAC10-16_159	-5.755	0.069	-0.246	-0.572	-1.369	-1.808
SUNTOP_FAC10-16_160	-6.008	0.065	-0.413	-0.294	-1.117	-2.450
SUNTOP_FAC10-16_161	-6.019	0.136	-0.361	-0.222	-1.622	-2.028
SUNTOP_FAC10-16_162	-5.786	0.073	-0.270	-0.337	-1.358	-1.768
SUNTOP_FAC10-16_163	-5.981	0.073	-0.260	-0.512	-1.308	-1.842
SUNTOP_FAC10-16_164	-5.935	0.061	-0.313	-0.562	-0.946	-2.159
SUNTOP_FAC10-16_165	-5.909	0.082	-0.295	-0.555	-1.251	-2.208
SUNTOP_FAC10-16_166	-5.865	0.059	-0.333	-0.321	-1.273	-2.125
SUNTOP_FAC10-16_167	-6.011	0.081	-0.359	-0.371	-1.285	-2.087
SUNTOP_FAC10-16_168	-5.909	0.067	-0.403	-0.222	-1.287	-2.245
SUNTOP_FAC10-16_169	-5.831	0.075	-0.336	-0.351	-1.382	-2.111
SUNTOP_FAC10-16_170	-5.996	0.131	-0.309	-0.693	-1.568	-2.595
SUNTOP_FAC10-16_171	-6.025	0.100	-0.311	-0.504	-1.413	-2.017
SUNTOP_FAC10-16_172	-5.980	0.108	-0.284	-0.434	-1.534	-1.991
SUNTOP_FAC10-16_173	-5.782	0.061	-0.299	-0.517	-1.249	-2.018
SUNTOP_FAC10-16_174	-5.923	0.086	-0.360	-0.345	-1.397	-2.266
SUNTOP_FAC10-16_175	-5.881	0.078	-0.351	-0.615	-1.482	-2.478
SUNTOP_FAC10-16_176	-5.988	0.095	-0.332	-0.351	-1.316	-1.899
SUNTOP_FAC10-16_177	-5.735	0.025	-0.284	-0.460	-1.040	-1.870
SUNTOP_FAC10-16_178	-6.024	0.031	-0.399	-0.440	-1.305	-2.199
SUNTOP_FAC10-16_179	-6.058	0.118	-0.299	-0.476	-1.466	-1.993
SUNTOP_FAC10-16_180	-6.066	0.071	-0.313	-0.392	-1.594	-2.025
SUNTOP_FAC10-16_181	-5.851	0.080	-0.325	-0.341	-1.376	-1.900
SUNTOP_FAC10-16_182	-5.982	0.069	-0.361	-0.383	-1.103	-2.261

Continued on next page

Table B.2 – continued from previous page

Genotype	*Intercept*	*abs(x)*	*y*	*abs(x)y*	*abs(x)²*	*y²*
SUNTOP_FAC10-16_183	-5.960	0.068	-0.385	-0.356	-1.339	-2.163
SUNTOP_FAC10-16_184	-5.956	0.082	-0.319	-0.445	-1.383	-2.060
SUNTOP_FAC10-16_185	-5.992	0.075	-0.385	-0.407	-1.374	-2.305
SUNTOP_FAC10-16_186	-5.885	0.085	-0.302	-0.425	-1.449	-1.886
SUNTOP_FAC10-16_187	-5.953	0.090	-0.347	-0.367	-1.338	-2.114
SUNTOP_FAC10-16_188	-6.383	0.110	-0.418	-0.585	-1.421	-2.276
SUNTOP_FAC10-16_189	-5.781	0.037	-0.285	-0.509	-1.260	-2.197
SUNTOP_FAC10-16_190	-5.973	0.083	-0.332	-0.393	-1.258	-1.951
SUNTOP_FAC10-16_191	-6.007	0.102	-0.309	-0.427	-1.450	-2.156
SUNTOP_PP	-6.143	0.058	-0.303	-0.459	-1.450	-1.965
SUNTOP_RIL114_299	-5.815	0.081	-0.277	-0.597	-1.492	-2.033
SUNTOP_RIL114_300	-6.044	0.121	-0.269	-0.510	-1.731	-2.098
SUNTOP_RIL114_301	-6.011	0.096	-0.336	-0.461	-1.487	-2.254
SUNTOP_RIL114_302	-5.808	0.073	-0.194	-0.542	-1.304	-1.861
SUNTOP_RIL114_303	-5.781	0.017	-0.346	-0.433	-1.205	-2.157
SUNTOP_RIL114_304	-5.883	0.051	-0.311	-0.427	-1.125	-2.028
SUNTOP_RIL114_305	-6.035	0.101	-0.301	-0.389	-1.316	-1.869
SUNTOP_RIL114_306	-5.861	0.045	-0.339	-0.408	-1.222	-2.201
SUNTOP_RIL114_307	-5.912	0.082	-0.323	-0.410	-1.277	-2.083
SUNTOP_RIL114_308	-5.884	0.065	-0.323	-0.386	-1.337	-2.154
SUNTOP_RIL114_309	-6.095	0.087	-0.361	-0.330	-1.241	-1.982
SUNTOP_RIL114_310	-6.003	0.101	-0.285	-0.501	-1.432	-2.208
SUNTOP_RIL114_311	-5.940	0.077	-0.347	-0.479	-1.224	-2.173
SUNTOP_RIL114_312	-5.918	0.054	-0.298	-0.410	-1.349	-1.957
SUNTOP_RIL114_313	-5.849	0.065	-0.276	-0.463	-1.361	-1.917
SUNTOP_RIL114_314	-5.876	0.037	-0.349	-0.359	-1.051	-2.000
SUNTOP_RIL114_315	-5.862	0.056	-0.319	-0.490	-1.224	-2.250
SUNTOP_RIL114_316	-5.870	0.081	-0.425	-0.150	-1.466	-2.142
SUNTOP_RIL114_317	-5.711	0.023	-0.283	-0.519	-1.162	-2.020
SUNTOP_RIL114_318	-5.823	0.064	-0.306	-0.415	-1.220	-1.924
SUNTOP_RIL114_319	-6.075	0.087	-0.361	-0.405	-1.381	-2.361
SUNTOP_RIL114_320	-6.141	0.138	-0.257	-0.592	-1.455	-2.108
SUNTOP_RIL114_321	-6.000	0.099	-0.336	-0.376	-1.414	-1.909
SUNTOP_RIL114_322	-5.945	0.025	-0.311	-0.377	-0.908	-1.990
SUNTOP_RIL114_323	-5.944	0.067	-0.300	-0.427	-1.233	-2.019
SUNTOP_RIL114_324	-5.883	0.110	-0.205	-0.550	-1.517	-1.744

Table B.2 – continued from previous page

Genotype	*Intercept*	*abs(x)*	*y*	*abs(x)y*	*abs(x)²*	*y²*
SUNTOP_RIL114_325	-6.304	0.187	-0.295	-0.601	-1.542	-2.049
SUNTOP_RIL114_326	-5.832	0.072	-0.272	-0.374	-1.276	-1.939
SUNTOP_RIL114_327	-5.816	0.025	-0.322	-0.504	-1.099	-2.107
SUNTOP_RIL114_328	-5.918	0.071	-0.321	-0.446	-1.332	-2.109
SUNTOP_RIL114_329	-5.833	0.089	-0.312	-0.552	-1.529	-2.098
SUNTOP_RIL114_330	-6.036	0.091	-0.327	-0.334	-1.246	-2.143
SUNTOP_RIL114_331	-5.816	0.080	-0.319	-0.512	-1.784	-2.007
SUNTOP_RIL114_333	-6.023	0.061	-0.361	-0.390	-1.258	-2.178
SUNTOP_RIL114_334	-5.918	0.077	-0.336	-0.362	-1.301	-2.006
SUNTOP_RIL114_335	-5.834	0.063	-0.323	-0.408	-1.352	-1.989
SUNTOP_RIL114_336	-5.910	0.024	-0.328	-0.389	-0.831	-1.930
SUNTOP_RIL114_337	-6.288	0.184	-0.324	-0.320	-1.898	-2.058
SUNTOP_RIL114_338	-5.837	0.063	-0.320	-0.387	-1.177	-1.894
SUNTOP_RIL114_339	-5.716	0.031	-0.282	-0.457	-1.244	-1.799
SUNTOP_RIL114_340	-6.016	0.099	-0.328	-0.368	-1.375	-1.950
SUNTOP_SB062_195	-5.904	0.028	-0.350	-0.353	-1.066	-2.184
SUNTOP_SB062_196	-5.752	0.071	-0.202	-0.735	-1.662	-1.727
SUNTOP_SB062_197	-5.914	0.081	-0.343	-0.376	-1.303	-2.072
SUNTOP_SB062_198	-5.769	0.019	-0.338	-0.390	-1.147	-1.963
SUNTOP_SB062_199	-5.941	0.103	-0.313	-0.427	-1.484	-1.794
SUNTOP_SB062_200	-5.968	0.093	-0.312	-0.556	-1.407	-1.986
SUNTOP_SB062_201	-5.915	0.062	-0.355	-0.529	-1.259	-2.189
SUNTOP_SB062_202	-5.928	0.081	-0.337	-0.569	-1.452	-2.167
SUNTOP_SB062_203	-5.856	0.061	-0.296	-0.464	-1.210	-2.153
SUNTOP_SB062_204	-5.903	0.027	-0.351	-0.258	-1.371	-2.072
SUNTOP_SB062_205	-5.886	0.081	-0.319	-0.439	-1.298	-2.055
SUNTOP_SB062_206	-6.055	0.106	-0.375	-0.307	-1.565	-2.111
SUNTOP_SB062_207	-6.082	0.082	-0.354	-0.335	-1.209	-1.930
SUNTOP_SB062_208	-6.034	0.096	-0.345	-0.343	-1.430	-2.200
SUNTOP_SB062_209	-5.946	0.130	-0.306	-0.162	-1.427	-1.827
SUNTOP_SB062_210	-5.937	0.080	-0.350	-0.497	-1.222	-2.206
SUNTOP_SB062_211	-6.031	0.071	-0.387	-0.364	-1.276	-1.944
SUNTOP_SB062_212	-5.869	0.042	-0.247	-0.587	-1.107	-1.749
SUNTOP_SB062_213	-5.947	0.083	-0.283	-0.550	-1.352	-1.925
SUNTOP_SB062_214	-5.893	0.086	-0.305	-0.509	-1.464	-2.089
SUNTOP_SB062_215	-5.954	0.094	-0.304	-0.314	-1.397	-1.986

Table B.2 – continued from previous page

Genotype	*Intercept*	*abs(x)*	*y*	*abs(x)y*	*abs(x)²*	*y²*
SUNTOP_SB062_216	-6.025	0.100	-0.354	-0.393	-1.684	-2.128
SUNTOP_SB062_217	-5.892	0.041	-0.353	-0.563	-1.298	-2.275
SUNTOP_SB062_218	-5.799	0.044	-0.243	-0.642	-1.426	-2.154
SUNTOP_SB062_219	-5.790	0.023	-0.321	-0.603	-1.046	-2.180
SUNTOP_SB062_220	-5.836	0.061	-0.305	-0.514	-1.339	-2.149
SUNTOP_SB062_221	-5.861	0.085	-0.337	-0.248	-1.444	-1.997
SUNTOP_SB062_222	-5.735	0.074	-0.266	-0.489	-1.451	-2.136
SUNTOP_SB062_223	-5.987	0.107	-0.160	-0.725	-1.846	-1.787
SUNTOP_SB062_224	-6.085	0.090	-0.357	-0.403	-1.376	-1.995
SUNTOP_SB062_225	-5.992	0.090	-0.342	-0.204	-1.366	-2.013
SUNTOP_SB062_226	-5.876	0.048	-0.373	-0.468	-1.306	-2.404
SUNTOP_SB062_227	-5.812	0.053	-0.312	-0.615	-1.367	-2.151
SUNTOP_SB062_228	-5.937	0.080	-0.247	-0.621	-1.342	-2.193
SUNTOP_SB062_229	-5.734	0.061	-0.276	-0.501	-1.393	-1.916
SUNTOP_SB062_230	-5.989	0.059	-0.323	-0.443	-1.042	-2.034
SUNTOP_SB062_231	-6.001	0.078	-0.354	-0.565	-1.418	-2.519
SUNTOP_SB062_232	-5.925	0.063	-0.361	-0.437	-1.250	-2.060
SUNTOP_SB062_233	-5.797	0.058	-0.289	-0.424	-1.262	-1.894
SUNTOP_SB062_234	-5.854	0.090	-0.310	-0.452	-1.399	-2.037
SUNTOP_SB062_235	-5.797	0.067	-0.249	-0.370	-1.252	-1.634
SUNTOP_SB062_236	-5.635	0.006	-0.322	-0.410	-1.136	-1.793
SUNTOP_SB062_237	-6.096	0.124	-0.367	-0.378	-1.547	-2.213
SUNTOP_SB062_238	-5.977	0.079	-0.327	-0.519	-1.405	-2.056
SUNTOP_SB062_239	-5.894	0.126	-0.176	-1.090	-1.946	-2.622
SUNTOP_SB062_240	-6.033	0.085	-0.328	-0.515	-1.404	-2.184
SUNTOP_SB062_241	-5.975	0.097	-0.303	-0.585	-1.276	-2.186
SUNTOP_SB062_242	-5.915	0.069	-0.364	-0.013	-1.222	-1.977
SUNTOP_SB062_243	-5.895	0.062	-0.353	-0.320	-1.166	-2.059
SUNTOP_SB062_244	-5.879	0.060	-0.365	-0.390	-1.429	-2.198
SUNTOP_SB062_245	-6.017	0.113	-0.270	-0.558	-1.419	-2.007
SUNTOP_SB062_246	-5.771	0.047	-0.288	-0.338	-1.245	-1.819
SUNTOP_SERI M82_247	-5.923	0.063	-0.321	-0.358	-1.187	-1.999
SUNTOP_SERI M82_248	-5.946	0.117	-0.255	-0.563	-1.497	-1.844
SUNTOP_SERI M82_249	-6.015	0.052	-0.338	-0.564	-1.417	-2.226
SUNTOP_SERI M82_250	-5.914	0.085	-0.349	-0.410	-1.331	-2.003
SUNTOP_SERI M82_251	-6.171	0.167	-0.285	-0.616	-1.445	-2.239

Table B.2 – continued from previous page

Genotype	Intercept	abs(x)	y	abs(x)y	abs(x)²	y²
SUNTOP_SERI M82_252	-5.887	0.051	-0.374	-0.535	-1.340	-2.053
SUNTOP_SERI M82_253	-5.949	0.099	-0.373	-0.291	-1.379	-2.020
SUNTOP_SERI M82_254	-5.825	0.034	-0.258	-0.456	-1.217	-1.781
SUNTOP_SERI M82_255	-5.984	0.078	-0.309	-0.523	-1.274	-2.211
SUNTOP_SERI M82_256	-6.025	0.089	-0.344	-0.474	-1.326	-2.109
SUNTOP_SERI M82_257	-5.841	0.094	-0.309	-0.529	-1.568	-1.999
SUNTOP_SERI M82_258	-5.975	0.054	-0.348	-0.422	-0.955	-2.205
SUNTOP_SERI M82_259	-5.922	0.080	-0.348	-0.368	-1.363	-1.996
SUNTOP_SERI M82_260	-5.963	0.064	-0.347	-0.340	-1.203	-2.029
SUNTOP_SERI M82_261	-5.853	0.074	-0.256	-0.413	-1.373	-1.856
SUNTOP_SERI M82_262	-5.818	0.054	-0.309	-0.538	-1.307	-2.109
SUNTOP_SERI M82_263	-5.778	0.014	-0.316	-0.436	-0.958	-1.930
SUNTOP_SERI M82_264	-5.914	0.071	-0.358	-0.349	-1.504	-2.084
SUNTOP_SERI M82_265	-5.844	0.098	-0.253	-0.491	-1.636	-1.977
SUNTOP_SERI M82_266	-5.879	0.057	-0.349	-0.348	-0.913	-1.961
SUNTOP_SERI M82_267	-5.889	0.077	-0.311	-0.480	-1.345	-2.004
SUNTOP_SERI M82_268	-5.861	0.049	-0.338	-0.619	-1.407	-2.401
SUNTOP_SERI M82_269	-5.848	0.060	-0.321	-0.358	-1.291	-1.890
SUNTOP_SERI M82_270	-5.783	0.069	-0.315	-0.485	-1.328	-2.046
SUNTOP_SERI M82_271	-5.919	0.066	-0.363	-0.427	-1.123	-2.315
SUNTOP_SERI M82_272	-5.908	0.072	-0.299	-0.476	-1.293	-2.133
SUNTOP_SERI M82_273	-5.936	0.078	-0.318	-0.400	-1.350	-1.995
SUNTOP_SERI M82_274	-6.120	0.095	-0.386	-0.326	-1.429	-2.149
SUNTOP_SERI M82_275	-6.086	0.090	-0.347	-0.548	-1.404	-2.164
SUNTOP_SERI M82_276	-5.905	0.077	-0.329	-0.394	-1.354	-2.121
SUNTOP_SERI M82_277	-5.783	0.007	-0.299	-0.432	-0.979	-1.996
SUNTOP_SERI M82_278	-6.093	0.082	-0.389	-0.295	-1.308	-2.103
SUNTOP_SERI M82_279	-5.947	0.056	-0.343	-0.460	-1.212	-2.307
SUNTOP_SERI M82_280	-5.895	0.061	-0.340	-0.351	-1.112	-2.040
SUNTOP_SERI M82_281	-5.872	0.076	-0.314	-0.449	-1.342	-2.057
SUNTOP_SERI M82_282	-5.981	0.096	-0.321	-0.373	-1.285	-1.958
SUNTOP_SERI M82_283	-5.997	0.073	-0.318	-0.406	-1.345	-1.987
SUNTOP_SERI M82_284	-5.893	0.064	-0.300	-0.371	-1.553	-2.184
SUNTOP_SERI M82_285	-5.820	0.056	-0.236	-0.522	-1.081	-1.850
SUNTOP_SERI M82_286	-5.716	0.023	-0.307	-0.483	-1.314	-2.055
SUNTOP_SERI M82_287	-5.956	0.060	-0.361	-0.520	-1.241	-2.308

Table B.2 – continued from previous page

Genotype	Intercept	abs(x)	y	abs(x)y	abs(x)²	y²
SUNTOP_SERI M82_288	-5.852	0.051	-0.308	-0.356	-1.150	-1.672
SUNTOP_SERI M82_289	-5.842	0.062	-0.259	-0.607	-1.245	-1.977
SUNTOP_SERI M82_290	-5.896	0.075	-0.247	-0.604	-1.340	-2.158
SUNTOP_SERI M82_291	-6.076	0.091	-0.378	-0.421	-1.180	-2.018
SUNTOP_SERI M82_292	-5.878	0.055	-0.351	-0.416	-1.093	-1.999
SUNTOP_SERI M82_294	-5.902	0.088	-0.246	-0.481	-1.348	-1.677
SUNTOP_SERI M82_295	-6.209	0.156	-0.340	-0.577	-1.856	-2.238
SUNTOP_SERI M82_296	-5.979	0.091	-0.300	-0.388	-1.297	-1.958
SUNTOP_SERI M82_297	-5.938	0.079	-0.356	-0.522	-1.355	-2.243
SUNTOP_SERI M82_298	-5.851	0.125	-0.280	-0.548	-1.790	-1.795
SUNTOP_SPITFIRE_1	-6.031	0.112	-0.215	-0.536	-1.261	-1.905
SUNTOP_SPITFIRE_10	-5.961	0.053	-0.365	-0.369	-1.230	-2.306
SUNTOP_SPITFIRE_12	-5.926	0.070	-0.363	-0.428	-1.402	-2.363
SUNTOP_SPITFIRE_13	-5.891	0.046	-0.289	-0.471	-1.205	-2.044
SUNTOP_SPITFIRE_14	-5.888	0.077	-0.294	-0.336	-1.432	-2.105
SUNTOP_SPITFIRE_15	-5.757	0.041	-0.256	-0.571	-1.287	-2.060
SUNTOP_SPITFIRE_16	-5.784	0.022	-0.313	-0.741	-1.334	-2.370
SUNTOP_SPITFIRE_17	-5.762	0.042	-0.307	-0.472	-1.316	-2.140
SUNTOP_SPITFIRE_18	-5.945	0.004	-0.226	-0.858	-1.212	-2.061
SUNTOP_SPITFIRE_19	-5.910	0.055	-0.344	-0.343	-1.113	-2.243
SUNTOP_SPITFIRE_2	-5.961	0.106	-0.300	-0.407	-1.564	-1.924
SUNTOP_SPITFIRE_20	-5.963	0.100	-0.375	-0.411	-1.566	-2.250
SUNTOP_SPITFIRE_21	-5.810	0.049	-0.327	-0.521	-1.332	-2.133
SUNTOP_SPITFIRE_22	-5.861	-0.008	-0.273	-0.541	-1.020	-2.095
SUNTOP_SPITFIRE_24	-5.963	0.098	-0.330	-0.438	-1.557	-2.336
SUNTOP_SPITFIRE_25	-6.097	0.119	-0.336	-0.450	-1.549	-2.255
SUNTOP_SPITFIRE_26	-5.888	0.076	-0.262	-0.448	-1.296	-1.849
SUNTOP_SPITFIRE_28	-5.880	0.084	-0.305	-0.406	-1.375	-2.130
SUNTOP_SPITFIRE_29	-5.899	0.060	-0.335	-0.533	-1.325	-2.232
SUNTOP_SPITFIRE_3	-5.953	0.095	-0.348	-0.414	-1.456	-2.239
SUNTOP_SPITFIRE_30	-5.845	0.082	-0.274	-0.303	-1.496	-1.884
SUNTOP_SPITFIRE_31	-5.947	0.079	-0.410	-0.439	-1.089	-2.495
SUNTOP_SPITFIRE_32	-6.103	0.092	-0.256	-0.590	-1.263	-2.257
SUNTOP_SPITFIRE_33	-6.135	0.127	-0.347	-0.451	-1.513	-2.224
SUNTOP_SPITFIRE_34	-5.846	0.086	-0.321	-0.454	-1.764	-2.233
SUNTOP_SPITFIRE_35	-6.067	0.113	-0.311	-0.578	-1.532	-2.286

Table B.2 – continued from previous page

Genotype	Intercept	abs(x)	y	abs(x)y	abs(x)²	y²
SUNTOP_SPITFIRE_36	-5.961	0.053	-0.394	-0.437	-1.296	-2.361
SUNTOP_SPITFIRE_38	-5.870	0.085	-0.257	-0.562	-1.336	-1.956
SUNTOP_SPITFIRE_39	-5.926	0.050	-0.359	-0.444	-1.299	-2.266
SUNTOP_SPITFIRE_4	-6.058	0.137	-0.267	-0.484	-1.781	-2.026
SUNTOP_SPITFIRE_40	-5.909	0.114	-0.332	-0.405	-1.552	-2.048
SUNTOP_SPITFIRE_41	-5.988	0.103	-0.318	-0.368	-1.394	-1.928
SUNTOP_SPITFIRE_42	-5.904	0.055	-0.310	-0.572	-1.342	-2.513
SUNTOP_SPITFIRE_43	-5.808	0.087	-0.249	-0.723	-1.606	-2.366
SUNTOP_SPITFIRE_44	-5.708	0.065	-0.252	-0.417	-1.344	-1.896
SUNTOP_SPITFIRE_46	-5.899	0.079	-0.297	-0.519	-1.350	-2.169
SUNTOP_SPITFIRE_47	-5.903	0.104	-0.311	-0.408	-1.453	-2.310
SUNTOP_SPITFIRE_48	-6.036	0.064	-0.348	-0.465	-1.295	-2.321
SUNTOP_SPITFIRE_5	-6.006	0.092	-0.259	-0.323	-1.363	-1.850
SUNTOP_SPITFIRE_50	-5.851	0.026	-0.377	-0.434	-1.193	-2.378
SUNTOP_SPITFIRE_51	-5.847	0.062	-0.324	-0.453	-1.303	-2.111
SUNTOP_SPITFIRE_52	-5.762	-0.017	-0.352	-0.580	-1.079	-2.338
SUNTOP_SPITFIRE_53	-5.948	0.076	-0.346	-0.353	-1.369	-2.141
SUNTOP_SPITFIRE_54	-5.914	0.038	-0.351	-0.545	-1.370	-2.534
SUNTOP_SPITFIRE_6	-5.864	0.067	-0.367	-0.384	-1.332	-2.423
SUNTOP_SPITFIRE_7	-5.884	0.077	-0.266	-0.458	-1.458	-2.102
SUNTOP_SPITFIRE_8	-5.936	0.089	-0.265	-0.542	-1.449	-2.108
SUNTOP_SPITFIRE_9	-5.908	0.060	-0.356	-0.339	-1.567	-2.209
SUNTOP_WYLIE_341	-5.824	0.043	-0.343	-0.608	-1.383	-2.246
SUNTOP_WYLIE_342	-5.834	0.081	-0.256	-0.558	-1.497	-2.040
SUNTOP_WYLIE_344	-5.672	0.004	-0.314	-0.285	-1.074	-2.132
SUNTOP_WYLIE_345	-5.957	0.068	-0.349	-0.389	-1.059	-2.321
SUNTOP_WYLIE_346	-5.891	0.073	-0.375	-0.506	-1.508	-2.356
SUNTOP_WYLIE_347	-6.052	0.083	-0.317	-0.484	-1.250	-2.016
SUNTOP_WYLIE_348	-5.982	0.067	-0.396	-0.421	-1.377	-2.548
SUNTOP_WYLIE_349	-5.903	0.081	-0.296	-0.441	-1.436	-2.088
SUNTOP_WYLIE_350	-6.045	0.067	-0.321	-0.441	-1.365	-2.109
SUNTOP_WYLIE_351	-5.888	0.077	-0.334	-0.246	-1.167	-1.997
SUNTOP_WYLIE_352	-5.897	0.059	-0.322	-0.325	-1.124	-2.099
SUNTOP_WYLIE_353	-5.798	0.052	-0.332	-0.390	-1.441	-2.156
SUNTOP_WYLIE_354	-6.050	0.086	-0.380	-0.296	-1.422	-2.197
SUNTOP_WYLIE_355	-6.005	0.057	-0.376	-0.471	-1.508	-2.157

Table B.2 – continued from previous page

Genotype	*Intercept*	*abs(x)*	*y*	*abs(x)y*	*abs(x)²*	*y²*
SUNTOP_WYLIE_356	-5.948	0.067	-0.356	-0.339	-1.315	-2.319
SUNTOP_WYLIE_357	-5.838	0.076	-0.312	-0.337	-1.395	-2.073
SUNTOP_WYLIE_358	-5.856	0.104	-0.300	-0.221	-1.797	-1.866
SUNTOP_WYLIE_359	-5.803	0.070	-0.341	-0.500	-1.253	-2.124
SUNTOP_WYLIE_360	-5.826	0.067	-0.263	-0.418	-1.383	-2.060
SUNTOP_WYLIE_361	-5.901	0.053	-0.345	-0.500	-1.411	-2.145
SUNTOP_WYLIE_362	-5.836	0.061	-0.296	-0.357	-1.258	-1.980
SUNTOP_WYLIE_363	-5.996	0.078	-0.419	-0.211	-1.264	-2.384
SUNTOP_WYLIE_364	-6.171	0.115	-0.363	-0.315	-1.427	-2.287
SUNTOP_WYLIE_365	-5.882	0.076	-0.314	-0.498	-1.494	-2.165
SUNTOP_WYLIE_366	-5.891	0.080	-0.278	-0.493	-1.363	-1.991
SUNTOP_WYLIE_367	-5.933	0.078	-0.339	-0.351	-1.384	-2.163
SUNTOP_WYLIE_368	-5.892	0.098	-0.310	-0.246	-1.404	-1.993
SUNTOP_WYLIE_369	-5.784	0.026	-0.342	-0.487	-1.329	-2.186
SUNTOP_WYLIE_371	-5.763	0.041	-0.273	-0.668	-1.281	-2.038
SUNTOP_WYLIE_372	-5.794	0.027	-0.347	-0.426	-1.286	-2.198
SUNTOP_WYLIE_373	-5.802	0.043	-0.317	-0.638	-1.151	-2.480
SUNTOP_WYLIE_374	-5.924	0.071	-0.314	-0.478	-1.371	-2.225
SUNTOP_WYLIE_376	-5.778	0.041	-0.365	-0.566	-1.459	-2.260
SUNTOP_WYLIE_377	-5.754	0.043	-0.330	-0.365	-1.382	-2.251
SUNTOP_WYLIE_378	-5.818	0.057	-0.326	-0.409	-1.243	-2.013
SUNTOP_WYLIE_379	-5.860	0.038	-0.349	-0.454	-1.250	-2.240
SUNTOP_WYLIE_380	-6.095	0.118	-0.365	-0.505	-1.384	-2.314
SUNTOP_WYLIE_381	-6.017	0.084	-0.408	-0.106	-1.294	-2.499
SUNTOP_WYLIE_382	-6.040	0.109	-0.372	-0.291	-1.678	-2.256
SUNTOP_ZWB10-37_383	-5.906	0.065	-0.320	-0.434	-1.279	-2.015
SUNTOP_ZWB10-37_384	-6.181	0.153	-0.385	-0.669	-1.738	-2.430
SUNTOP_ZWB10-37_385	-5.825	0.042	-0.317	-0.527	-1.324	-2.051
SUNTOP_ZWB10-37_386	-5.860	0.071	-0.315	-0.521	-1.448	-2.089
SUNTOP_ZWB10-37_387	-6.102	0.147	-0.406	-0.527	-1.966	-2.492
SUNTOP_ZWB10-37_388	-5.874	0.018	-0.330	-0.477	-1.141	-2.293
SUNTOP_ZWB10-37_389	-6.039	0.117	-0.285	-0.465	-1.634	-2.057
SUNTOP_ZWB10-37_390	-5.927	0.105	-0.330	-0.612	-1.698	-2.242
SUNTOP_ZWB10-37_392	-6.229	0.062	-0.396	-0.520	-1.174	-2.508
SUNTOP_ZWB10-37_393	-5.987	0.080	-0.351	-0.633	-1.405	-2.207
SUNTOP_ZWB10-37_394	-5.855	0.048	-0.343	-0.470	-1.163	-2.147

Table B.2 – continued from previous page

Genotype	*Intercept*	*abs(x)*	*y*	*abs(x)y*	*abs(x)²*	*y²*
SUNTOP_ZWB10-37_395	-5.981	0.070	-0.309	-0.474	-1.326	-2.161
SUNTOP_ZWB10-37_396	-5.937	0.069	-0.330	-0.393	-1.185	-2.006
SUNTOP_ZWB10-37_397	-6.062	0.109	-0.408	-0.391	-1.557	-2.374
SUNTOP_ZWB10-37_398	-5.960	0.053	-0.344	-0.427	-1.134	-2.081
SUNTOP_ZWB10-37_400	-5.873	0.063	-0.320	-0.461	-1.294	-2.112
SUNTOP_ZWB10-37_403	-5.780	0.076	-0.265	-0.442	-1.411	-1.964
SUNTOP_ZWB10-37_404	-5.918	0.071	-0.321	-0.446	-1.332	-2.109
SUNTOP_ZWB10-37_405	-5.797	0.061	-0.289	-0.440	-1.321	-1.785
SUNTOP_ZWB10-37_406	-6.007	0.088	-0.318	-0.500	-1.307	-2.145
SUNTOP_ZWB10-37_407	-5.951	0.059	-0.371	-0.243	-1.050	-2.089
SUNTOP_ZWB10-37_408	-6.248	0.090	-0.393	-0.436	-1.185	-2.272
SUNTOP_ZWB10-37_409	-5.958	0.040	-0.378	-0.386	-1.104	-2.142
SUNTOP_ZWB10-37_410	-5.901	0.087	-0.264	-0.517	-1.440	-1.952
SUNTOP_ZWB10-37_411	-5.929	0.088	-0.286	-0.405	-1.500	-1.966
SUNTOP_ZWB10-37_412	-5.807	0.003	-0.249	-0.613	-1.178	-1.995
SUNTOP_ZWB10-37_413	-6.216	0.095	-0.413	-0.463	-1.457	-2.225
SUNTOP_ZWB10-37_414	-5.958	0.097	-0.304	-0.527	-1.487	-2.098
SUNTOP_ZWB10-37_415	-5.545	-0.016	-0.242	-0.546	-1.052	-1.991
SUNTOP_ZWB10-37_416	-5.969	0.077	-0.365	-0.501	-1.398	-2.446
SUNTOP_ZWB10-37_417	-5.773	0.087	-0.241	-0.226	-1.520	-1.551
SUNTOP_ZWB10-37_418	-5.885	0.073	-0.360	-0.175	-1.316	-2.092
SUNTOP_ZWB10-37_419	-5.823	0.080	-0.251	-0.424	-1.459	-1.921
SUNTOP_ZWB10-37_420	-5.921	0.074	-0.342	-0.432	-1.381	-2.333
SUNTOP_ZWB10-37_422	-5.896	0.051	-0.337	-0.486	-1.147	-2.076
SUNTOP_ZWB10-37_423	-5.920	0.061	-0.262	-0.461	-1.220	-1.898
SUNTOP_ZWB10-37_424	-6.103	0.052	-0.401	-0.300	-1.099	-2.425
SUNTOP_ZWW10-128_425	-5.979	0.076	-0.292	-0.493	-1.210	-2.114
SUNTOP_ZWW10-128_426	-6.005	0.109	-0.328	-0.440	-1.517	-1.988
SUNTOP_ZWW10-128_427	-5.927	0.092	-0.319	-0.494	-1.358	-2.189
SUNTOP_ZWW10-128_429	-5.807	0.084	-0.287	-0.329	-1.409	-1.716
SUNTOP_ZWW10-128_430	-6.038	0.065	-0.374	-0.412	-0.987	-2.192
SUNTOP_ZWW10-128_432	-5.885	0.064	-0.334	-0.364	-1.273	-2.083
SUNTOP_ZWW10-128_433	-5.883	0.048	-0.287	-0.577	-1.305	-2.213
SUNTOP_ZWW10-128_434	-5.850	0.181	-0.397	-0.362	-2.168	-2.090
SUNTOP_ZWW10-128_435	-6.051	0.102	-0.316	-0.478	-1.423	-2.104
SUNTOP_ZWW10-128_436	-5.937	0.060	-0.295	-0.363	-0.950	-1.884

Table B.2 – continued from previous page

Genotype	Intercept	abs(x)	y	abs(x)y	abs(x)^2	y^2
SUNTOP_ZWW10-128_437	-6.041	0.077	-0.340	-0.529	-1.304	-2.391
SUNTOP_ZWW10-128_438	-6.103	0.055	-0.375	-0.319	-1.254	-2.711
SUNTOP_ZWW10-128_439	-5.958	0.098	-0.380	-0.342	-1.419	-2.222
SUNTOP_ZWW10-128_440	-6.025	0.056	-0.287	-0.353	-1.708	-1.801
SUNTOP_ZWW10-128_441	-6.045	0.080	-0.370	-0.317	-1.310	-2.352
SUNTOP_ZWW10-128_443	-5.992	0.095	-0.337	-0.395	-1.402	-2.071
SUNTOP_ZWW10-128_444	-5.907	0.069	-0.287	-0.488	-1.398	-2.072
SUNTOP_ZWW10-128_445	-5.766	0.024	-0.212	-0.373	-0.990	-1.683
SUNTOP_ZWW10-128_446	-5.889	0.059	-0.319	-0.493	-1.319	-2.078
SUNTOP_ZWW10-128_448	-6.070	0.101	-0.300	-0.449	-1.332	-2.057
SUNTOP_ZWW10-128_449	-5.871	0.055	-0.320	-0.383	-1.185	-1.937
SUNTOP_ZWW10-128_450	-6.029	0.065	-0.330	-0.410	-1.121	-2.061
SUNTOP_ZWW10-128_451	-6.075	0.078	-0.381	-0.380	-1.343	-2.170
SUNTOP_ZWW10-128_452	-5.908	0.082	-0.302	-0.546	-1.424	-2.150
SUNTOP_ZWW10-128_453	-6.072	0.068	-0.323	-0.335	-1.309	-1.992
SUNTOP_ZWW10-128_454	-5.877	0.063	-0.288	-0.481	-1.371	-2.010
SUNTOP_ZWW10-128_455	-6.029	0.075	-0.290	-0.457	-1.291	-2.022
SUNTOP_ZWW10-128_456	-5.889	0.044	-0.315	-0.373	-1.087	-1.996
SUNTOP_ZWW10-128_457	-5.761	0.061	-0.295	-0.456	-1.384	-2.024
SUNTOP_ZWW10-128_458	-5.854	0.079	-0.291	-0.309	-1.433	-1.756
SUNTOP_ZWW10-128_459	-5.811	0.029	-0.265	-0.377	-1.315	-1.824
SUNTOP_ZWW10-128_460	-5.862	0.064	-0.337	-0.366	-1.312	-2.075
SUNTOP_ZWW10-128_461	-5.933	0.078	-0.291	-0.462	-1.352	-1.950
SUNTOP_ZWW10-128_462	-5.816	0.055	-0.305	-0.474	-1.284	-2.026
SUNTOP_ZWW10-128_463	-5.660	0.027	-0.263	-0.453	-1.101	-1.803
SUNTOP_ZWW10-128_464	-5.992	0.085	-0.330	-0.398	-1.413	-1.873
SUNTOP_ZWW10-128_465	-5.909	0.072	-0.339	-0.324	-1.058	-1.908
SUNTOP_ZWW10-128_466	-5.637	0.053	-0.250	-0.629	-1.569	-1.764
ZWB10-37_P1	-6.168	0.068	-0.363	-0.901	-1.278	-2.998
ZWW10-128_PP	-5.829	0.082	-0.338	-0.417	-1.412	-1.889

B.3 Multivariate unweighted genotype predictions

Table B.3: The genotype predictions for the unweighted multivariate linear mixed model, where all predictions are generated from one model. The full set of genotype predictions are presented here, and it is important to note that these predictions are on the transformed data scale with the exception of *intercept* which did not require transforming.

Genotype	*Intercept*	y^2
DHARWAR DRY_PP	-5.857	-2.113
DRYSDALE_PP	-6.013	-2.467
EGA GREGORY_PP	-5.836	-2.119
EGA WYLIE_PP	-6.158	-2.568
FAC10-16_P1	-5.742	-2.081
MACE_PP	-5.746	-1.951
MACE_SB062_123	-5.740	-1.997
RIL114_PP	-5.947	-2.126
SB062_PP	-5.889	-1.865
SERI M82_PP	-6.150	-2.577
SPITFIRE-P9	-5.806	-2.134
SUNTOP_DHARWAH DRY_1	-5.890	-2.150
SUNTOP_DHARWAH DRY_10	-5.813	-2.002
SUNTOP_DHARWAH DRY_11	-5.808	-1.928
SUNTOP_DHARWAH DRY_12	-5.824	-2.118
SUNTOP_DHARWAH DRY_13	-5.927	-2.184
SUNTOP_DHARWAH DRY_14	-5.944	-2.091
SUNTOP_DHARWAH DRY_15	-5.849	-2.107
SUNTOP_DHARWAH DRY_16	-6.071	-2.308
SUNTOP_DHARWAH DRY_17	-5.885	-1.986
SUNTOP_DHARWAH DRY_18	-5.947	-2.230
SUNTOP_DHARWAH DRY_19	-6.118	-2.416
SUNTOP_DHARWAH DRY_2	-6.028	-2.152
SUNTOP_DHARWAH DRY_20	-6.062	-2.348
SUNTOP_DHARWAH DRY_21	-5.942	-2.242
SUNTOP_DHARWAH DRY_22	-6.113	-2.396
SUNTOP_DHARWAH DRY_23	-5.808	-2.041
SUNTOP_DHARWAH DRY_24	-6.026	-2.123
SUNTOP_DHARWAH DRY_25	-5.836	-2.132

Continued on next page

Genotype	Intercept	y^2
SUNTOP_DHARWAH DRY_26	-6.061	-2.421
SUNTOP_DHARWAH DRY_27	-6.123	-2.400
SUNTOP_DHARWAH DRY_28	-6.131	-2.233
SUNTOP_DHARWAH DRY_29	-5.982	-2.375
SUNTOP_DHARWAH DRY_3	-5.727	-1.765
SUNTOP_DHARWAH DRY_30	-5.934	-1.991
SUNTOP_DHARWAH DRY_31	-5.777	-1.944
SUNTOP_DHARWAH DRY_32	-6.000	-2.395
SUNTOP_DHARWAH DRY_33	-5.950	-2.238
SUNTOP_DHARWAH DRY_34	-5.835	-2.037
SUNTOP_DHARWAH DRY_35	-5.865	-2.069
SUNTOP_DHARWAH DRY_36	-5.926	-2.127
SUNTOP_DHARWAH DRY_37	-5.829	-2.087
SUNTOP_DHARWAH DRY_38	-6.057	-2.351
SUNTOP_DHARWAH DRY_39	-5.895	-2.158
SUNTOP_DHARWAH DRY_4	-5.797	-1.959
SUNTOP_DHARWAH DRY_40	-5.764	-2.018
SUNTOP_DHARWAH DRY_41	-5.951	-2.161
SUNTOP_DHARWAH DRY_42	-5.918	-2.344
SUNTOP_DHARWAH DRY_43	-6.146	-2.403
SUNTOP_DHARWAH DRY_44	-5.878	-2.181
SUNTOP_DHARWAH DRY_45	-5.970	-2.114
SUNTOP_DHARWAH DRY_46	-6.110	-2.439
SUNTOP_DHARWAH DRY_47	-5.881	-2.059
SUNTOP_DHARWAH DRY_48	-5.826	-2.011
SUNTOP_DHARWAH DRY_49	-6.020	-2.181
SUNTOP_DHARWAH DRY_5	-5.950	-2.230
SUNTOP_DHARWAH DRY_50	-5.809	-1.994
SUNTOP_DHARWAH DRY_51	-6.245	-2.777
SUNTOP_DHARWAH DRY_52	-5.903	-2.158
SUNTOP_DHARWAH DRY_6	-5.822	-1.978
SUNTOP_DHARWAH DRY_7	-6.082	-2.486
SUNTOP_DHARWAH DRY_8	-5.798	-2.073
SUNTOP_DHARWAH DRY_9	-5.856	-2.102
SUNTOP_DRYSDALE_100	-5.901	-2.168
SUNTOP_DRYSDALE_101	-5.964	-2.151

Genotype	*Intercept*	y^2
SUNTOP_DRYSDALE_102	-5.942	-2.210
SUNTOP_DRYSDALE_103	-5.961	-2.300
SUNTOP_DRYSDALE_104	-6.002	-2.360
SUNTOP_DRYSDALE_53	-6.249	-2.685
SUNTOP_DRYSDALE_54	-5.727	-2.054
SUNTOP_DRYSDALE_55	-6.008	-2.522
SUNTOP_DRYSDALE_56	-6.111	-2.463
SUNTOP_DRYSDALE_57	-5.848	-2.081
SUNTOP_DRYSDALE_58	-6.146	-2.443
SUNTOP_DRYSDALE_59	-6.043	-2.365
SUNTOP_DRYSDALE_60	-5.917	-2.285
SUNTOP_DRYSDALE_61	-5.928	-2.170
SUNTOP_DRYSDALE_62	-5.928	-2.240
SUNTOP_DRYSDALE_64	-6.248	-2.453
SUNTOP_DRYSDALE_65	-5.886	-2.121
SUNTOP_DRYSDALE_66	-5.878	-2.105
SUNTOP_DRYSDALE_67	-5.877	-2.086
SUNTOP_DRYSDALE_68	-5.875	-2.131
SUNTOP_DRYSDALE_69	-5.925	-2.319
SUNTOP_DRYSDALE_70	-5.956	-2.122
SUNTOP_DRYSDALE_71	-5.978	-2.239
SUNTOP_DRYSDALE_72	-6.100	-2.559
SUNTOP_DRYSDALE_73	-6.084	-2.257
SUNTOP_DRYSDALE_74	-5.967	-2.210
SUNTOP_DRYSDALE_75	-5.896	-2.111
SUNTOP_DRYSDALE_76	-5.946	-2.178
SUNTOP_DRYSDALE_77	-6.209	-2.326
SUNTOP_DRYSDALE_78	-5.879	-2.097
SUNTOP_DRYSDALE_79	-6.069	-2.286
SUNTOP_DRYSDALE_80	-6.024	-2.266
SUNTOP_DRYSDALE_81	-6.114	-2.234
SUNTOP_DRYSDALE_83	-5.853	-2.107
SUNTOP_DRYSDALE_84	-5.990	-2.291
SUNTOP_DRYSDALE_85	-6.030	-2.285
SUNTOP_DRYSDALE_86	-5.939	-2.170
SUNTOP_DRYSDALE_87	-6.088	-2.400

Genotype	Intercept	y^2
SUNTOP_DRYSDALE_88	-5.843	-2.004
SUNTOP_DRYSDALE_89	-5.777	-2.062
SUNTOP_DRYSDALE_90	-6.007	-2.202
SUNTOP_DRYSDALE_91	-5.758	-1.938
SUNTOP_DRYSDALE_92	-5.975	-2.166
SUNTOP_DRYSDALE_93	-6.130	-2.299
SUNTOP_DRYSDALE_94	-5.982	-2.245
SUNTOP_DRYSDALE_95	-5.986	-2.450
SUNTOP_DRYSDALE_96	-5.852	-2.027
SUNTOP_DRYSDALE_97	-6.011	-2.262
SUNTOP_DRYSDALE_98	-5.964	-2.307
SUNTOP_DRYSDALE_99	-5.946	-2.157
SUNTOP_EGA GREGORY_108	-5.863	-2.072
SUNTOP_EGA GREGORY_109	-5.945	-2.264
SUNTOP_EGA GREGORY_110	-6.188	-2.435
SUNTOP_EGA GREGORY_111	-5.888	-2.282
SUNTOP_EGA GREGORY_112	-5.744	-1.864
SUNTOP_EGA GREGORY_113	-6.006	-2.131
SUNTOP_EGA GREGORY_114	-5.958	-2.277
SUNTOP_EGA GREGORY_115	-5.878	-2.038
SUNTOP_EGA GREGORY_116	-6.017	-2.250
SUNTOP_EGA GREGORY_117	-5.923	-2.301
SUNTOP_EGA GREGORY_118	-5.944	-2.197
SUNTOP_EGA GREGORY_119	-5.720	-2.087
SUNTOP_EGA GREGORY_120	-5.867	-2.373
SUNTOP_EGA GREGORY_121	-5.924	-2.167
SUNTOP_EGA GREGORY_122	-5.834	-2.019
SUNTOP_EGA GREGORY_123	-5.889	-2.051
SUNTOP_EGA GREGORY_124	-5.867	-2.149
SUNTOP_EGA GREGORY_125	-5.969	-2.245
SUNTOP_EGA GREGORY_126	-5.914	-2.215
SUNTOP_EGA GREGORY_127	-5.975	-2.333
SUNTOP_EGA GREGORY_128	-5.746	-1.910
SUNTOP_EGA GREGORY_129	-5.824	-2.160
SUNTOP_EGA GREGORY_130	-6.215	-2.445
SUNTOP_EGA GREGORY_131	-5.743	-2.013

Genotype	Intercept	y^2
SUNTOP_EGA GREGORY_132	-5.999	-2.270
SUNTOP_EGA GREGORY_133	-6.000	-2.188
SUNTOP_EGA GREGORY_134	-6.021	-2.253
SUNTOP_EGA GREGORY_135	-5.953	-2.077
SUNTOP_EGA GREGORY_136	-6.044	-2.238
SUNTOP_EGA GREGORY_137	-5.948	-2.298
SUNTOP_EGA GREGORY_138	-5.902	-2.165
SUNTOP_EGA GREGORY_139	-5.911	-2.269
SUNTOP_EGA GREGORY_140	-6.175	-2.676
SUNTOP_EGA GREGORY_141	-5.918	-2.102
SUNTOP_EGA GREGORY_142	-5.952	-2.170
SUNTOP_EGA GREGORY_143	-5.875	-2.176
SUNTOP_EGA GREGORY_144	-6.086	-2.298
SUNTOP_EGA GREGORY_145	-5.949	-2.063
SUNTOP_EGA GREGORY_146	-5.828	-2.086
SUNTOP_EGA GREGORY_147	-6.027	-2.404
SUNTOP_EGA GREGORY_148	-5.961	-2.150
SUNTOP_EGA GREGORY_149	-5.810	-1.991
SUNTOP_FAC10-16_150	-5.972	-2.267
SUNTOP_FAC10-16_151	-5.954	-2.163
SUNTOP_FAC10-16_152	-5.940	-2.027
SUNTOP_FAC10-16_153	-5.983	-2.275
SUNTOP_FAC10-16_154	-5.878	-2.122
SUNTOP_FAC10-16_155	-5.866	-2.077
SUNTOP_FAC10-16_156	-5.863	-2.163
SUNTOP_FAC10-16_157	-6.116	-2.264
SUNTOP_FAC10-16_158	-5.808	-2.064
SUNTOP_FAC10-16_159	-5.789	-1.938
SUNTOP_FAC10-16_160	-6.123	-2.587
SUNTOP_FAC10-16_161	-6.013	-2.176
SUNTOP_FAC10-16_162	-5.749	-1.850
SUNTOP_FAC10-16_163	-5.956	-2.071
SUNTOP_FAC10-16_164	-5.954	-2.193
SUNTOP_FAC10-16_165	-5.957	-2.250
SUNTOP_FAC10-16_166	-5.893	-2.159
SUNTOP_FAC10-16_167	-5.998	-2.213

Genotype	Intercept	y^2
SUNTOP_FAC10-16_168	-5.959	-2.236
SUNTOP_FAC10-16_169	-5.846	-2.107
SUNTOP_FAC10-16_170	-6.075	-2.476
SUNTOP_FAC10-16_171	-6.038	-2.256
SUNTOP_FAC10-16_172	-5.970	-2.092
SUNTOP_FAC10-16_173	-5.824	-2.061
SUNTOP_FAC10-16_174	-5.968	-2.256
SUNTOP_FAC10-16_175	-6.093	-2.589
SUNTOP_FAC10-16_176	-5.949	-2.062
SUNTOP_FAC10-16_177	-5.786	-1.970
SUNTOP_FAC10-16_178	-6.044	-2.284
SUNTOP_FAC10-16_179	-6.041	-2.188
SUNTOP_FAC10-16_180	-6.127	-2.251
SUNTOP_FAC10-16_181	-5.851	-2.015
SUNTOP_FAC10-16_182	-6.044	-2.364
SUNTOP_FAC10-16_183	-5.973	-2.225
SUNTOP_FAC10-16_184	-5.959	-2.156
SUNTOP_FAC10-16_185	-6.039	-2.328
SUNTOP_FAC10-16_186	-5.872	-2.015
SUNTOP_FAC10-16_187	-6.007	-2.326
SUNTOP_FAC10-16_188	-6.373	-2.629
SUNTOP_FAC10-16_189	-5.886	-2.335
SUNTOP_FAC10-16_190	-5.983	-2.109
SUNTOP_FAC10-16_191	-6.079	-2.326
SUNTOP_PP	-6.175	-2.136
SUNTOP_RIL114_299	-5.855	-2.077
SUNTOP_RIL114_300	-6.045	-2.230
SUNTOP_RIL114_301	-6.072	-2.355
SUNTOP_RIL114_302	-5.843	-2.031
SUNTOP_RIL114_303	-5.819	-2.152
SUNTOP_RIL114_304	-5.894	-2.098
SUNTOP_RIL114_305	-6.000	-2.079
SUNTOP_RIL114_306	-5.943	-2.291
SUNTOP_RIL114_307	-5.937	-2.163
SUNTOP_RIL114_308	-5.920	-2.202
SUNTOP_RIL114_309	-6.047	-2.179

Genotype	Intercept	y^2
SUNTOP_RIL114_310	-6.095	-2.362
SUNTOP_RIL114_311	-5.955	-2.213
SUNTOP_RIL114_312	-5.906	-1.988
SUNTOP_RIL114_313	-5.826	-1.969
SUNTOP_RIL114_314	-5.894	-2.103
SUNTOP_RIL114_315	-5.927	-2.279
SUNTOP_RIL114_316	-5.897	-2.149
SUNTOP_RIL114_317	-5.759	-1.995
SUNTOP_RIL114_318	-5.824	-1.978
SUNTOP_RIL114_319	-6.318	-2.783
SUNTOP_RIL114_320	-6.121	-2.291
SUNTOP_RIL114_321	-5.975	-2.097
SUNTOP_RIL114_322	-5.909	-2.026
SUNTOP_RIL114_323	-5.933	-2.089
SUNTOP_RIL114_324	-5.849	-1.953
SUNTOP_RIL114_325	-6.211	-2.302
SUNTOP_RIL114_326	-5.848	-1.990
SUNTOP_RIL114_327	-5.866	-2.134
SUNTOP_RIL114_328	-5.950	-2.193
SUNTOP_RIL114_329	-5.873	-2.125
SUNTOP_RIL114_330	-6.043	-2.271
SUNTOP_RIL114_331	-5.855	-2.068
SUNTOP_RIL114_333	-6.055	-2.294
SUNTOP_RIL114_334	-5.920	-2.113
SUNTOP_RIL114_335	-5.864	-2.081
SUNTOP_RIL114_336	-5.899	-2.059
SUNTOP_RIL114_337	-6.215	-2.339
SUNTOP_RIL114_338	-5.858	-2.042
SUNTOP_RIL114_339	-5.739	-1.907
SUNTOP_RIL114_340	-5.990	-2.083
SUNTOP_SB062_195	-5.995	-2.363
SUNTOP_SB062_196	-5.711	-1.759
SUNTOP_SB062_197	-5.934	-2.150
SUNTOP_SB062_198	-5.816	-2.039
SUNTOP_SB062_199	-5.905	-1.994
SUNTOP_SB062_200	-5.950	-2.118

Genotype	*Intercept*	y^2
SUNTOP_SB062_201	-5.948	-2.210
SUNTOP_SB062_202	-5.950	-2.201
SUNTOP_SB062_203	-5.900	-2.171
SUNTOP_SB062_204	-5.931	-2.187
SUNTOP_SB062_205	-5.931	-2.144
SUNTOP_SB062_206	-6.105	-2.384
SUNTOP_SB062_207	-6.150	-2.213
SUNTOP_SB062_208	-6.106	-2.333
SUNTOP_SB062_209	-5.889	-2.003
SUNTOP_SB062_210	-5.972	-2.238
SUNTOP_SB062_211	-6.002	-2.133
SUNTOP_SB062_212	-5.858	-1.903
SUNTOP_SB062_213	-5.950	-2.123
SUNTOP_SB062_214	-5.923	-2.176
SUNTOP_SB062_215	-5.937	-2.061
SUNTOP_SB062_216	-6.030	-2.251
SUNTOP_SB062_217	-5.957	-2.314
SUNTOP_SB062_218	-5.863	-2.223
SUNTOP_SB062_219	-5.851	-2.158
SUNTOP_SB062_220	-5.885	-2.159
SUNTOP_SB062_221	-5.888	-2.093
SUNTOP_SB062_222	-5.824	-2.159
SUNTOP_SB062_223	-5.917	-1.980
SUNTOP_SB062_224	-6.068	-2.207
SUNTOP_SB062_225	-5.991	-2.153
SUNTOP_SB062_226	-6.013	-2.548
SUNTOP_SB062_227	-5.872	-2.155
SUNTOP_SB062_228	-5.951	-2.188
SUNTOP_SB062_229	-5.770	-1.983
SUNTOP_SB062_230	-6.035	-2.253
SUNTOP_SB062_231	-6.098	-2.475
SUNTOP_SB062_232	-5.935	-2.153
SUNTOP_SB062_233	-5.784	-1.955
SUNTOP_SB062_234	-5.879	-2.119
SUNTOP_SB062_235	-5.768	-1.846
SUNTOP_SB062_236	-5.702	-1.896

Genotype	Intercept	y^2
SUNTOP_SB062_237	-6.122	-2.341
SUNTOP_SB062_238	-5.975	-2.169
SUNTOP_SB062_239	-5.976	-2.357
SUNTOP_SB062_240	-6.085	-2.332
SUNTOP_SB062_241	-6.004	-2.263
SUNTOP_SB062_242	-5.923	-2.121
SUNTOP_SB062_243	-5.922	-2.150
SUNTOP_SB062_244	-5.922	-2.220
SUNTOP_SB062_245	-6.007	-2.140
SUNTOP_SB062_246	-5.745	-1.868
SUNTOP_SERI M82_247	-5.954	-2.115
SUNTOP_SERI M82_248	-5.921	-2.039
SUNTOP_SERI M82_249	-6.047	-2.322
SUNTOP_SERI M82_250	-5.929	-2.094
SUNTOP_SERI M82_251	-6.134	-2.377
SUNTOP_SERI M82_252	-5.913	-2.139
SUNTOP_SERI M82_253	-5.961	-2.129
SUNTOP_SERI M82_254	-5.793	-1.854
SUNTOP_SERI M82_255	-6.064	-2.475
SUNTOP_SERI M82_256	-6.033	-2.233
SUNTOP_SERI M82_257	-5.868	-2.072
SUNTOP_SERI M82_258	-6.002	-2.263
SUNTOP_SERI M82_259	-5.911	-2.074
SUNTOP_SERI M82_260	-5.966	-2.169
SUNTOP_SERI M82_261	-5.861	-1.922
SUNTOP_SERI M82_262	-5.819	-2.039
SUNTOP_SERI M82_263	-5.811	-2.009
SUNTOP_SERI M82_264	-5.951	-2.197
SUNTOP_SERI M82_265	-5.838	-2.007
SUNTOP_SERI M82_266	-5.899	-2.082
SUNTOP_SERI M82_267	-5.890	-2.023
SUNTOP_SERI M82_268	-5.952	-2.331
SUNTOP_SERI M82_269	-5.859	-2.040
SUNTOP_SERI M82_270	-5.843	-2.090
SUNTOP_SERI M82_271	-5.967	-2.274
SUNTOP_SERI M82_272	-5.940	-2.199

Genotype	Intercept	y^2
SUNTOP_SERI M82_273	-5.930	-2.105
SUNTOP_SERI M82_274	-6.175	-2.337
SUNTOP_SERI M82_275	-6.095	-2.298
SUNTOP_SERI M82_276	-5.937	-2.190
SUNTOP_SERI M82_277	-5.795	-1.994
SUNTOP_SERI M82_278	-6.088	-2.257
SUNTOP_SERI M82_279	-6.044	-2.443
SUNTOP_SERI M82_280	-5.911	-2.118
SUNTOP_SERI M82_281	-5.854	-2.040
SUNTOP_SERI M82_282	-5.961	-2.122
SUNTOP_SERI M82_283	-6.001	-2.097
SUNTOP_SERI M82_284	-5.934	-2.212
SUNTOP_SERI M82_285	-5.842	-1.977
SUNTOP_SERI M82_286	-5.796	-2.068
SUNTOP_SERI M82_287	-5.983	-2.306
SUNTOP_SERI M82_288	-5.827	-1.936
SUNTOP_SERI M82_289	-5.860	-2.081
SUNTOP_SERI M82_290	-5.933	-2.198
SUNTOP_SERI M82_291	-6.068	-2.253
SUNTOP_SERI M82_292	-5.882	-2.082
SUNTOP_SERI M82_294	-5.890	-1.917
SUNTOP_SERI M82_295	-6.173	-2.368
SUNTOP_SERI M82_296	-5.982	-2.042
SUNTOP_SERI M82_297	-5.945	-2.205
SUNTOP_SERI M82_298	-5.854	-2.010
SUNTOP_SPITFIRE_1	-6.020	-2.064
SUNTOP_SPITFIRE_10	-6.049	-2.413
SUNTOP_SPITFIRE_12	-6.001	-2.362
SUNTOP_SPITFIRE_13	-5.847	-1.978
SUNTOP_SPITFIRE_14	-5.933	-2.187
SUNTOP_SPITFIRE_15	-5.793	-2.051
SUNTOP_SPITFIRE_16	-5.889	-2.270
SUNTOP_SPITFIRE_17	-5.814	-2.112
SUNTOP_SPITFIRE_18	-5.961	-2.194
SUNTOP_SPITFIRE_19	-5.980	-2.326
SUNTOP_SPITFIRE_2	-5.944	-2.076

Table B.3 – continued from previous page

Genotype	Intercept	y^2
SUNTOP_SPITFIRE_20	-5.991	-2.277
SUNTOP_SPITFIRE_21	-5.874	-2.151
SUNTOP_SPITFIRE_22	-5.908	-2.178
SUNTOP_SPITFIRE_24	-6.086	-2.531
SUNTOP_SPITFIRE_25	-6.194	-2.459
SUNTOP_SPITFIRE_26	-5.854	-1.964
SUNTOP_SPITFIRE_28	-5.911	-2.172
SUNTOP_SPITFIRE_29	-5.969	-2.305
SUNTOP_SPITFIRE_3	-6.021	-2.370
SUNTOP_SPITFIRE_30	-5.796	-1.915
SUNTOP_SPITFIRE_31	-6.013	-2.366
SUNTOP_SPITFIRE_32	-6.094	-2.351
SUNTOP_SPITFIRE_33	-6.186	-2.399
SUNTOP_SPITFIRE_34	-5.916	-2.217
SUNTOP_SPITFIRE_35	-6.129	-2.419
SUNTOP_SPITFIRE_36	-6.047	-2.373
SUNTOP_SPITFIRE_38	-5.878	-2.072
SUNTOP_SPITFIRE_39	-5.983	-2.301
SUNTOP_SPITFIRE_4	-6.029	-2.220
SUNTOP_SPITFIRE_40	-5.927	-2.137
SUNTOP_SPITFIRE_41	-5.968	-2.123
SUNTOP_SPITFIRE_42	-6.025	-2.465
SUNTOP_SPITFIRE_43	-5.928	-2.401
SUNTOP_SPITFIRE_44	-5.687	-1.802
SUNTOP_SPITFIRE_46	-5.962	-2.272
SUNTOP_SPITFIRE_47	-5.981	-2.343
SUNTOP_SPITFIRE_48	-6.254	-2.742
SUNTOP_SPITFIRE_5	-5.979	-2.108
SUNTOP_SPITFIRE_50	-5.952	-2.353
SUNTOP_SPITFIRE_51	-5.849	-2.129
SUNTOP_SPITFIRE_52	-5.874	-2.292
SUNTOP_SPITFIRE_53	-5.973	-2.210
SUNTOP_SPITFIRE_54	-6.052	-2.586
SUNTOP_SPITFIRE_6	-5.970	-2.376
SUNTOP_SPITFIRE_7	-5.895	-2.129
SUNTOP_SPITFIRE_8	-5.955	-2.181

Genotype	*Intercept*	y^2
SUNTOP_SPITFIRE_9	-5.965	-2.287
SUNTOP_WYLIE_341	-5.890	-2.188
SUNTOP_WYLIE_342	-5.864	-2.102
SUNTOP_WYLIE_344	-5.739	-2.055
SUNTOP_WYLIE_345	-6.016	-2.325
SUNTOP_WYLIE_346	-5.954	-2.291
SUNTOP_WYLIE_347	-6.061	-2.176
SUNTOP_WYLIE_348	-6.094	-2.515
SUNTOP_WYLIE_349	-5.911	-2.129
SUNTOP_WYLIE_350	-6.195	-2.426
SUNTOP_WYLIE_351	-5.914	-2.122
SUNTOP_WYLIE_352	-5.936	-2.182
SUNTOP_WYLIE_353	-5.862	-2.151
SUNTOP_WYLIE_354	-6.087	-2.324
SUNTOP_WYLIE_355	-6.014	-2.251
SUNTOP_WYLIE_356	-6.092	-2.577
SUNTOP_WYLIE_357	-5.882	-2.136
SUNTOP_WYLIE_358	-5.880	-2.061
SUNTOP_WYLIE_359	-5.864	-2.128
SUNTOP_WYLIE_360	-5.849	-2.092
SUNTOP_WYLIE_361	-5.930	-2.186
SUNTOP_WYLIE_362	-5.823	-1.994
SUNTOP_WYLIE_363	-6.117	-2.510
SUNTOP_WYLIE_364	-6.231	-2.496
SUNTOP_WYLIE_365	-5.936	-2.209
SUNTOP_WYLIE_366	-5.890	-2.072
SUNTOP_WYLIE_367	-5.970	-2.236
SUNTOP_WYLIE_368	-5.893	-2.079
SUNTOP_WYLIE_369	-5.866	-2.177
SUNTOP_WYLIE_371	-5.839	-2.089
SUNTOP_WYLIE_372	-5.852	-2.156
SUNTOP_WYLIE_373	-5.920	-2.278
SUNTOP_WYLIE_374	-5.993	-2.354
SUNTOP_WYLIE_376	-5.870	-2.217
SUNTOP_WYLIE_377	-5.881	-2.293
SUNTOP_WYLIE_378	-5.836	-2.054

Table B.3 – continued from previous page

Genotype	Intercept	y^2
SUNTOP_WYLIE_379	-5.925	-2.251
SUNTOP_WYLIE_380	-6.110	-2.357
SUNTOP_WYLIE_381	-6.097	-2.502
SUNTOP_WYLIE_382	-6.150	-2.476
SUNTOP_ZWB10-37_383	-5.919	-2.128
SUNTOP_ZWB10-37_384	-6.178	-2.430
SUNTOP_ZWB10-37_385	-5.859	-2.088
SUNTOP_ZWB10-37_386	-5.879	-2.121
SUNTOP_ZWB10-37_387	-6.177	-2.593
SUNTOP_ZWB10-37_388	-5.935	-2.266
SUNTOP_ZWB10-37_389	-6.020	-2.190
SUNTOP_ZWB10-37_390	-5.993	-2.342
SUNTOP_ZWB10-37_392	-6.185	-2.457
SUNTOP_ZWB10-37_393	-6.043	-2.270
SUNTOP_ZWB10-37_394	-5.903	-2.165
SUNTOP_ZWB10-37_395	-6.048	-2.321
SUNTOP_ZWB10-37_396	-5.941	-2.123
SUNTOP_ZWB10-37_397	-6.108	-2.423
SUNTOP_ZWB10-37_398	-5.967	-2.173
SUNTOP_ZWB10-37_400	-5.898	-2.166
SUNTOP_ZWB10-37_403	-5.818	-2.037
SUNTOP_ZWB10-37_404	-5.950	-2.193
SUNTOP_ZWB10-37_405	-5.801	-1.932
SUNTOP_ZWB10-37_406	-6.006	-2.226
SUNTOP_ZWB10-37_407	-5.961	-2.178
SUNTOP_ZWB10-37_408	-6.200	-2.421
SUNTOP_ZWB10-37_409	-5.972	-2.204
SUNTOP_ZWB10-37_410	-5.923	-2.088
SUNTOP_ZWB10-37_411	-5.916	-2.055
SUNTOP_ZWB10-37_412	-5.841	-2.072
SUNTOP_ZWB10-37_413	-6.258	-2.617
SUNTOP_ZWB10-37_414	-5.975	-2.201
SUNTOP_ZWB10-37_415	-5.538	-1.763
SUNTOP_ZWB10-37_416	-6.089	-2.550
SUNTOP_ZWB10-37_417	-5.784	-1.882
SUNTOP_ZWB10-37_418	-5.899	-2.188

Genotype	Intercept	y^2
SUNTOP_ZWB10-37_419	-5.794	-1.927
SUNTOP_ZWB10-37_420	-6.043	-2.507
SUNTOP_ZWB10-37_422	-5.915	-2.147
SUNTOP_ZWB10-37_423	-5.918	-2.082
SUNTOP_ZWB10-37_424	-6.234	-2.656
SUNTOP_ZWW10-128_425	-5.998	-2.219
SUNTOP_ZWW10-128_426	-5.994	-2.130
SUNTOP_ZWW10-128_427	-5.974	-2.253
SUNTOP_ZWW10-128_429	-5.809	-1.950
SUNTOP_ZWW10-128_430	-6.059	-2.298
SUNTOP_ZWW10-128_432	-5.918	-2.163
SUNTOP_ZWW10-128_433	-5.979	-2.405
SUNTOP_ZWW10-128_434	-5.886	-2.135
SUNTOP_ZWW10-128_435	-6.062	-2.235
SUNTOP_ZWW10-128_436	-5.904	-2.031
SUNTOP_ZWW10-128_437	-6.167	-2.652
SUNTOP_ZWW10-128_438	-6.143	-2.558
SUNTOP_ZWW10-128_439	-5.991	-2.263
SUNTOP_ZWW10-128_440	-5.979	-2.034
SUNTOP_ZWW10-128_441	-6.126	-2.466
SUNTOP_ZWW10-128_443	-5.993	-2.190
SUNTOP_ZWW10-128_444	-5.899	-2.084
SUNTOP_ZWW10-128_445	-5.741	-1.819
SUNTOP_ZWW10-128_446	-5.909	-2.136
SUNTOP_ZWW10-128_448	-6.042	-2.176
SUNTOP_ZWW10-128_449	-5.866	-2.027
SUNTOP_ZWW10-128_450	-6.012	-2.152
SUNTOP_ZWW10-128_451	-6.105	-2.313
SUNTOP_ZWW10-128_452	-5.970	-2.251
SUNTOP_ZWW10-128_453	-6.102	-2.210
SUNTOP_ZWW10-128_454	-5.864	-2.036
SUNTOP_ZWW10-128_455	-6.049	-2.241
SUNTOP_ZWW10-128_456	-5.886	-2.069
SUNTOP_ZWW10-128_457	-5.781	-2.051
SUNTOP_ZWW10-128_458	-5.792	-1.833
SUNTOP_ZWW10-128_459	-5.804	-1.931

Genotype	*Intercept*	y^2
SUNTOP_ZWW10-128_460	-5.887	-2.117
SUNTOP_ZWW10-128_461	-5.930	-2.088
SUNTOP_ZWW10-128_462	-5.838	-2.059
SUNTOP_ZWW10-128_463	-5.778	-2.045
SUNTOP_ZWW10-128_464	-5.963	-2.078
SUNTOP_ZWW10-128_465	-5.918	-2.105
SUNTOP_ZWW10-128_466	-5.691	-1.866
ZWB10-37_P1	-6.257	-2.911
ZWW10-128_PP	-5.830	-1.972

B.4 Multivariate weighted genotype predictions

Table B.4: The genotype predictions for the weighted multivariate linear mixed model, where all predictions are generated from one model. The full set of genotype predictions are presented here, and it is important to note that these predictions are on the transformed data scale with the exception of *intercept* which did not require transforming.

Genotype	*Intercept*	$abs(x)^2$	y^2
DHARWAR DRY_PP	-5.729	-1.070	-1.951
DRYSDALE_PP	-6.037	-1.253	-2.572
EGA GREGORY_PP	-5.681	-1.037	-1.791
EGA WYLIE_PP	-6.223	-1.635	-2.629
FAC10-16_P1	-5.653	-1.176	-1.859
MACE_PP	-5.701	-1.276	-1.792
MACE_SB062_123	-5.706	-1.176	-1.899
RIL114_PP	-5.851	-1.238	-1.938
SB062_PP	-5.722	-1.029	-1.709
SERI M82_PP	-6.137	-1.393	-2.565
SPITFIRE-P9	-5.819	-1.398	-1.989
SUNTOP_DHARWAH DRY_1	-5.826	-1.181	-2.065
SUNTOP_DHARWAH DRY_10	-5.737	-1.204	-1.853
SUNTOP_DHARWAH DRY_11	-5.739	-1.286	-1.753
SUNTOP_DHARWAH DRY_12	-5.748	-1.057	-2.039
SUNTOP_DHARWAH DRY_13	-5.931	-1.425	-2.099

Genotype	Intercept	$abs(x)^2$	y^2
SUNTOP_DHARWAH DRY_14	-5.796	-1.039	-1.979
SUNTOP_DHARWAH DRY_15	-5.933	-1.657	-2.019
SUNTOP_DHARWAH DRY_16	-6.122	-1.599	-2.296
SUNTOP_DHARWAH DRY_17	-5.819	-1.324	-1.855
SUNTOP_DHARWAH DRY_18	-5.815	-0.973	-2.172
SUNTOP_DHARWAH DRY_19	-6.085	-1.291	-2.425
SUNTOP_DHARWAH DRY_2	-5.971	-1.519	-1.964
SUNTOP_DHARWAH DRY_20	-6.017	-1.350	-2.300
SUNTOP_DHARWAH DRY_21	-5.918	-1.284	-2.204
SUNTOP_DHARWAH DRY_22	-6.315	-1.994	-2.471
SUNTOP_DHARWAH DRY_23	-5.631	-1.082	-1.727
SUNTOP_DHARWAH DRY_24	-5.972	-1.376	-2.073
SUNTOP_DHARWAH DRY_25	-5.834	-1.351	-2.055
SUNTOP_DHARWAH DRY_26	-6.070	-1.308	-2.488
SUNTOP_DHARWAH DRY_27	-6.086	-1.300	-2.406
SUNTOP_DHARWAH DRY_28	-5.910	-1.304	-2.016
SUNTOP_DHARWAH DRY_29	-6.006	-1.422	-2.354
SUNTOP_DHARWAH DRY_3	-5.566	-1.197	-1.404
SUNTOP_DHARWAH DRY_30	-5.903	-1.502	-1.917
SUNTOP_DHARWAH DRY_31	-5.650	-1.031	-1.774
SUNTOP_DHARWAH DRY_32	-6.018	-1.338	-2.407
SUNTOP_DHARWAH DRY_33	-6.032	-1.587	-2.207
SUNTOP_DHARWAH DRY_34	-5.736	-1.066	-1.925
SUNTOP_DHARWAH DRY_35	-5.826	-1.306	-1.950
SUNTOP_DHARWAH DRY_36	-5.843	-1.170	-2.038
SUNTOP_DHARWAH DRY_37	-5.877	-1.536	-1.976
SUNTOP_DHARWAH DRY_38	-6.031	-1.273	-2.375
SUNTOP_DHARWAH DRY_39	-5.891	-1.391	-2.076
SUNTOP_DHARWAH DRY_4	-5.611	-0.942	-1.735
SUNTOP_DHARWAH DRY_40	-5.524	-0.860	-1.655
SUNTOP_DHARWAH DRY_41	-5.842	-1.020	-2.130
SUNTOP_DHARWAH DRY_42	-5.947	-1.043	-2.580
SUNTOP_DHARWAH DRY_43	-6.222	-1.661	-2.454
SUNTOP_DHARWAH DRY_44	-5.915	-1.432	-2.084
SUNTOP_DHARWAH DRY_45	-6.055	-1.776	-2.023
SUNTOP_DHARWAH DRY_46	-6.147	-1.477	-2.505

Genotype	Intercept	$abs(x)^2$	y^2
SUNTOP_DHARWAH DRY_47	-5.824	-1.231	-1.976
SUNTOP_DHARWAH DRY_48	-5.789	-1.379	-1.837
SUNTOP_DHARWAH DRY_49	-5.911	-1.164	-2.091
SUNTOP_DHARWAH DRY_5	-5.775	-0.848	-2.171
SUNTOP_DHARWAH DRY_50	-5.717	-1.176	-1.827
SUNTOP_DHARWAH DRY_51	-6.476	-1.713	-3.123
SUNTOP_DHARWAH DRY_52	-5.889	-1.313	-2.103
SUNTOP_DHARWAH DRY_6	-5.761	-1.373	-1.764
SUNTOP_DHARWAH DRY_7	-6.167	-1.321	-2.742
SUNTOP_DHARWAH DRY_8	-5.788	-1.262	-1.960
SUNTOP_DHARWAH DRY_9	-5.668	-0.830	-1.968
SUNTOP_DRYSDALE_100	-5.832	-1.217	-2.060
SUNTOP_DRYSDALE_101	-5.806	-0.947	-2.101
SUNTOP_DRYSDALE_102	-5.931	-1.369	-2.155
SUNTOP_DRYSDALE_103	-5.892	-1.125	-2.263
SUNTOP_DRYSDALE_104	-5.939	-1.186	-2.299
SUNTOP_DRYSDALE_53	-6.305	-1.396	-2.887
SUNTOP_DRYSDALE_54	-5.515	-0.680	-1.884
SUNTOP_DRYSDALE_55	-6.110	-1.500	-2.554
SUNTOP_DRYSDALE_56	-6.194	-1.362	-2.704
SUNTOP_DRYSDALE_57	-5.870	-1.350	-2.065
SUNTOP_DRYSDALE_58	-6.052	-1.104	-2.483
SUNTOP_DRYSDALE_59	-6.018	-1.303	-2.361
SUNTOP_DRYSDALE_60	-5.852	-1.149	-2.191
SUNTOP_DRYSDALE_61	-5.774	-0.950	-2.064
SUNTOP_DRYSDALE_62	-5.907	-1.263	-2.215
SUNTOP_DRYSDALE_64	-6.161	-1.325	-2.483
SUNTOP_DRYSDALE_65	-5.642	-0.728	-1.979
SUNTOP_DRYSDALE_66	-5.805	-1.185	-2.005
SUNTOP_DRYSDALE_67	-5.810	-1.279	-1.936
SUNTOP_DRYSDALE_68	-5.778	-1.045	-2.068
SUNTOP_DRYSDALE_69	-5.816	-1.024	-2.245
SUNTOP_DRYSDALE_70	-5.897	-1.332	-2.021
SUNTOP_DRYSDALE_71	-6.083	-1.704	-2.214
SUNTOP_DRYSDALE_72	-6.244	-1.598	-2.726
SUNTOP_DRYSDALE_73	-6.138	-1.690	-2.222

Genotype	Intercept	$abs(x)^2$	y^2
SUNTOP_DRYSDALE_74	-5.881	-1.178	-2.134
SUNTOP_DRYSDALE_75	-5.845	-1.289	-1.995
SUNTOP_DRYSDALE_76	-5.888	-1.222	-2.134
SUNTOP_DRYSDALE_77	-6.168	-1.571	-2.254
SUNTOP_DRYSDALE_78	-5.898	-1.466	-2.012
SUNTOP_DRYSDALE_79	-5.977	-1.140	-2.267
SUNTOP_DRYSDALE_80	-5.955	-1.177	-2.253
SUNTOP_DRYSDALE_81	-6.162	-1.752	-2.142
SUNTOP_DRYSDALE_83	-5.763	-1.132	-1.938
SUNTOP_DRYSDALE_84	-6.041	-1.336	-2.427
SUNTOP_DRYSDALE_85	-6.080	-1.549	-2.280
SUNTOP_DRYSDALE_86	-5.982	-1.534	-2.110
SUNTOP_DRYSDALE_87	-6.075	-1.357	-2.422
SUNTOP_DRYSDALE_88	-5.884	-1.587	-1.877
SUNTOP_DRYSDALE_89	-5.655	-0.987	-1.905
SUNTOP_DRYSDALE_90	-6.150	-1.874	-2.193
SUNTOP_DRYSDALE_91	-5.631	-1.087	-1.733
SUNTOP_DRYSDALE_92	-5.898	-1.358	-2.047
SUNTOP_DRYSDALE_93	-6.103	-1.475	-2.264
SUNTOP_DRYSDALE_94	-5.969	-1.365	-2.203
SUNTOP_DRYSDALE_95	-5.939	-1.250	-2.313
SUNTOP_DRYSDALE_96	-5.807	-1.324	-1.898
SUNTOP_DRYSDALE_97	-5.989	-1.316	-2.248
SUNTOP_DRYSDALE_98	-6.054	-1.598	-2.288
SUNTOP_DRYSDALE_99	-5.924	-1.366	-2.095
SUNTOP_EGA GREGORY_108	-5.790	-1.149	-1.995
SUNTOP_EGA GREGORY_109	-5.842	-1.055	-2.207
SUNTOP_EGA GREGORY_110	-5.998	-1.139	-2.344
SUNTOP_EGA GREGORY_111	-5.771	-0.981	-2.176
SUNTOP_EGA GREGORY_112	-5.607	-1.001	-1.717
SUNTOP_EGA GREGORY_113	-6.009	-1.629	-1.980
SUNTOP_EGA GREGORY_114	-5.884	-1.220	-2.158
SUNTOP_EGA GREGORY_115	-5.774	-1.248	-1.833
SUNTOP_EGA GREGORY_116	-6.020	-1.397	-2.238
SUNTOP_EGA GREGORY_117	-5.910	-1.316	-2.237
SUNTOP_EGA GREGORY_118	-5.856	-1.152	-2.122

Genotype	Intercept	$abs(x)^2$	y^2
SUNTOP_EGA GREGORY_119	-5.595	-0.877	-1.961
SUNTOP_EGA GREGORY_120	-5.914	-1.003	-2.599
SUNTOP_EGA GREGORY_121	-5.929	-1.398	-2.106
SUNTOP_EGA GREGORY_122	-5.811	-1.373	-1.899
SUNTOP_EGA GREGORY_123	-5.771	-1.207	-1.807
SUNTOP_EGA GREGORY_124	-5.748	-1.181	-1.886
SUNTOP_EGA GREGORY_125	-5.952	-1.285	-2.237
SUNTOP_EGA GREGORY_126	-5.872	-1.177	-2.207
SUNTOP_EGA GREGORY_127	-5.965	-1.423	-2.181
SUNTOP_EGA GREGORY_128	-5.670	-1.133	-1.766
SUNTOP_EGA GREGORY_129	-5.740	-1.042	-2.078
SUNTOP_EGA GREGORY_130	-6.317	-1.818	-2.509
SUNTOP_EGA GREGORY_131	-5.556	-0.780	-1.858
SUNTOP_EGA GREGORY_132	-6.048	-1.601	-2.199
SUNTOP_EGA GREGORY_133	-5.952	-1.358	-2.134
SUNTOP_EGA GREGORY_134	-5.999	-1.399	-2.200
SUNTOP_EGA GREGORY_135	-6.374	-2.743	-2.031
SUNTOP_EGA GREGORY_136	-6.069	-1.968	-2.001
SUNTOP_EGA GREGORY_137	-5.785	-0.692	-2.399
SUNTOP_EGA GREGORY_138	-5.807	-1.148	-2.032
SUNTOP_EGA GREGORY_139	-5.835	-1.080	-2.225
SUNTOP_EGA GREGORY_140	-6.261	-1.529	-2.793
SUNTOP_EGA GREGORY_141	-5.887	-1.380	-1.998
SUNTOP_EGA GREGORY_142	-5.931	-1.381	-2.100
SUNTOP_EGA GREGORY_143	-5.839	-1.354	-2.033
SUNTOP_EGA GREGORY_144	-6.099	-1.532	-2.286
SUNTOP_EGA GREGORY_145	-5.780	-1.264	-1.724
SUNTOP_EGA GREGORY_146	-5.741	-1.119	-1.960
SUNTOP_EGA GREGORY_147	-5.989	-1.253	-2.351
SUNTOP_EGA GREGORY_148	-5.889	-1.291	-2.061
SUNTOP_EGA GREGORY_149	-5.692	-1.115	-1.826
SUNTOP_FAC10-16_150	-5.998	-1.349	-2.340
SUNTOP_FAC10-16_151	-5.940	-1.408	-2.089
SUNTOP_FAC10-16_152	-5.961	-1.611	-1.923
SUNTOP_FAC10-16_153	-5.952	-1.225	-2.283
SUNTOP_FAC10-16_154	-5.884	-1.452	-2.004

Genotype	Intercept	$abs(x)^2$	y^2
SUNTOP_FAC10-16_155	-5.730	-1.025	-1.935
SUNTOP_FAC10-16_156	-5.712	-0.868	-2.085
SUNTOP_FAC10-16_157	-6.270	-2.064	-2.249
SUNTOP_FAC10-16_158	-5.678	-1.033	-1.924
SUNTOP_FAC10-16_159	-5.666	-1.245	-1.665
SUNTOP_FAC10-16_160	-6.057	-1.149	-2.575
SUNTOP_FAC10-16_161	-6.082	-1.749	-2.093
SUNTOP_FAC10-16_162	-5.632	-1.215	-1.585
SUNTOP_FAC10-16_163	-5.856	-1.366	-1.848
SUNTOP_FAC10-16_164	-5.814	-0.923	-2.164
SUNTOP_FAC10-16_165	-5.920	-1.230	-2.226
SUNTOP_FAC10-16_166	-5.841	-1.202	-2.082
SUNTOP_FAC10-16_167	-5.981	-1.363	-2.155
SUNTOP_FAC10-16_168	-5.944	-1.269	-2.260
SUNTOP_FAC10-16_169	-5.845	-1.306	-2.042
SUNTOP_FAC10-16_170	-6.246	-1.629	-2.711
SUNTOP_FAC10-16_171	-6.012	-1.520	-2.088
SUNTOP_FAC10-16_172	-6.017	-1.647	-2.036
SUNTOP_FAC10-16_173	-5.706	-1.122	-1.876
SUNTOP_FAC10-16_174	-5.996	-1.401	-2.279
SUNTOP_FAC10-16_175	-6.067	-1.440	-2.505
SUNTOP_FAC10-16_176	-5.898	-1.380	-1.922
SUNTOP_FAC10-16_177	-5.537	-0.857	-1.688
SUNTOP_FAC10-16_178	-6.032	-1.374	-2.274
SUNTOP_FAC10-16_179	-6.057	-1.622	-2.083
SUNTOP_FAC10-16_180	-6.151	-1.820	-2.152
SUNTOP_FAC10-16_181	-5.793	-1.331	-1.838
SUNTOP_FAC10-16_182	-5.957	-1.117	-2.347
SUNTOP_FAC10-16_183	-5.980	-1.375	-2.207
SUNTOP_FAC10-16_184	-5.957	-1.432	-2.092
SUNTOP_FAC10-16_185	-6.099	-1.465	-2.412
SUNTOP_FAC10-16_186	-5.841	-1.442	-1.835
SUNTOP_FAC10-16_187	-5.948	-1.362	-2.141
SUNTOP_FAC10-16_188	-6.524	-1.824	-2.833
SUNTOP_FAC10-16_189	-5.757	-1.098	-2.049
SUNTOP_FAC10-16_190	-5.876	-1.299	-1.960

Genotype	Intercept	$abs(x)^2$	y^2
SUNTOP_FAC10-16_191	-6.090	-1.572	-2.269
SUNTOP_PP	-6.084	-1.568	-2.057
SUNTOP_RIL114_299	-5.831	-1.409	-1.928
SUNTOP_RIL114_300	-6.166	-1.898	-2.181
SUNTOP_RIL114_301	-6.130	-1.605	-2.362
SUNTOP_RIL114_302	-5.709	-1.217	-1.750
SUNTOP_RIL114_303	-5.745	-1.054	-2.042
SUNTOP_RIL114_304	-5.779	-1.078	-1.985
SUNTOP_RIL114_305	-5.930	-1.428	-1.916
SUNTOP_RIL114_306	-5.851	-1.145	-2.164
SUNTOP_RIL114_307	-5.872	-1.262	-2.060
SUNTOP_RIL114_308	-5.897	-1.298	-2.130
SUNTOP_RIL114_309	-6.003	-1.378	-2.092
SUNTOP_RIL114_310	-6.077	-1.515	-2.305
SUNTOP_RIL114_311	-5.922	-1.224	-2.199
SUNTOP_RIL114_312	-5.859	-1.357	-1.931
SUNTOP_RIL114_313	-5.762	-1.289	-1.805
SUNTOP_RIL114_314	-5.751	-1.004	-1.972
SUNTOP_RIL114_315	-5.873	-1.156	-2.221
SUNTOP_RIL114_316	-5.933	-1.440	-2.111
SUNTOP_RIL114_317	-5.622	-0.972	-1.843
SUNTOP_RIL114_318	-5.690	-1.109	-1.795
SUNTOP_RIL114_319	-6.243	-1.571	-2.610
SUNTOP_RIL114_320	-6.169	-1.664	-2.264
SUNTOP_RIL114_321	-5.952	-1.511	-1.952
SUNTOP_RIL114_322	-5.745	-0.885	-1.986
SUNTOP_RIL114_323	-5.872	-1.252	-2.026
SUNTOP_RIL114_324	-5.792	-1.513	-1.649
SUNTOP_RIL114_325	-6.288	-1.823	-2.257
SUNTOP_RIL114_326	-5.739	-1.193	-1.831
SUNTOP_RIL114_327	-5.715	-0.975	-1.996
SUNTOP_RIL114_328	-5.915	-1.332	-2.109
SUNTOP_RIL114_329	-5.893	-1.475	-2.033
SUNTOP_RIL114_330	-6.008	-1.312	-2.250
SUNTOP_RIL114_331	-5.944	-1.777	-1.906
SUNTOP_RIL114_333	-6.020	-1.338	-2.274

Genotype	Intercept	$abs(x)^2$	y^2
SUNTOP_RIL114_334	-5.862	-1.297	-1.993
SUNTOP_RIL114_335	-5.780	-1.264	-1.895
SUNTOP_RIL114_336	-5.684	-0.794	-1.920
SUNTOP_RIL114_337	-6.496	-2.293	-2.429
SUNTOP_RIL114_338	-5.713	-1.113	-1.815
SUNTOP_RIL114_339	-5.585	-1.073	-1.634
SUNTOP_RIL114_340	-5.963	-1.471	-2.000
SUNTOP_SB062_195	-5.836	-1.020	-2.181
SUNTOP_SB062_196	-5.718	-1.571	-1.540
SUNTOP_SB062_197	-5.881	-1.295	-2.053
SUNTOP_SB062_198	-5.658	-0.989	-1.856
SUNTOP_SB062_199	-5.865	-1.535	-1.757
SUNTOP_SB062_200	-5.937	-1.458	-1.995
SUNTOP_SB062_201	-5.918	-1.245	-2.197
SUNTOP_SB062_202	-5.982	-1.466	-2.176
SUNTOP_SB062_203	-5.830	-1.146	-2.109
SUNTOP_SB062_204	-5.899	-1.361	-2.058
SUNTOP_SB062_205	-5.854	-1.272	-2.029
SUNTOP_SB062_206	-6.126	-1.727	-2.200
SUNTOP_SB062_207	-5.941	-1.328	-1.987
SUNTOP_SB062_208	-6.102	-1.543	-2.311
SUNTOP_SB062_209	-5.869	-1.465	-1.812
SUNTOP_SB062_210	-5.932	-1.222	-2.233
SUNTOP_SB062_211	-5.940	-1.379	-1.992
SUNTOP_SB062_212	-5.663	-1.074	-1.666
SUNTOP_SB062_213	-5.884	-1.392	-1.926
SUNTOP_SB062_214	-5.926	-1.456	-2.065
SUNTOP_SB062_215	-5.930	-1.449	-2.006
SUNTOP_SB062_216	-6.140	-1.792	-2.218
SUNTOP_SB062_217	-5.939	-1.263	-2.275
SUNTOP_SB062_218	-5.821	-1.300	-2.030
SUNTOP_SB062_219	-5.738	-0.932	-2.117
SUNTOP_SB062_220	-5.845	-1.254	-2.083
SUNTOP_SB062_221	-5.852	-1.412	-1.928
SUNTOP_SB062_222	-5.769	-1.276	-1.978
SUNTOP_SB062_223	-6.027	-1.946	-1.791

Genotype	Intercept	$abs(x)^2$	y^2
SUNTOP_SB062_224	-6.018	-1.505	-2.046
SUNTOP_SB062_225	-5.961	-1.443	-2.051
SUNTOP_SB062_226	-5.966	-1.241	-2.408
SUNTOP_SB062_227	-5.841	-1.282	-2.080
SUNTOP_SB062_228	-5.970	-1.353	-2.225
SUNTOP_SB062_229	-5.689	-1.254	-1.758
SUNTOP_SB062_230	-5.851	-1.064	-2.081
SUNTOP_SB062_231	-6.220	-1.531	-2.668
SUNTOP_SB062_232	-5.880	-1.250	-2.069
SUNTOP_SB062_233	-5.685	-1.146	-1.767
SUNTOP_SB062_234	-5.853	-1.351	-1.998
SUNTOP_SB062_235	-5.611	-1.167	-1.521
SUNTOP_SB062_236	-5.485	-0.896	-1.604
SUNTOP_SB062_237	-6.202	-1.728	-2.356
SUNTOP_SB062_238	-5.984	-1.477	-2.102
SUNTOP_SB062_239	-6.299	-1.969	-2.690
SUNTOP_SB062_240	-6.106	-1.537	-2.319
SUNTOP_SB062_241	-5.980	-1.311	-2.243
SUNTOP_SB062_242	-5.830	-1.216	-1.966
SUNTOP_SB062_243	-5.807	-1.114	-2.034
SUNTOP_SB062_244	-5.945	-1.400	-2.180
SUNTOP_SB062_245	-6.006	-1.524	-2.074
SUNTOP_SB062_246	-5.643	-1.118	-1.694
SUNTOP_SERI M82_247	-5.832	-1.179	-1.996
SUNTOP_SERI M82_248	-5.898	-1.552	-1.831
SUNTOP_SERI M82_249	-6.076	-1.508	-2.298
SUNTOP_SERI M82_250	-5.872	-1.334	-1.990
SUNTOP_SERI M82_251	-6.209	-1.584	-2.417
SUNTOP_SERI M82_252	-5.866	-1.316	-2.020
SUNTOP_SERI M82_253	-5.923	-1.410	-2.023
SUNTOP_SERI M82_254	-5.668	-1.137	-1.680
SUNTOP_SERI M82_255	-5.987	-1.314	-2.260
SUNTOP_SERI M82_256	-6.014	-1.425	-2.176
SUNTOP_SERI M82_257	-5.886	-1.549	-1.928
SUNTOP_SERI M82_258	-5.876	-0.957	-2.258
SUNTOP_SERI M82_259	-5.886	-1.376	-1.982

Genotype	Intercept	$abs(x)^2$	y^2
SUNTOP_SERI M82_260	-5.879	-1.232	-2.045
SUNTOP_SERI M82_261	-5.772	-1.335	-1.770
SUNTOP_SERI M82_262	-5.805	-1.215	-2.023
SUNTOP_SERI M82_263	-5.618	-0.867	-1.827
SUNTOP_SERI M82_264	-5.980	-1.540	-2.094
SUNTOP_SERI M82_265	-5.890	-1.600	-1.894
SUNTOP_SERI M82_266	-5.695	-0.863	-1.933
SUNTOP_SERI M82_267	-5.853	-1.327	-1.971
SUNTOP_SERI M82_268	-6.016	-1.365	-2.419
SUNTOP_SERI M82_269	-5.728	-1.214	-1.780
SUNTOP_SERI M82_270	-5.761	-1.222	-1.936
SUNTOP_SERI M82_271	-5.920	-1.099	-2.331
SUNTOP_SERI M82_272	-5.900	-1.274	-2.131
SUNTOP_SERI M82_273	-5.893	-1.373	-1.993
SUNTOP_SERI M82_274	-6.180	-1.656	-2.323
SUNTOP_SERI M82_275	-6.125	-1.566	-2.291
SUNTOP_SERI M82_276	-5.915	-1.344	-2.115
SUNTOP_SERI M82_277	-5.585	-0.796	-1.832
SUNTOP_SERI M82_278	-6.087	-1.475	-2.253
SUNTOP_SERI M82_279	-5.978	-1.214	-2.364
SUNTOP_SERI M82_280	-5.793	-1.078	-2.006
SUNTOP_SERI M82_281	-5.839	-1.287	-1.994
SUNTOP_SERI M82_282	-5.895	-1.331	-1.983
SUNTOP_SERI M82_283	-5.961	-1.436	-2.046
SUNTOP_SERI M82_284	-5.992	-1.548	-2.175
SUNTOP_SERI M82_285	-5.657	-1.003	-1.763
SUNTOP_SERI M82_286	-5.706	-1.145	-1.927
SUNTOP_SERI M82_287	-6.001	-1.254	-2.379
SUNTOP_SERI M82_288	-5.641	-1.104	-1.597
SUNTOP_SERI M82_289	-5.753	-1.167	-1.901
SUNTOP_SERI M82_290	-5.914	-1.318	-2.149
SUNTOP_SERI M82_291	-5.961	-1.276	-2.091
SUNTOP_SERI M82_292	-5.764	-1.055	-1.962
SUNTOP_SERI M82_294	-5.745	-1.359	-1.607
SUNTOP_SERI M82_295	-6.405	-2.146	-2.434
SUNTOP_SERI M82_296	-5.908	-1.367	-1.986

Genotype	Intercept	$abs(x)^2$	y^2
SUNTOP_SERI M82_297	-5.990	-1.371	-2.265
SUNTOP_SERI M82_298	-5.892	-1.802	-1.702
SUNTOP_SPITFIRE_1	-5.918	-1.341	-1.967
SUNTOP_SPITFIRE_10	-6.013	-1.257	-2.395
SUNTOP_SPITFIRE_12	-6.041	-1.404	-2.403
SUNTOP_SPITFIRE_13	-5.796	-1.145	-1.988
SUNTOP_SPITFIRE_14	-5.911	-1.407	-2.074
SUNTOP_SPITFIRE_15	-5.696	-1.114	-1.887
SUNTOP_SPITFIRE_16	-5.896	-1.233	-2.324
SUNTOP_SPITFIRE_17	-5.734	-1.128	-1.974
SUNTOP_SPITFIRE_18	-5.886	-1.220	-2.088
SUNTOP_SPITFIRE_19	-5.876	-1.066	-2.253
SUNTOP_SPITFIRE_2	-5.970	-1.657	-1.927
SUNTOP_SPITFIRE_20	-6.080	-1.611	-2.289
SUNTOP_SPITFIRE_21	-5.813	-1.225	-2.047
SUNTOP_SPITFIRE_22	-5.741	-0.942	-2.029
SUNTOP_SPITFIRE_24	-6.148	-1.636	-2.436
SUNTOP_SPITFIRE_25	-6.280	-1.792	-2.488
SUNTOP_SPITFIRE_26	-5.755	-1.261	-1.766
SUNTOP_SPITFIRE_28	-5.898	-1.342	-2.097
SUNTOP_SPITFIRE_29	-5.941	-1.301	-2.241
SUNTOP_SPITFIRE_3	-6.039	-1.492	-2.287
SUNTOP_SPITFIRE_30	-5.800	-1.456	-1.764
SUNTOP_SPITFIRE_31	-5.994	-1.075	-2.539
SUNTOP_SPITFIRE_32	-6.136	-1.421	-2.430
SUNTOP_SPITFIRE_33	-6.268	-1.760	-2.445
SUNTOP_SPITFIRE_34	-6.053	-1.752	-2.207
SUNTOP_SPITFIRE_35	-6.242	-1.725	-2.485
SUNTOP_SPITFIRE_36	-6.037	-1.314	-2.427
SUNTOP_SPITFIRE_38	-5.805	-1.302	-1.893
SUNTOP_SPITFIRE_39	-5.982	-1.301	-2.313
SUNTOP_SPITFIRE_4	-6.186	-1.971	-2.133
SUNTOP_SPITFIRE_40	-5.962	-1.571	-2.043
SUNTOP_SPITFIRE_41	-5.935	-1.471	-1.962
SUNTOP_SPITFIRE_42	-6.075	-1.323	-2.579
SUNTOP_SPITFIRE_43	-5.968	-1.501	-2.274

Genotype	Intercept	$abs(x)^2$	y^2
SUNTOP_SPITFIRE_44	-5.583	-1.114	-1.625
SUNTOP_SPITFIRE_46	-5.925	-1.330	-2.164
SUNTOP_SPITFIRE_47	-6.014	-1.441	-2.325
SUNTOP_SPITFIRE_48	-6.137	-1.418	-2.508
SUNTOP_SPITFIRE_5	-5.916	-1.451	-1.889
SUNTOP_SPITFIRE_50	-5.899	-1.118	-2.352
SUNTOP_SPITFIRE_51	-5.813	-1.207	-2.026
SUNTOP_SPITFIRE_52	-5.777	-0.946	-2.263
SUNTOP_SPITFIRE_53	-5.980	-1.410	-2.184
SUNTOP_SPITFIRE_54	-6.083	-1.352	-2.586
SUNTOP_SPITFIRE_6	-5.995	-1.273	-2.445
SUNTOP_SPITFIRE_7	-5.919	-1.437	-2.073
SUNTOP_SPITFIRE_8	-5.983	-1.493	-2.133
SUNTOP_SPITFIRE_9	-6.019	-1.576	-2.210
SUNTOP_WYLIE_341	-5.904	-1.314	-2.200
SUNTOP_WYLIE_342	-5.853	-1.433	-1.951
SUNTOP_WYLIE_344	-5.595	-0.828	-1.948
SUNTOP_WYLIE_345	-5.933	-1.051	-2.367
SUNTOP_WYLIE_346	-6.038	-1.493	-2.361
SUNTOP_WYLIE_347	-5.974	-1.325	-2.111
SUNTOP_WYLIE_348	-6.198	-1.453	-2.704
SUNTOP_WYLIE_349	-5.930	-1.439	-2.072
SUNTOP_WYLIE_350	-6.108	-1.530	-2.308
SUNTOP_WYLIE_351	-5.780	-1.122	-1.951
SUNTOP_WYLIE_352	-5.820	-1.086	-2.089
SUNTOP_WYLIE_353	-5.864	-1.385	-2.058
SUNTOP_WYLIE_354	-6.110	-1.539	-2.318
SUNTOP_WYLIE_355	-6.077	-1.607	-2.227
SUNTOP_WYLIE_356	-6.039	-1.345	-2.406
SUNTOP_WYLIE_357	-5.851	-1.333	-2.023
SUNTOP_WYLIE_358	-5.933	-1.811	-1.804
SUNTOP_WYLIE_359	-5.790	-1.152	-2.054
SUNTOP_WYLIE_360	-5.824	-1.323	-1.970
SUNTOP_WYLIE_361	-5.942	-1.405	-2.139
SUNTOP_WYLIE_362	-5.737	-1.157	-1.868
SUNTOP_WYLIE_363	-6.073	-1.312	-2.486

Genotype	Intercept	$abs(x)^2$	y^2
SUNTOP_WYLIE_364	-6.291	-1.698	-2.542
SUNTOP_WYLIE_365	-5.957	-1.482	-2.136
SUNTOP_WYLIE_366	-5.848	-1.343	-1.944
SUNTOP_WYLIE_367	-5.978	-1.412	-2.193
SUNTOP_WYLIE_368	-5.869	-1.393	-1.955
SUNTOP_WYLIE_369	-5.802	-1.186	-2.090
SUNTOP_WYLIE_371	-5.731	-1.184	-1.910
SUNTOP_WYLIE_372	-5.812	-1.154	-2.133
SUNTOP_WYLIE_373	-5.893	-1.014	-2.469
SUNTOP_WYLIE_374	-5.975	-1.371	-2.246
SUNTOP_WYLIE_376	-5.856	-1.304	-2.148
SUNTOP_WYLIE_377	-5.811	-1.206	-2.137
SUNTOP_WYLIE_378	-5.728	-1.124	-1.894
SUNTOP_WYLIE_379	-5.879	-1.172	-2.220
SUNTOP_WYLIE_380	-6.154	-1.492	-2.434
SUNTOP_WYLIE_381	-6.139	-1.347	-2.626
SUNTOP_WYLIE_382	-6.210	-1.843	-2.352
SUNTOP_ZWB10-37_383	-5.835	-1.250	-1.979
SUNTOP_ZWB10-37_384	-6.391	-1.988	-2.582
SUNTOP_ZWB10-37_385	-5.791	-1.225	-1.969
SUNTOP_ZWB10-37_386	-5.886	-1.409	-2.026
SUNTOP_ZWB10-37_387	-6.431	-2.167	-2.650
SUNTOP_ZWB10-37_388	-5.873	-1.072	-2.276
SUNTOP_ZWB10-37_389	-6.102	-1.739	-2.135
SUNTOP_ZWB10-37_390	-6.086	-1.727	-2.256
SUNTOP_ZWB10-37_392	-6.295	-1.406	-2.740
SUNTOP_ZWB10-37_393	-6.047	-1.470	-2.285
SUNTOP_ZWB10-37_394	-5.806	-1.086	-2.098
SUNTOP_ZWB10-37_395	-6.013	-1.396	-2.249
SUNTOP_ZWB10-37_396	-5.832	-1.179	-1.994
SUNTOP_ZWB10-37_397	-6.231	-1.704	-2.515
SUNTOP_ZWB10-37_398	-5.873	-1.143	-2.110
SUNTOP_ZWB10-37_400	-5.845	-1.237	-2.054
SUNTOP_ZWB10-37_403	-5.735	-1.280	-1.819
SUNTOP_ZWB10-37_404	-5.915	-1.332	-2.109
SUNTOP_ZWB10-37_405	-5.684	-1.228	-1.678

Genotype	Intercept	$abs(x)^2$	y^2
SUNTOP_ZWB10-37_406	-6.006	-1.374	-2.221
SUNTOP_ZWB10-37_407	-5.827	-1.034	-2.098
SUNTOP_ZWB10-37_408	-6.250	-1.453	-2.550
SUNTOP_ZWB10-37_409	-5.885	-1.107	-2.173
SUNTOP_ZWB10-37_410	-5.879	-1.444	-1.925
SUNTOP_ZWB10-37_411	-5.930	-1.536	-1.958
SUNTOP_ZWB10-37_412	-5.714	-1.080	-1.895
SUNTOP_ZWB10-37_413	-6.369	-1.771	-2.646
SUNTOP_ZWB10-37_414	-6.012	-1.551	-2.137
SUNTOP_ZWB10-37_415	-5.403	-0.726	-1.643
SUNTOP_ZWB10-37_416	-6.145	-1.456	-2.579
SUNTOP_ZWB10-37_417	-5.620	-1.448	-1.347
SUNTOP_ZWB10-37_418	-5.860	-1.275	-2.047
SUNTOP_ZWB10-37_419	-5.784	-1.382	-1.806
SUNTOP_ZWB10-37_420	-6.034	-1.388	-2.389
SUNTOP_ZWB10-37_422	-5.815	-1.114	-2.045
SUNTOP_ZWB10-37_423	-5.774	-1.195	-1.852
SUNTOP_ZWB10-37_424	-6.127	-1.200	-2.611
SUNTOP_ZWW10-128_425	-5.936	-1.243	-2.179
SUNTOP_ZWW10-128_426	-6.012	-1.617	-2.023
SUNTOP_ZWW10-128_427	-5.971	-1.368	-2.223
SUNTOP_ZWW10-128_429	-5.656	-1.302	-1.552
SUNTOP_ZWW10-128_430	-5.929	-1.025	-2.269
SUNTOP_ZWW10-128_432	-5.850	-1.229	-2.062
SUNTOP_ZWW10-128_433	-5.903	-1.260	-2.192
SUNTOP_ZWW10-128_434	-6.198	-2.255	-2.099
SUNTOP_ZWW10-128_435	-6.068	-1.542	-2.193
SUNTOP_ZWW10-128_436	-5.726	-0.944	-1.872
SUNTOP_ZWW10-128_437	-6.131	-1.387	-2.537
SUNTOP_ZWW10-128_438	-6.256	-1.330	-2.891
SUNTOP_ZWW10-128_439	-6.020	-1.448	-2.265
SUNTOP_ZWW10-128_440	-6.029	-1.846	-1.841
SUNTOP_ZWW10-128_441	-6.128	-1.417	-2.487
SUNTOP_ZWW10-128_443	-6.002	-1.488	-2.124
SUNTOP_ZWW10-128_444	-5.911	-1.397	-2.053
SUNTOP_ZWW10-128_445	-5.500	-0.852	-1.521

Continued on next page

Genotype	*Intercept*	$abs(x)^2$	y^2
SUNTOP_ZWW10-128_446	-5.866	-1.287	-2.046
SUNTOP_ZWW10-128_448	-6.043	-1.475	-2.157
SUNTOP_ZWW10-128_449	-5.753	-1.138	-1.876
SUNTOP_ZWW10-128_450	-5.923	-1.179	-2.129
SUNTOP_ZWW10-128_451	-6.112	-1.505	-2.317
SUNTOP_ZWW10-128_452	-5.947	-1.422	-2.140
SUNTOP_ZWW10-128_453	-6.023	-1.478	-2.106
SUNTOP_ZWW10-128_454	-5.837	-1.331	-1.943
SUNTOP_ZWW10-128_455	-5.970	-1.383	-2.082
SUNTOP_ZWW10-128_456	-5.740	-1.019	-1.941
SUNTOP_ZWW10-128_457	-5.724	-1.220	-1.868
SUNTOP_ZWW10-128_458	-5.754	-1.395	-1.672
SUNTOP_ZWW10-128_459	-5.710	-1.235	-1.731
SUNTOP_ZWW10-128_460	-5.837	-1.251	-2.028
SUNTOP_ZWW10-128_461	-5.870	-1.370	-1.937
SUNTOP_ZWW10-128_462	-5.773	-1.199	-1.945
SUNTOP_ZWW10-128_463	-5.494	-0.894	-1.605
SUNTOP_ZWW10-128_464	-5.924	-1.498	-1.893
SUNTOP_ZWW10-128_465	-5.718	-1.017	-1.855
SUNTOP_ZWW10-128_466	-5.592	-1.318	-1.549
ZWB10-37_P1	-6.369	-1.346	-3.191
ZWW10-128_PP	-5.802	-1.374	-1.847